GEOLOGIC INTERPRETATION FROM WELL LOGS

STANDARD OIL COMPANY OF CALIFORNIA

SAN FRANCISCO

1967

GEOLOGIC INTERPRETATION FROM WELL LOGS

INTRODUCTION

The purpose of this manual is to compile under one cover the principles of well log correlation, together with examples of lithologic interpretation and expressions of stratigraphic and structural features which can sometimes be recognized on well logs.

For the past 35 years, geologists and engineers have correlated electric and radioactivity logs. During the first 20 years, this correlation consisted of a comparison of log curves checked by paleontologic dating and lithologic information from cores and cuttings. Very little consideration was given to the electrochemical and petrophysical fundamentals and relationships that determine the amplitudes and shapes of the various curves. Quantitative analysis was relegated to the log analyst, usually an engineer, whose primary interests were porosity and hydrocarbon saturation.

Advancing technology during the last 15 years has provided a multiplicity of electric, acoustic, and radioactivity logs which have greatly enhanced both qualitative and quantitative interpretation, but for all except the expert log analyst, correlation and geologic interpretation seem to be more difficult than with the simpler appearing logs of the past. Modern drilling fluids and drilling practices have also contributed to the confusion. Geologists and petroleum engineers must therefore acquire a basic understanding of petrophysics and quantitative log interpretation. These subjects are now well covered by Company manuals by Mr. J. E. Walstrom, by Chevron Research reports, and by several published texts. Geologic interpretation and correlation of modern logs are not adequately covered; hence the need for a supplemental manual designed primarily for the exploration geologist.

About half of the log examples and accompanying descriptions for this compilation were taken from the 1959 W.O.I. manual, "Stratigraphic and Structural Interpretations from Well Logs," the 1959 Chevron West manual, "Qualitative Use of Well Logs," Chevron Research memoranda and reports, and Schlumberger Interpretation Techniques. The balance of the examples were contributed by the editor and the following individuals from the Standard of California family:

C. A. Bengston	Chevron Research
F. L. Campbell	Chevron Research
L. R. Litsey	Chevron Calco
C. D. Jones	Chevron Exploration
B. B. Cooley	Chevron Sotex
C. F. Lamb	Chevron Sotex
C. V. Moore	Chevron Sotex
R. E. Murphy	Chevron Sotex
W. L. Turner	Chevron Sotex
J. R. Lishman	Chevron Standard
D. W. Organ	Chevron Standard
E. C. Bowman	Chevron West

J. E. Dryden	Western Operations, Inc.
D. N. Helmuth	Western Operations, Inc.
R. R. Johnston	Western Operations, Inc.
R. L. Manly	Western Operations, Inc.
H. E. Nagle	Western Operations, Inc.

Many other examples were not included because, in the editors' judgment, the interpretation was unclear or ambiguous, or a better example of the same feature was available. Because of the differences in background and experience in local areas of the various contributors, some may prefer local examples to those selected for the compilation. The manual is in loose-leaf form for that reason and also so that additional material may be added in each section.

As research progresses in computer applications to well log analysis and lithologic interpretation, computer logs and plots should be included in this manual. The experimental logs now available were not included at this time, because they could be misleading. At the present state of the art, the geologist should be working toward a better understanding of the influence of various rock properties on the basic measurements made by logging tools. He will then be better equipped to interpret and analyze the computer logs derived from these measurements.

J. C. Wells
Editor
May 1967

CONTENTS

PART 4. STRUCTURAL INTERPRETATION FROM LOGS

Steep Dips
Unconformities
Normal Faults
Reverse Faulting and Overturning
Structural Interpretations from Dipmeter Data

PART 5. HYDRODYNAMICS AND ABNORMAL PRESSURE EFFECTS

Transition from Fresh Water to Salt Water
Hydrodynamic Effects
Abnormal Pressure Effects on Well Logs

PART 1

CORRELATION

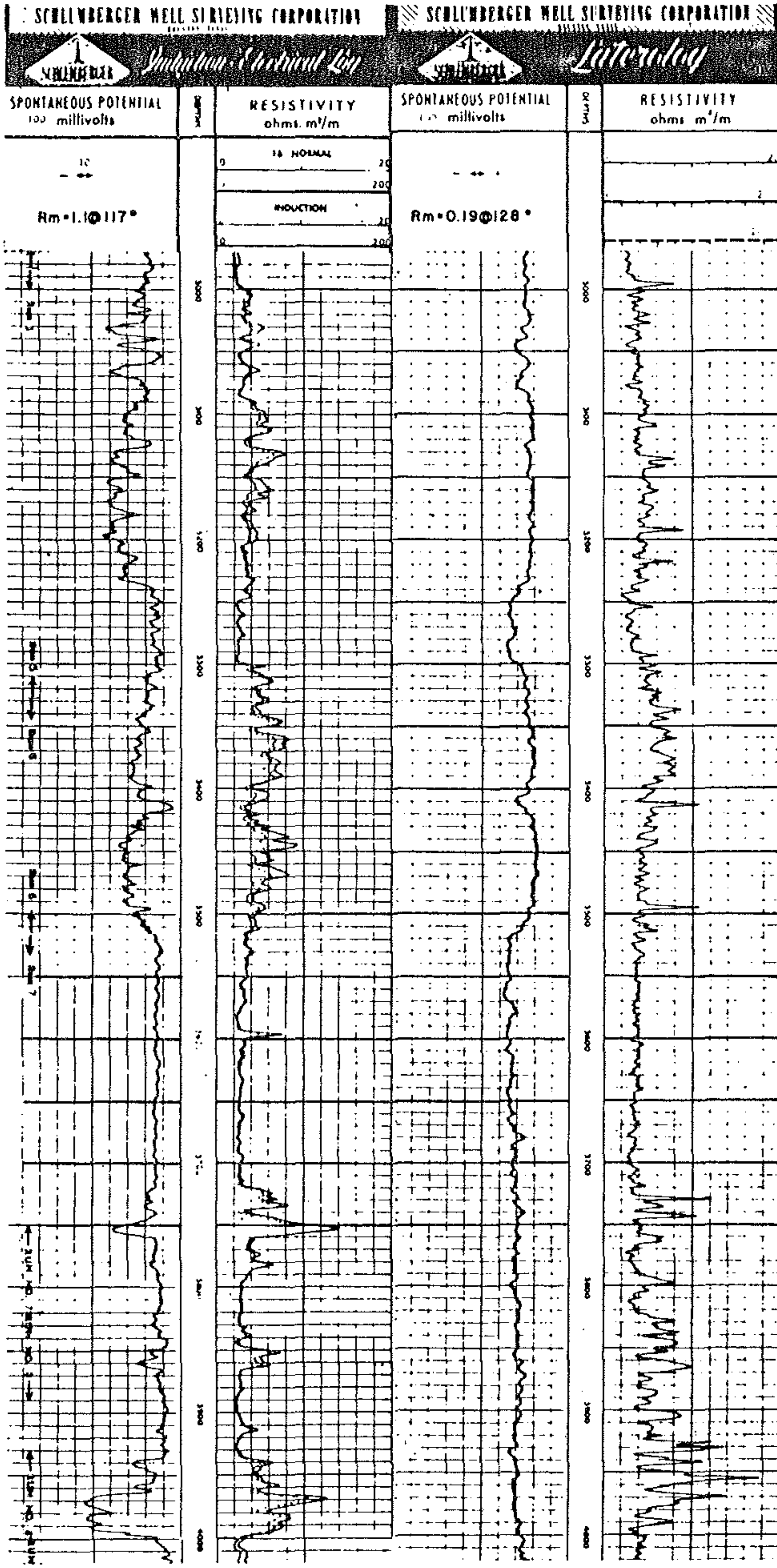

ELECTRIC LOG
IN FRESH
WATER MUD

(ORIGINAL HOLE)

COMPARED
WITH

LATEROLOG
IN SALT MUD

(REDRILL)

Note positive
S.P. opposite
sands in salt mud.

KERN
COUNTY,
CALIFORNIA

Figure 1-1

COMPARISON OF

ELECTRIC LOG
WITH
INTERVAL VELOCITY LOG

GRAPEVINE AREA CALIFORNIA

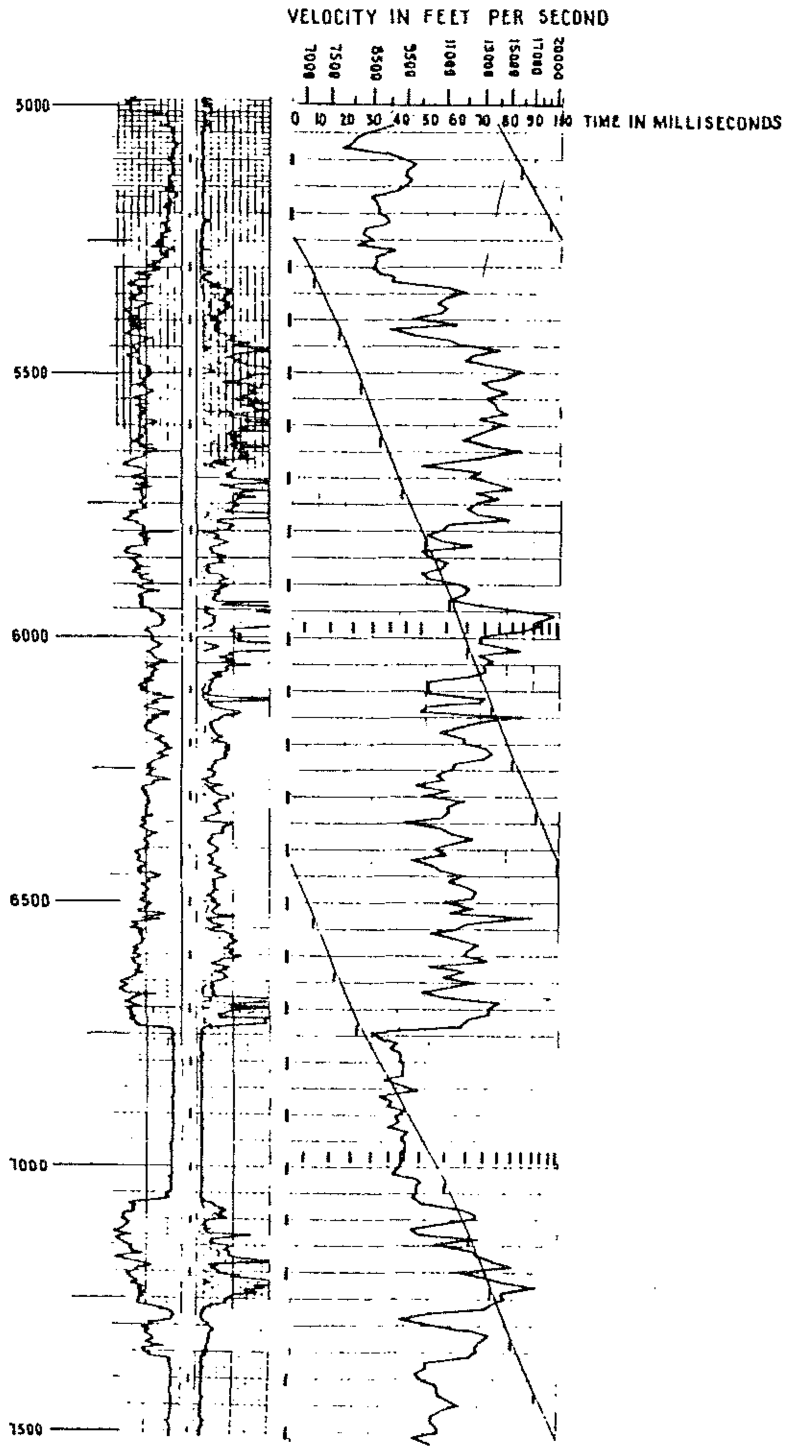

Figure 1-2

LITHOLOGIC CORRELATION

The first step in any correlation problem is to assemble all the electric logs, core and cuttings descriptions, and paleontological data that are available. In some areas, radioactivity logs and velocity logs may also be quite helpful. Then, before attempting any correlation, the logs should be studied critically and compared with the lithology, as shown in the descriptions of cores and cuttings. If the geologist is not familiar with the section, core samples where available should also be examined and compared with the written descriptions and electric logs because descriptions of the same type of material by different geologists often vary considerably.

After the geologist has become familiar with the material available, the regional perspective should be established. This is usually done by choosing the most complete core records, and in some cases measured outcrop sections, as starting points in several parts of the area and comparing paleontological data to establish time relations. The geologist is then ready to begin correlating logs.

Regional correlation is usually best accomplished by first comparing large stratigraphic units and correlating by general over-all character because individual marker beds may not be continuous and facies changes and structural complications may cause confusion if smaller units are used. Confusion may also result from using electric logs which do not properly reflect the lithology or which were recorded under different conditions. (See Figures 1-3 to 1-11.)

Large stratigraphic units which can be correlated over broad areas may be predominantly sand, or shale, or carbonates, or they may be quite variable with one or more persistent beds that are easily recognizable. The S.P. curve is normally used for correlating sand and silicous shale intervals although sometimes the resistivity curves must be used in conjunction. Large shale intervals usually show more detail on the conductivity curve or amplified short normal of the induction-electric or standard electric logs, and the Laterolog-8 on the logarithmic scale of the DIL system also shows excellent detail in low resistivity intervals. In some areas, the ohm-meter value of shale resistivity in a particular interval or a sequence of intervals may be correlated. When attempting to correlate shale resistivities quantitatively it may be necessary to correct the short normal curve for the size of the hole and the mud resistivity. In carbonate sections, the gamma ray curve is used for detailed correlation because the high resistivity effect on the S.P. produces a rounded and sluggish-looking curve. (See Figure 2-14).

When the broad regional stratigraphic correlations have been established, the next problem becomes one of breaking down the larger stratigraphic units into environment of deposition as illustrated in Part 2 of this manual. The S.P. curve can be very helpful for this purpose in sand-shale sections because its pattern normally reflects ratios of shale or argillaceous material to clean sands. This does not mean a decrease in self-potential is necessarily a measure of decreased permeability. It means a decrease in self-potential indicates an increase in argillaceous material provided there is no change in formation water salinity. Dipmeter plots used with electric logs may indicate the direction of sand transport and may help to identify individual sands. This stratigraphic application of the dipmeter has proven to be very helpful in California and South Louisiana.

Some specific rock types or groups show more or less definite characteristics or log patterns as illustrated in Part 3 of this manual. In most cases, however, these patterns are not sufficiently diagnostic to be used without corroborating evidence from cuttings, cores, or sidewall samples.

CORRELATION

Type of Log	Formations to Which Applicable	Type of Mud	Advantages and Special Merits	Limitations	Precautions
SP	Any except those of very high resistivity.	Any conductive* mud so long as Rmf is not equal to Rw.	Sharply defines contacts between shales and porous nonshales.	Affected by lateral changes in formation water salinity, loses character as Rmf/Rw approaches unity, as e/d becomes quite small and as Rt/Rm and Rs/Rm become quite large.	Proper scale must be chosen to provide desired definition.
Short Normal	Low and moderate resistivities.	Any conductive* mud except saturated or nearly saturated salt muds.	Wide selection of scales provides adequate correlation character over wide range of resistivities.	Reflects variations in Rmf, ROS and Di and extremely sensitive to e/spacing as e approaches spacing; reverses but has characteristic shape when e equals or is less than the spacing.	Care must be taken in selecting proper scale for correlation realizing that this generally is not the same as the desired scale for formation evaluation work. Amplified scale best in long shale sections.
Lateral	Any	Same	Always gives marked "kicks" in right direction for thin resistive streaks with characteristic shadow zone and false peak below.	Poor definition of thin conductive beds surrounded by thick resistive formations.	Effect of adjacent beds on shape of curve must always be considered.
Induction	Low and moderate resistivities.	Same	Conductivity curve is particularly useful through long intervals of low resistivity.	Does not always indicate thin resistive streaks.	Care must be taken in selecting proper scale.
Laterologs (Guard electrode)	Any	Any conductive* mud but best with muds of lower resistivity.	Sharp bed delineation.		Hyperbolic scale generally best for correlation work.
Micrylog	Any	Any conductive* mud except saturated or nearly saturated salt muds.	Extremely detailed. Excellent supplement to amplified short normal through long intervals of negligible resistivity contrast and substitute for long lateral for delineating thin resistive markers.		
Gamma Ray	Any	Any	Reflects only natural radioactivity which for most formations exhibits less lateral variation than do electrical char[illegible]istics. Not affected by [illegible] hole conditions or formation	Low radioactivity contrasts cannot always be overcome simply by changing scale as can low electrical contrasts.	Quality of log severely affected by choice of logging speed, time constant, instrument sensitivity and scale.

Sonic (Interval Velocity) (Acoustic)	Any	Any. (Response in empty holes unknown)	Measures a basic characteristic of the formations. It is not materially affected by changes in Rm, Rw, Sw, or (within limits) d.	Gives abnormal readings in high porosity, unconsolidated, noninvaded gas (and sometimes oil) bearing sands and through zones of extreme fracturing.	Optimum bias setting must be selected to avoid excessive cycle skipping or electrical noise.
Density (Gamma - Gamma)	Any	Any	Records basic parameter, density, of the formations. Two receiver, compensated log effective through casing.		

LITHOLOGY

SP	Any except those of extreme resistivity.	Any conductive mud so long as Rmf is not equal to Rw.	Distinguishes between shales and nonshales.	Same as for correlation work.	Same as for correlation work.
Gamma Ray	Any	Any	Not affected by bore hole conditions.	Local relationship between radioactivity and lithology must be known. Always same limitation as for correlation work.	Same as for correlation work.
Sonic	Consolidated	Any fluid	Records basic parameter, velocity, of the formations. Where adequate knowledge of porosity and fluid content is available, formation velocity can be related to Lithology.	Same as for correlation work.	Same as for correlation work.
Density	Any	Any	Records basic parameter, density, of the formations. Where porosity and fluid content are known, rock type may be identified.	Sensitive to sharp irregularities in the bore wall.	Proper calibration essential. Should be checked against core analysis if possible.

*Conductive is used under Type of Mud, in the general sense and does not refer to degree: Includes all drilling fluids with a continuous water phase.

TIME LINE CORRELATION

The electric log markers most frequently used as time lines are bentonite beds because of their distinctive pattern, as shown on Figures 3-8 to 3-10, and their widespread occurrence. In some areas where volcanic activity was restricted to short time intervals, dense basalt flows which usually show a distinctive pattern (Figure 3-29) may be used. Basalts are particularly useful in continental sequences where bentonites might suffer more from differential erosion.

Sedimentary deposits often cross time lines, but there are some blanket type deposits that may be recognized, particularly on gamma ray logs. Glauconitic sands, often associated with rapid transgression following a period of erosion, are quite distinctive particularly in areas where the sediments ordinarily show low radioactivity (Figure 3-13). Thin radioactive shales may be good time markers particularly in pre-tertiary rocks. Potash beds may be correlatable in saline basins (Figure 3-28), and coal beds in continental basins (Figure 3-16).

In some areas easily recognizable necks or shoulders have been observed on both the S.P. and short spacing resistivity curves at formation boundaries and sometimes within a particular formation. The lithologic differences reflected by these distinctive changes in electrical characteristics are not always apparent and may be immaterial provided they check with paleontological data.

ADVERSE PHYSICAL AND CHEMICAL EFFECTS

The following examples (Figure 1-3 to 1-11) show some of the correlation and interpretation problems caused by the drilling fluid and the electrical circuitry. Fortunately, effects as severe as those illustrated are rare in most areas, but geologists should be alert for unusual appearing logs.

Despite quality control checks, poorly calibrated logs and mechanical effects which could have been corrected do slip by occasionally. These effects may be severe enough to hamper correlation as well as quantitative interpretation. All questions regarding log quality should be brought to the attention of an experienced development geologist or a Company log analyst.

S.P. AND WATER SALINITY

The SP log is a good indicator of sands. However, the SP deflection is dependent on the contrast between the mud and formation water salinity and may not always show sands. Other factors such as streaming potential and Ca or Mg ion can affect SP deflection.

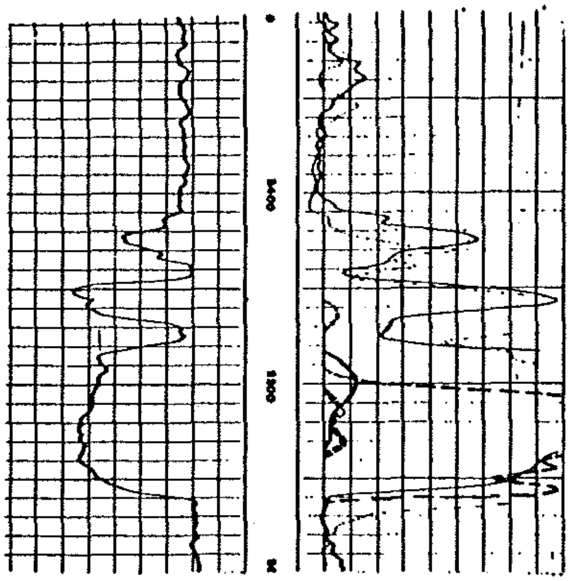

Typical SP deflection when mud is much fresher than formation water.

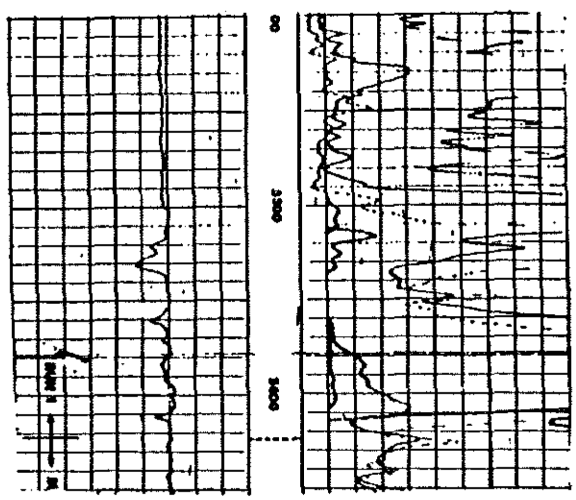

Formation water and mud have approximately the same salinity, resulting in almost no SP deflection. The mud salinity is approximately the same as the upper example; therefore, the formation water is much fresher than above.

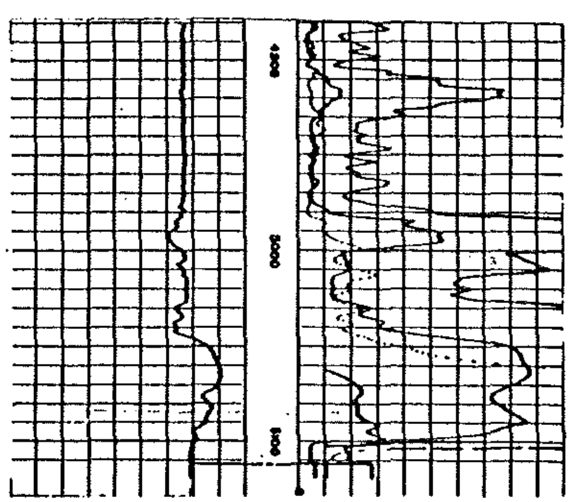

Reversed SP resulting from the formation water being fresher than the mud filtrate.

NORTH PARK BASIN

Figure 1-3

RELATIONSHIP OF MUD TYPE TO IDENTIFICATION AND CORRELATION OF SANDS

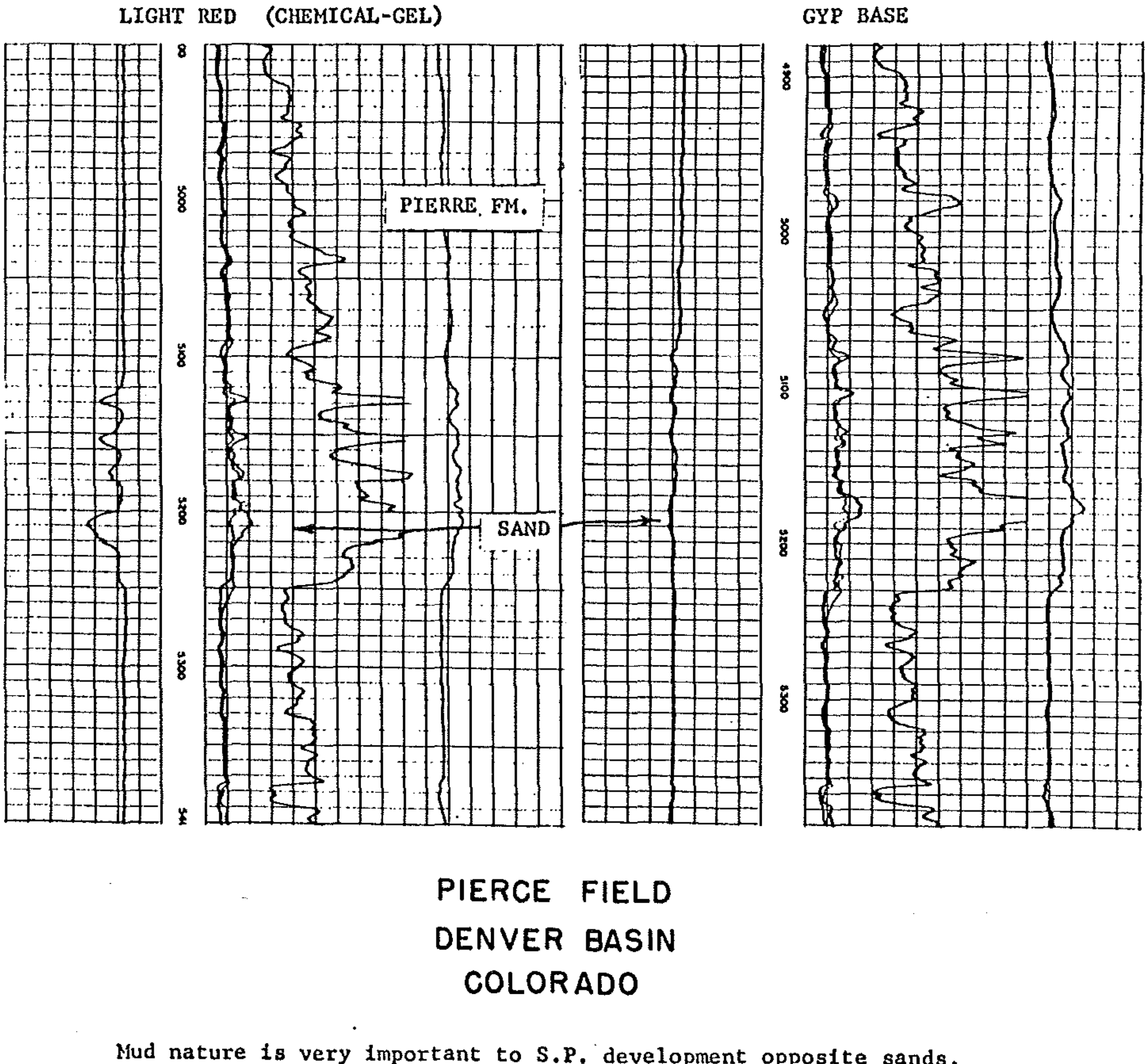

PIERCE FIELD
DENVER BASIN
COLORADO

Mud nature is very important to S.P. development opposite sands. Although low contrast between mud and formation resistivities will result in a log as shown on the right, the depressed S.P. in example on the right is caused by the nature of the Gyp Base drilling fluid. Care must be taken when correlating or making sand counts to account for changes in drilling fluid

Figure 1-4

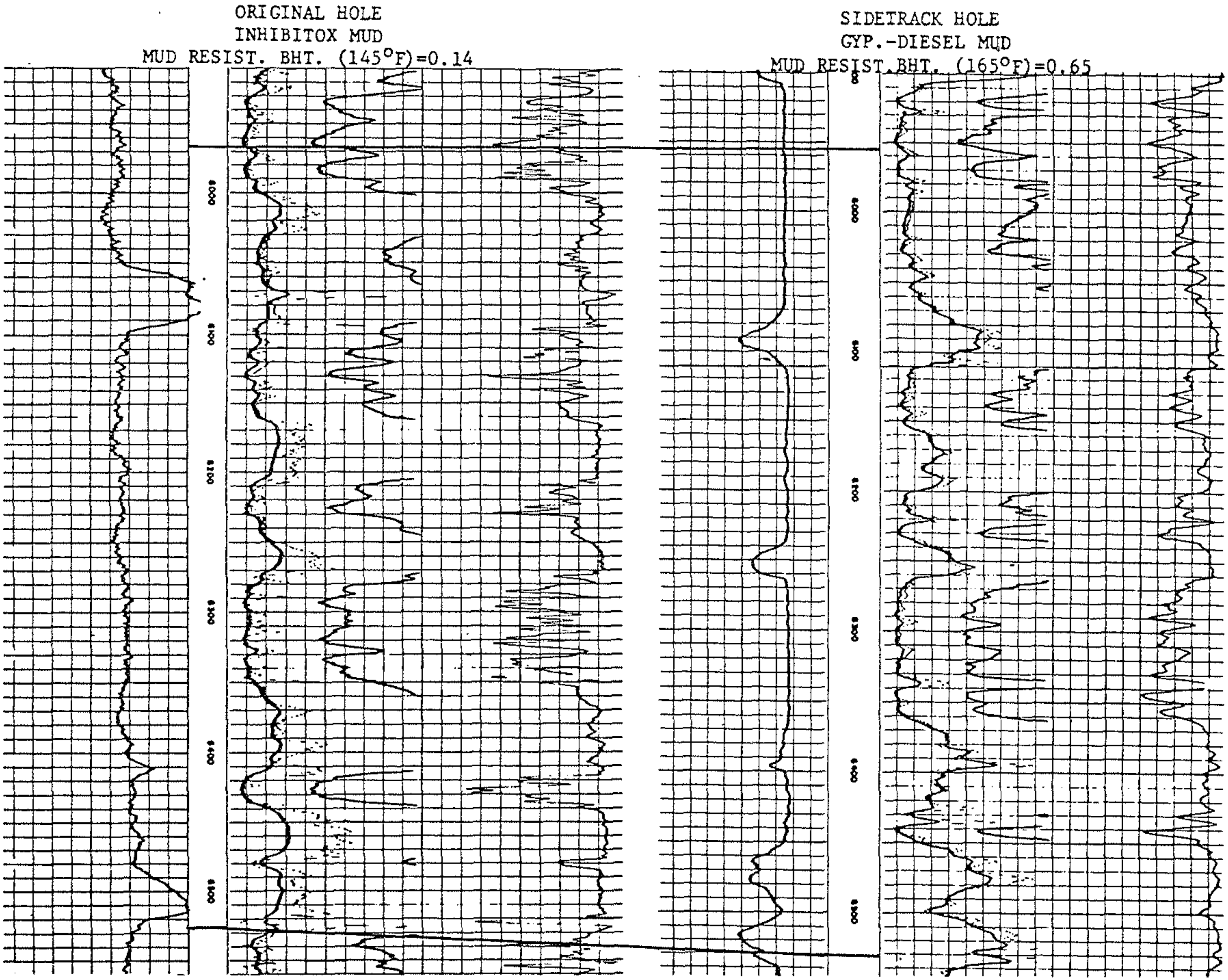

EFFECT OF DRILLING FLUID ON E-LOG CHARACTER

Figure 1-5

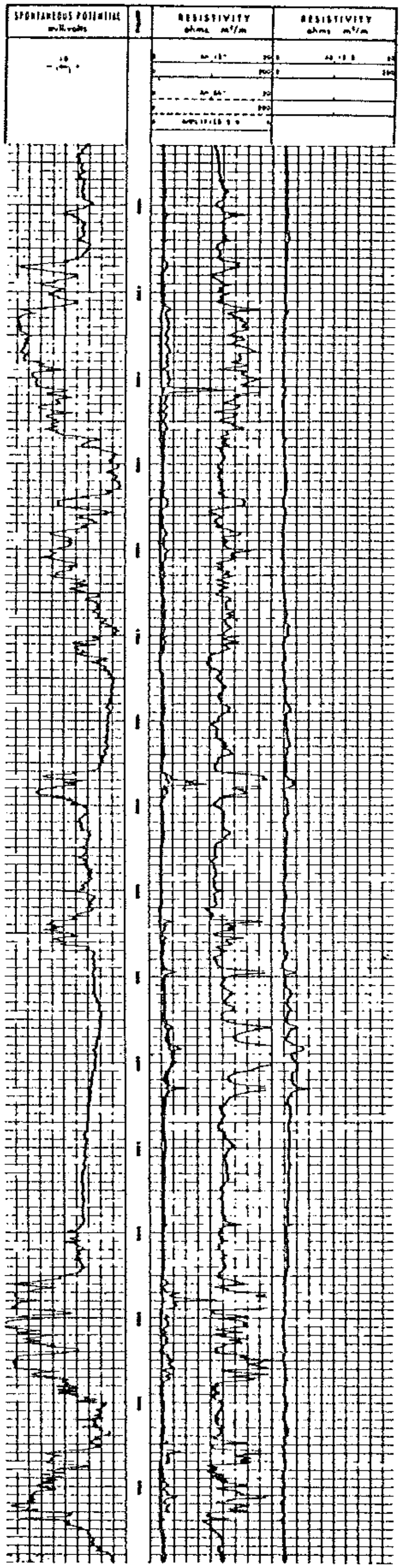

DOWNHOLE GROUND

EFFECT ON THE

S.P. CURVE

The shifting shale base line is caused by a long ground electrode moving with the logging sonde and being affected by the average potential of the 100'-200' interval which it straddles. Downhole grounds are sometimes necessary to avoid adverse surface effects particularly in metropolitan areas. This S.P. curve cannot be interpreted quantitatively, and the curving base line must be carefully considered in qualitative interpretation and correlation.

Figure 1-6

RESITIVITY REVERSAL
FROM CRITICAL BED THICKNESS

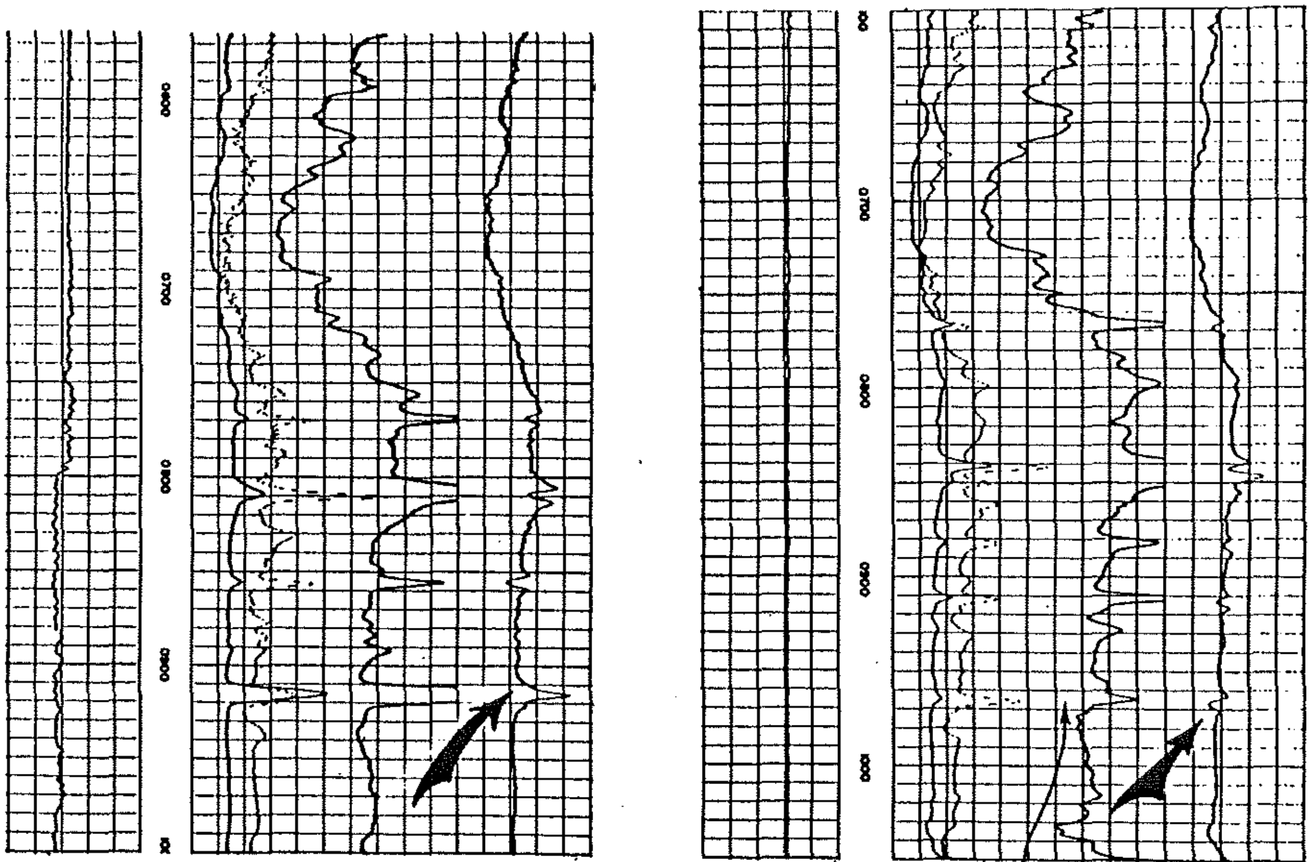

DENVER BASIN
COLORADO

Resistive bed between 16" and 64" thick.

Interval 910-920 feet on log to left shows a resistive bed on all three curves. Log on right side shows a well defined resistive bed only on the lateral curve. The long normal on the right hand log is affected by critical bed thickness and actually shows resistivity reversal. Normal curves always show resistivity reversal in beds of high resistivity when the bed thickness is less than the log spacing. When correlating by normal curve character, the bed thickness should be considered.

Figure 1-7

EFFECT OF WELL-BORE FLUID ON RADIOACTIVITY LOGGING

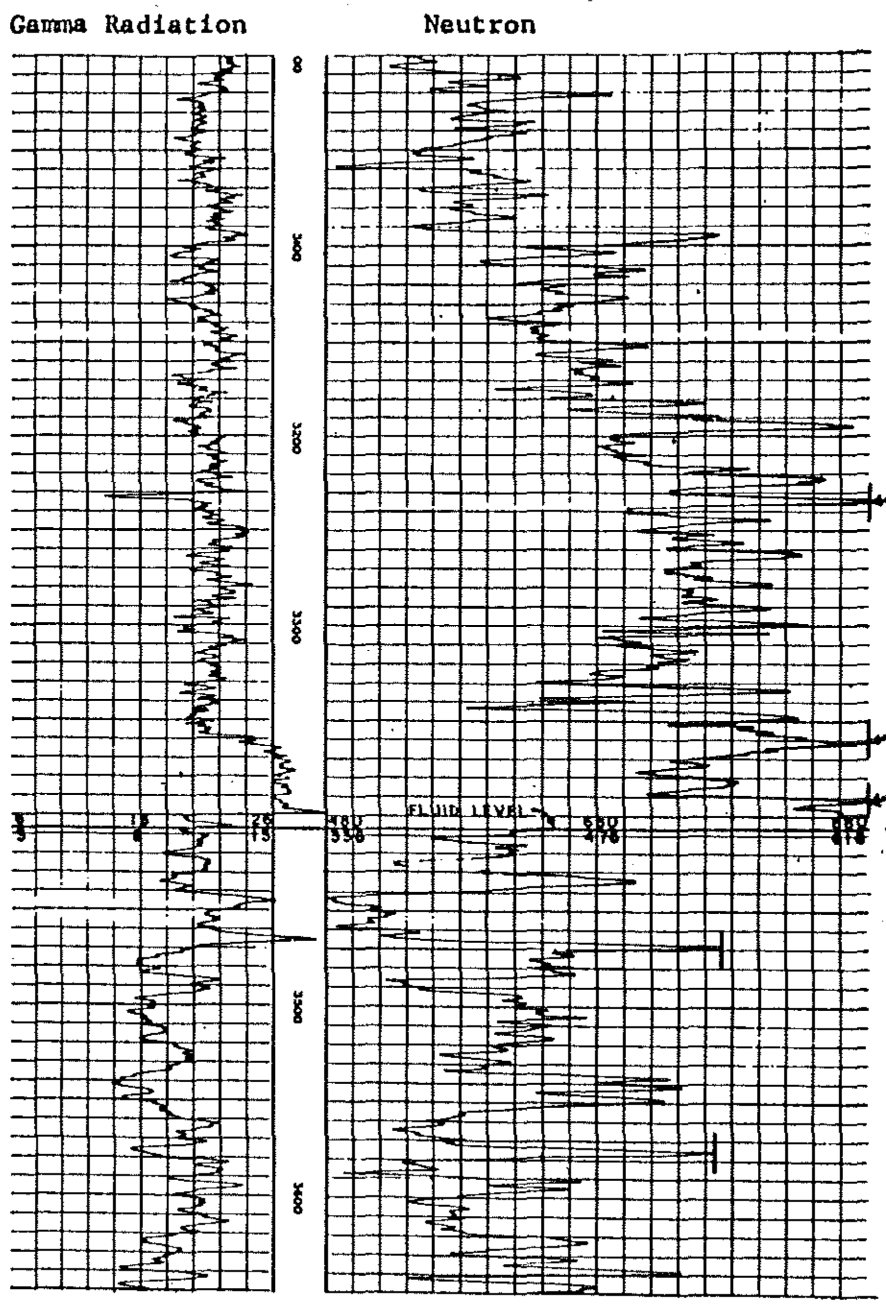

GYPSUM BASIN
COLORADO

Well bore fluid depresses gamma ray and neutron activity. Unmarked fluid levels may resemble formational boundaries.

Figure 1-8

POROSITY INDUCED FROM WASHOUT OF MATRIX

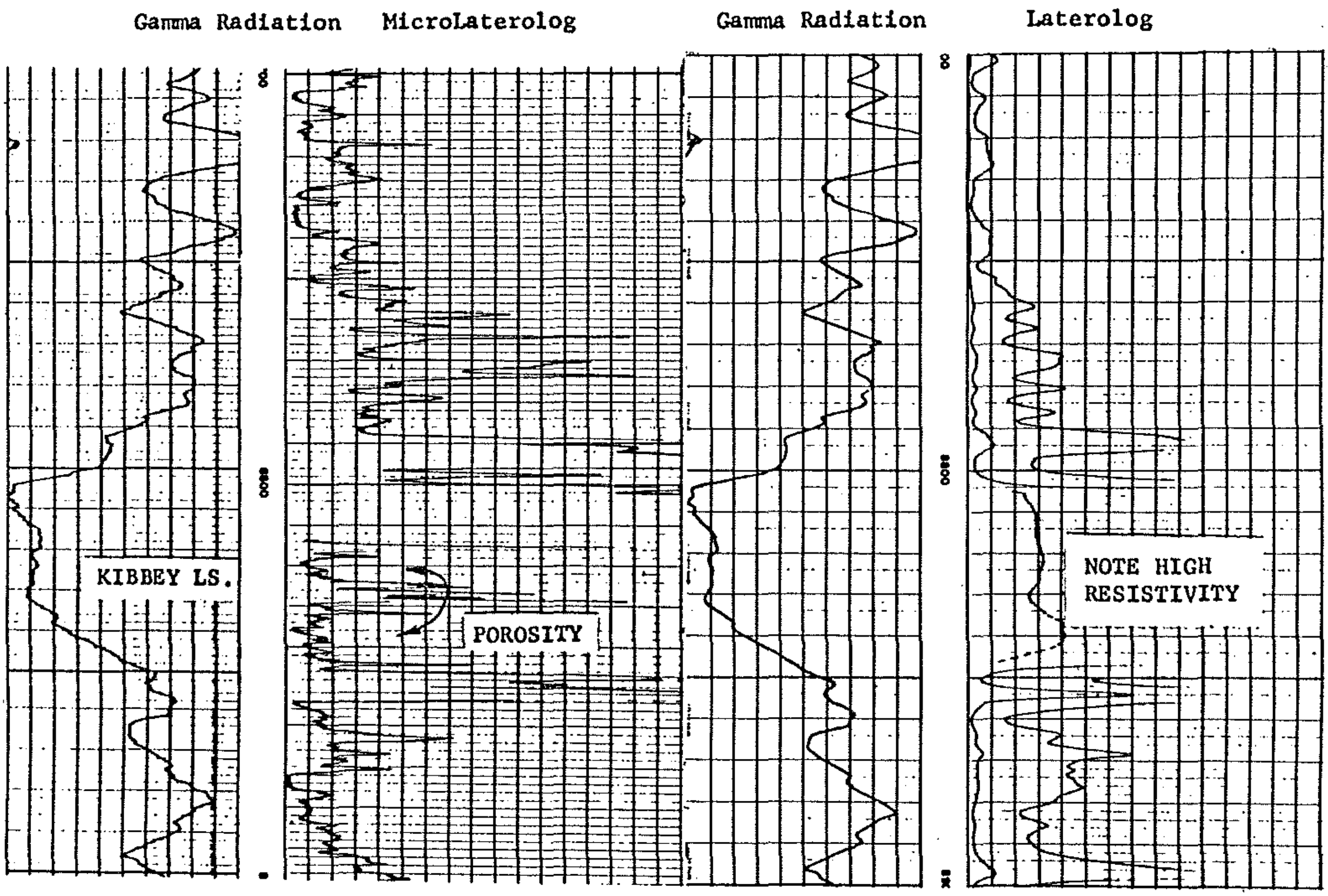

WILLISTON BASIN
NORTH DAKOTA

Porosity as shown by MicroLaterolog has been caused by washout of salt cement from fragmental limestone. The Laterolog with a deeper investigation, reads beyond the washout zone and the high resistivity is indicative of low porosity. This particular circumstance could be easily confused with oil saturation. Sample examination is necessary for interpretation.

Figure 1-9

SEVERE HOLE WASHOUT

IN ABNORMALLY HIGH PRESSURE SAND

IVAN RIVER, ALASKA

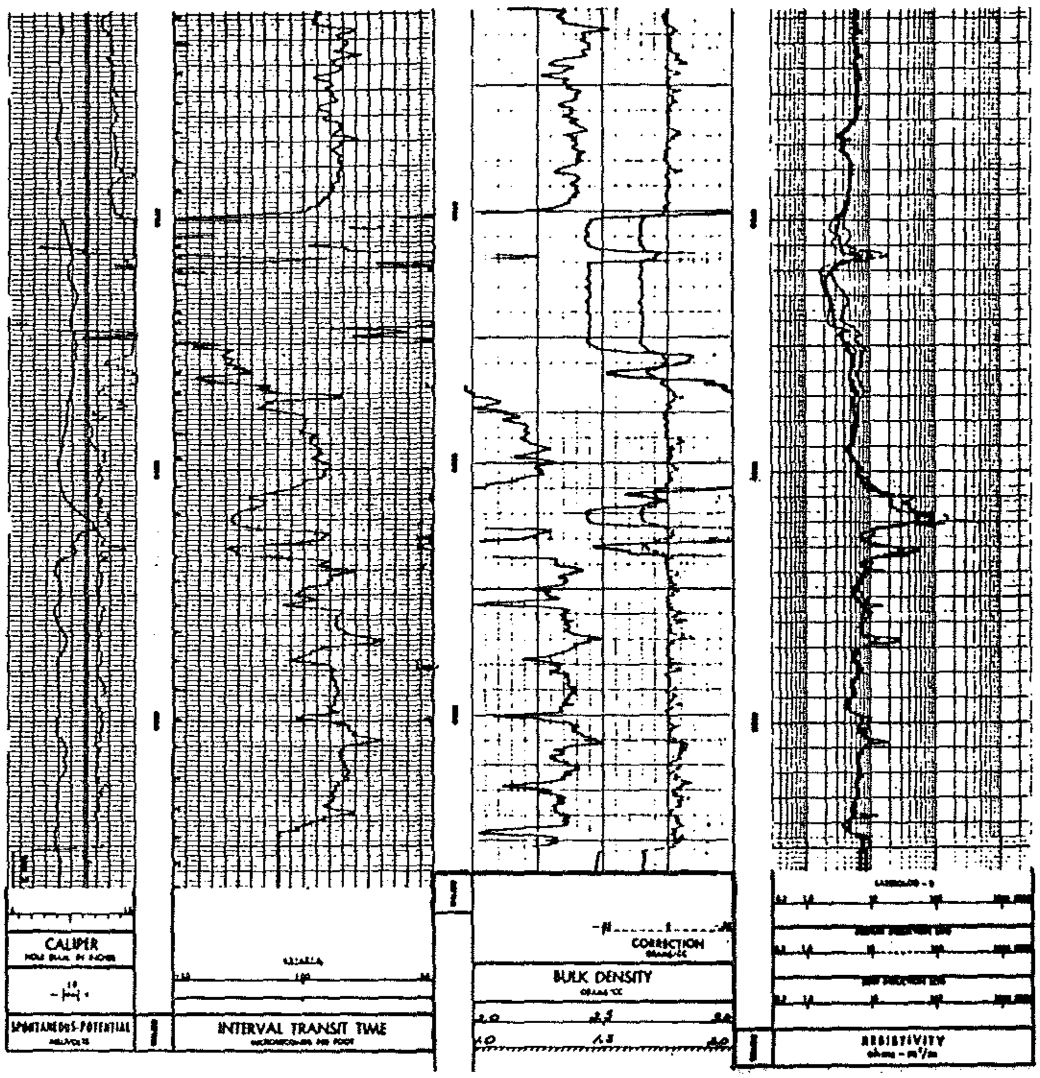

In the interval 8700' - 8750', the S.P. curve is reversed, mud travel time is recorded on the Sonic log, mud density on the density log, and even the deep induction curve is affected primarily by mud resistivity. Fortunately, cavities such as this are rare in permeable sands.

TD: 8760±?

Figure 1-10

HIGH PRESSURE SALT WATER INFLUX

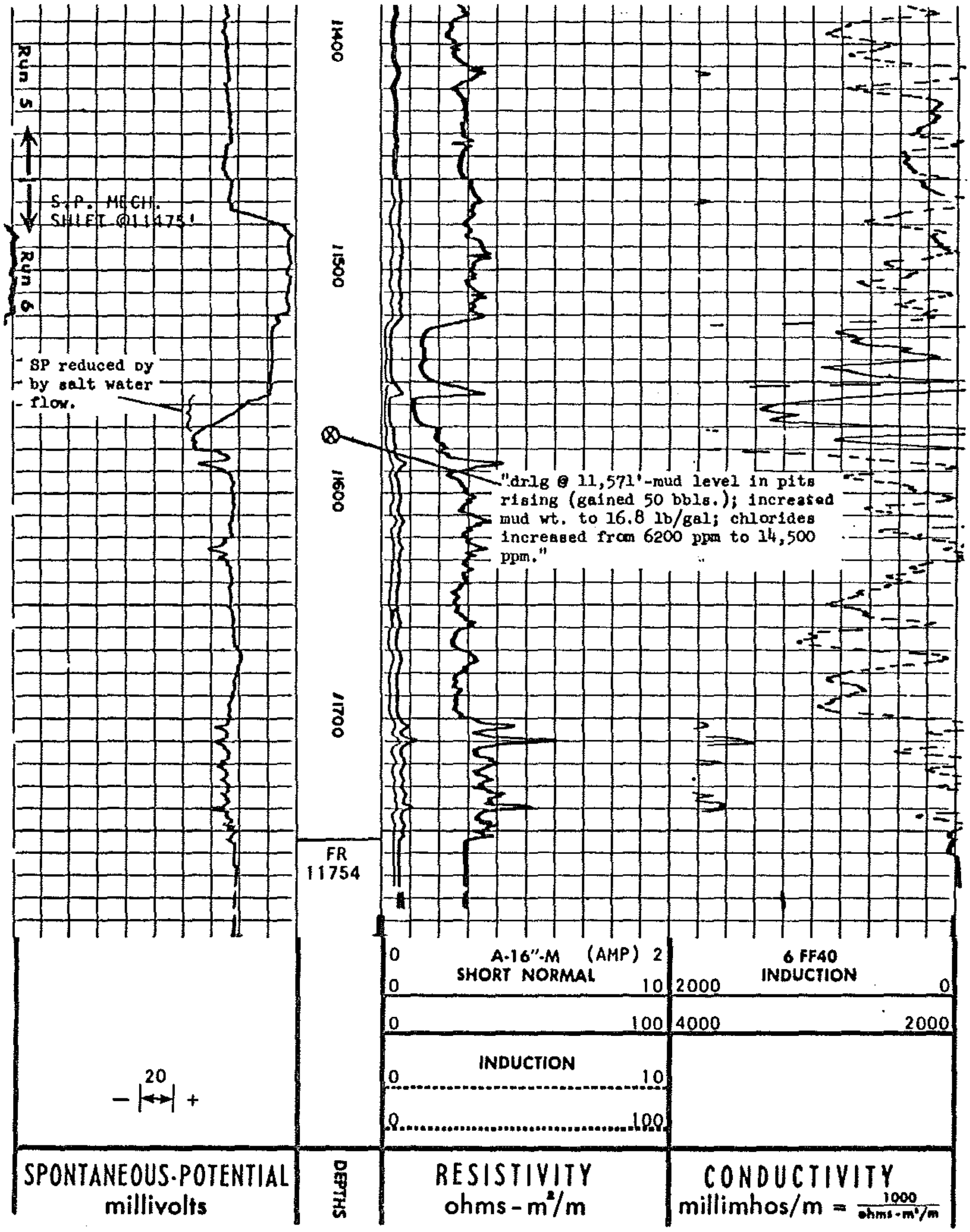

Figure 1-11

LOGARITHMIC VERSUS LINEAR SCALES

The re-introduction of logarithmic scales by Schlumberger in 1962 caused some consternation among geologists unfamiliar with that type of format. The older generation will remember that Schlumberger recorded resistivity curves on a logarithmic scale in the middle thirties, but that was a non-focused two curve system and there was no particular advantage to the logarithmic scale except for greater detail in low resistivity intervals. This detail was later restored on the linear scale with the expanded normal curve.

The Dual Induction-Laterolog 8 Survey (DIL) provides, in a single surveying operation, three focused resistivity measurements and an S.P. curve. It was designed to determine depth of invasion and provide a good value of true resistivity where the deep induction curve was affected by invasion. The logarithmic scale was chosen primarily to facilitate the quantitative evaluation of invasion from the ratios of the resistivity values recorded by the three curves. On this scale, the horizontal separation between any two curves is the ratio of the resistivity values.

Contrary to early experience with non-focused systems, the logarithmic scale now improves the readability of a three-curve focused system. It provides greater detail in the low resistivity range and eliminates confusing offscale traces and scale changes. All resistivity curves are on the same scale and the expanded and ten times scales are eliminated.

Detailed correlation is facilitated by the logarithmic scale, particularly between wells where the resistivity contrast is large, as shown on Figure 1-12. Two of the logs are linear recordings of 16" normal and lLd induction curves; the other two are logarithmic records of the LL8 and lLd curves. Major features are readily correlated between any two of the four logs. Furthermore, the few minor features that are apparent on the 16" normal curve are readily correlated with the LL8 recordings. However, as is frequently the case, the normal curves are quite rounded and afford little detail for precise correlations, particularly when the hole diameter is large and/or there is a high contrast between formation and mud resistivities. The LL8 curves provide a much sharper bed delineation and more detailed information.

COMPARISON OF CORRELATIONS - LOGARITHMIC SCALE OF LL8-ILD VS LINEAR SCALE OF 16 IN. NORMAL-ILD

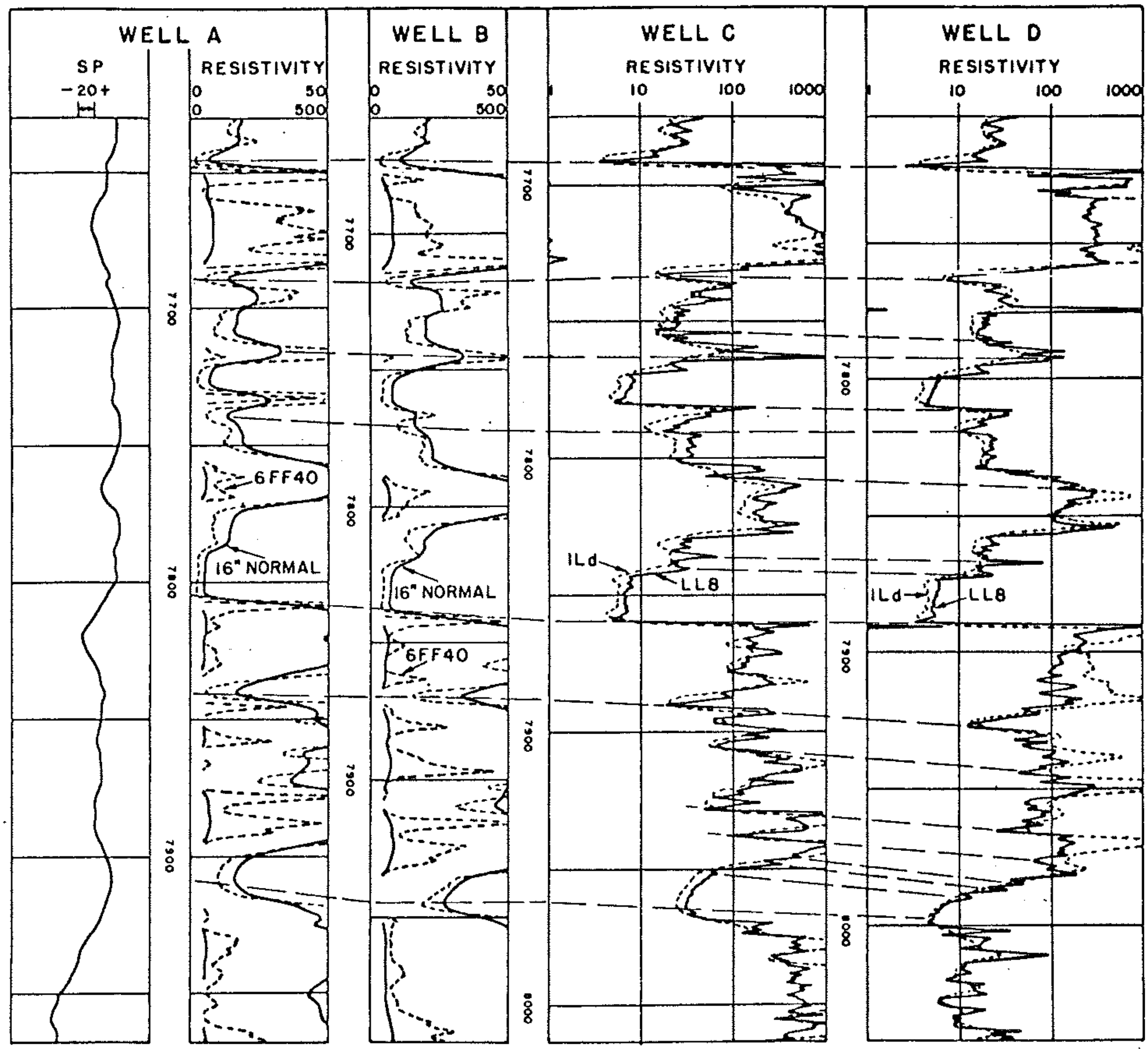

Figure 1-12

PART 2

INTERPRETATION OF DEPOSITIONAL ENVIRONMENT FROM LOGS

The accompanying examples are excellent illustrations of the four electric log patterns described by Mr. Nadler. However, before using such patterns, particularly in a new area, the following points should be considered:

First, the S.P. curve on the electric log should be used exclusively, as was done by Mr. Nadler, as the resistivity curves are more affected by formation fluid. Also, finely interbedded sands and shales may approximate the appearance of both transgressive and regressive environments on three-electrode resistivity logs because of masking and false resistivity effects.

Second, the type of mud used in the hole and the relation of its salinity to that of the formation water should be checked. Lime-treated mud is particularly detrimental to the S.P. log causing erratic behavior in many cases, and in fresh water areas, the S.P. curve is considerably dampened and may even be reversed if the salinity of the mud is greater than that of the formation water. (See Figures 1-3 to 1-5). In such cases, the gamma ray curve may be substituted for the S.P. curve provided that the natural radioactivity is primarily a function of clay or shale content.

Third, the relationship between the S.P. curve and sand permeability is not always as clear-cut as might be implied from the examples shown. Siliceous shales, like those of the upper Miocene in California, often show electric log patterns similar to those shown by channel sands. (See Figure 3-5). This is partly a result of fracturing and partly the high concentration of silica, as compared with clay minerals, in the cherty or diatomaceous beds.

Fourth, electrical disturbances (both natural and man-made) may cause erratic behavior of the S.P. curve. A scratched electrode effect, ordinarily caused by pulling through a tight spot in the hole, may look very much like a transgressive sand pattern, and drift of the S.P. curve, if not properly evaluated, may also cause an erroneous interpretation.

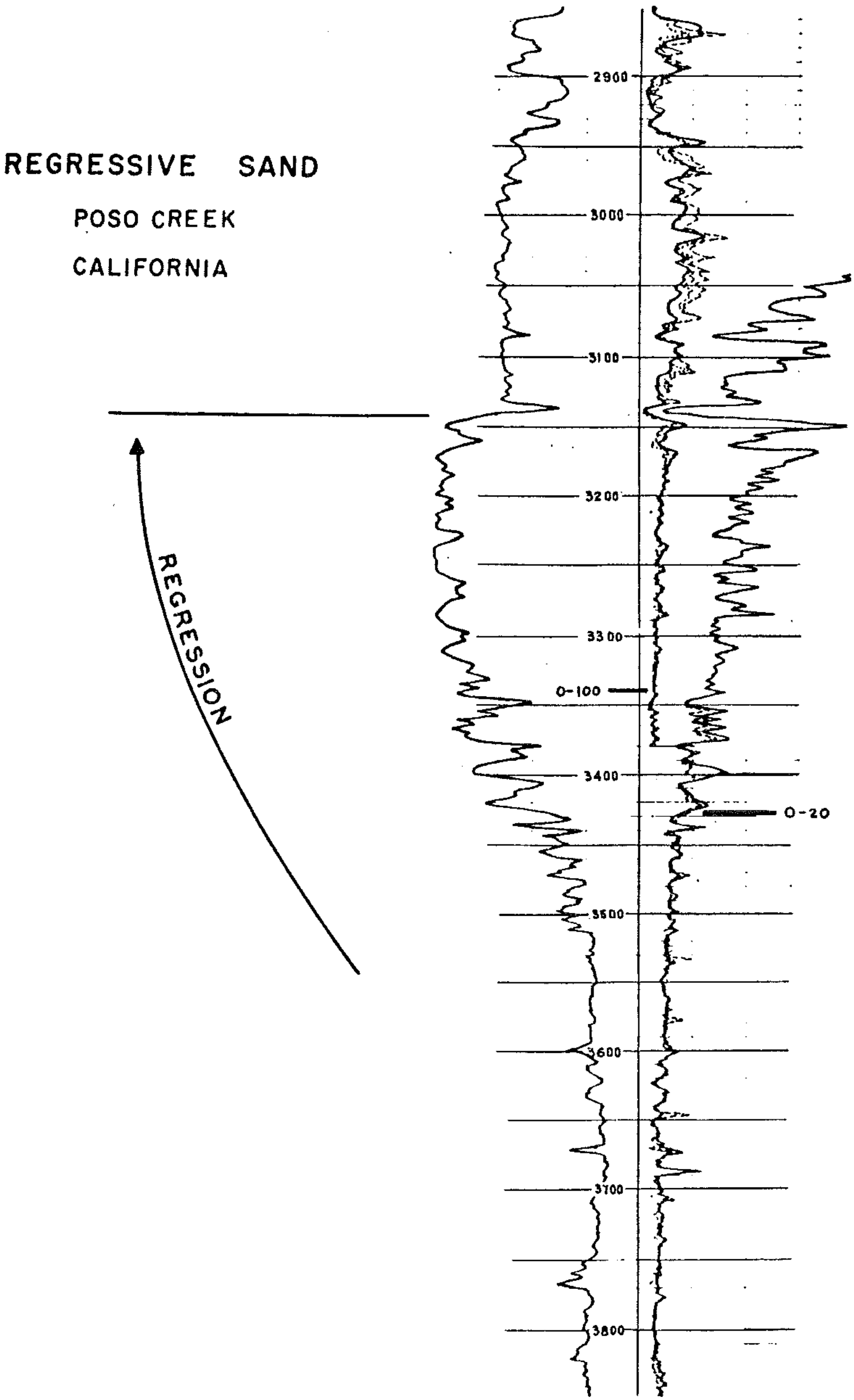

Figure 2-1

LITHOLOGY FROM LOGS
STRUCTURAL INTERPRETATION FROM LOGS
HYDRODYNAMICS AND ABNORMAL PRESSURE EFFECTS

SANDSTONE

CYCLIC REGRESSIVE SANDSTONES OF THE CRETACEOUS FRONTIER FM OF CENTRAL WYOMING

WERTZ FIELD, WYOMING

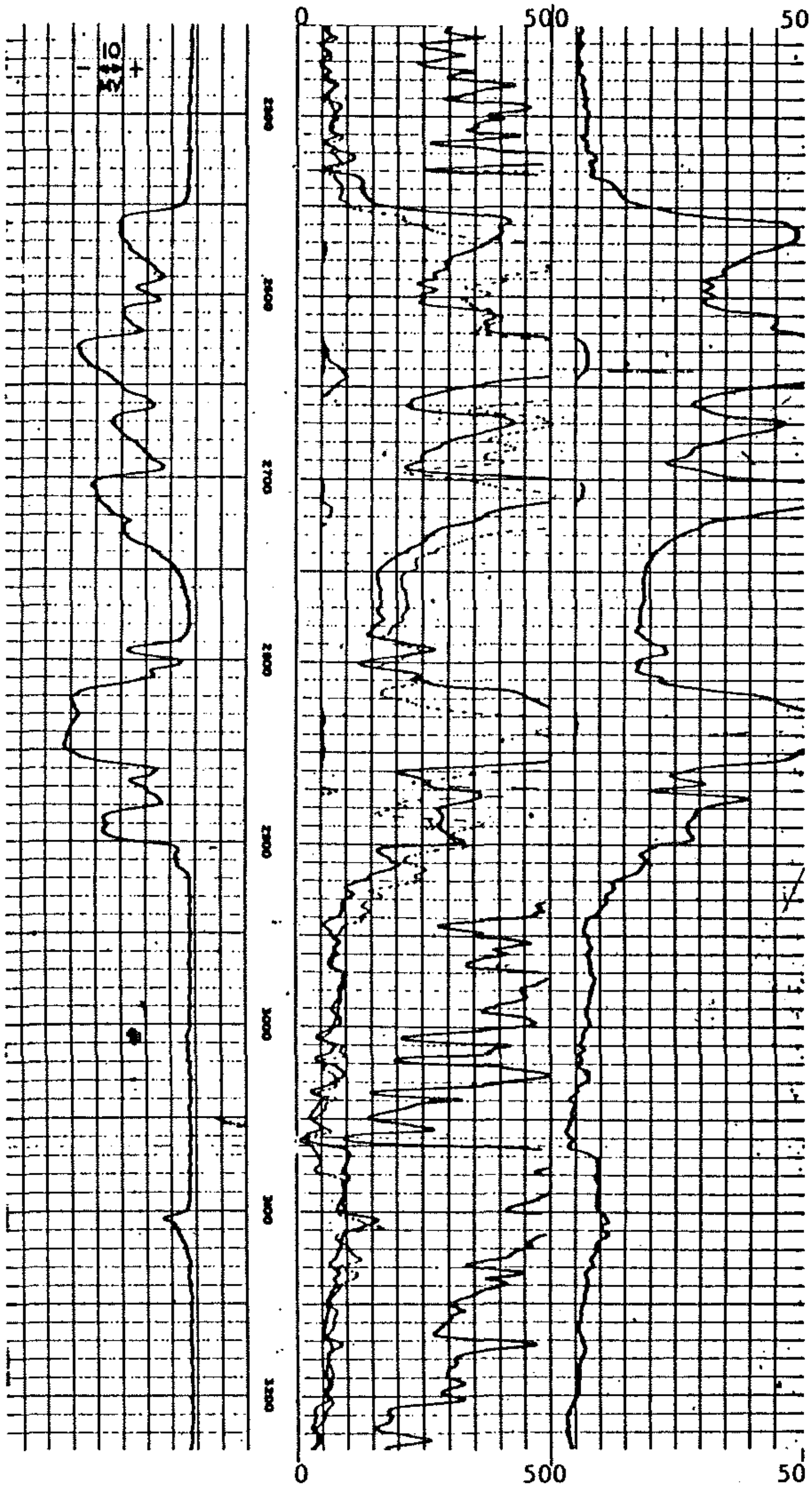

Figure 2-2

TRANSGRESSIVE SAND

CASTAIC FIELD
CALIFORNIA

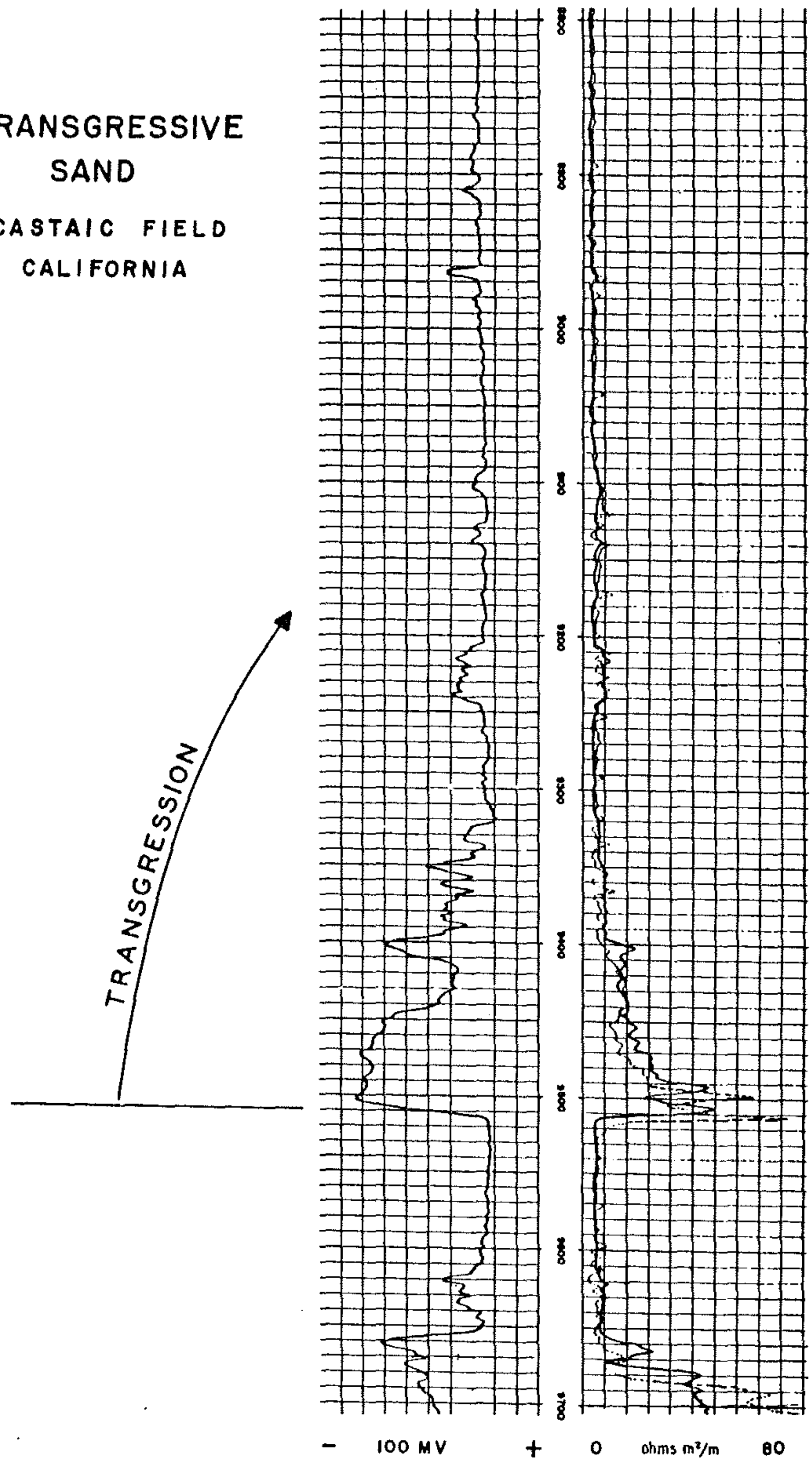

Figure 2-3

OFFSHORE BAR

COALINGA NOSE
CALIFORNIA

Note Uniform Character
Of S.P. Curve.

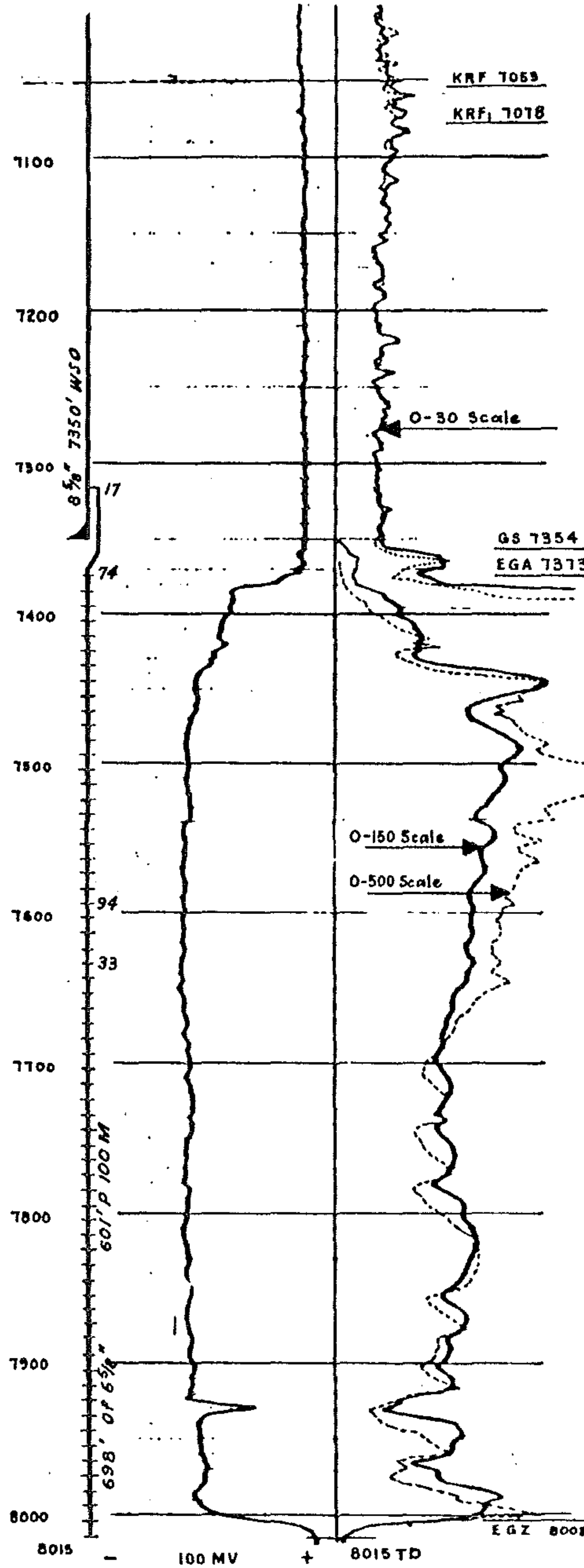

Figure 2-4

BAR SAND

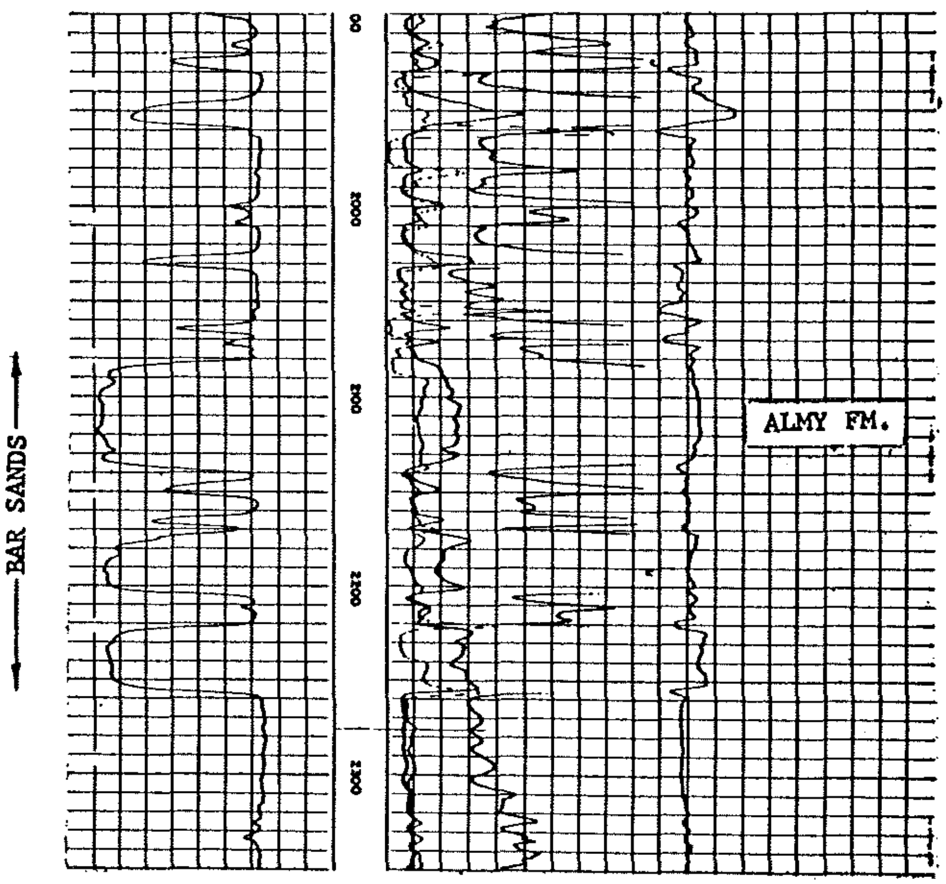

GREEN RIVER BASIN
WYOMING

Bar sands are characterized by the lack of thin shale interbeds, massive sand character and blocky S.P. shape.

Figure 2-5

CHANNEL SAND

ELK HILLS

CALIFORNIA

Coarse, Gritty Sand Interbedded With Fine Sand And Brown Shale.

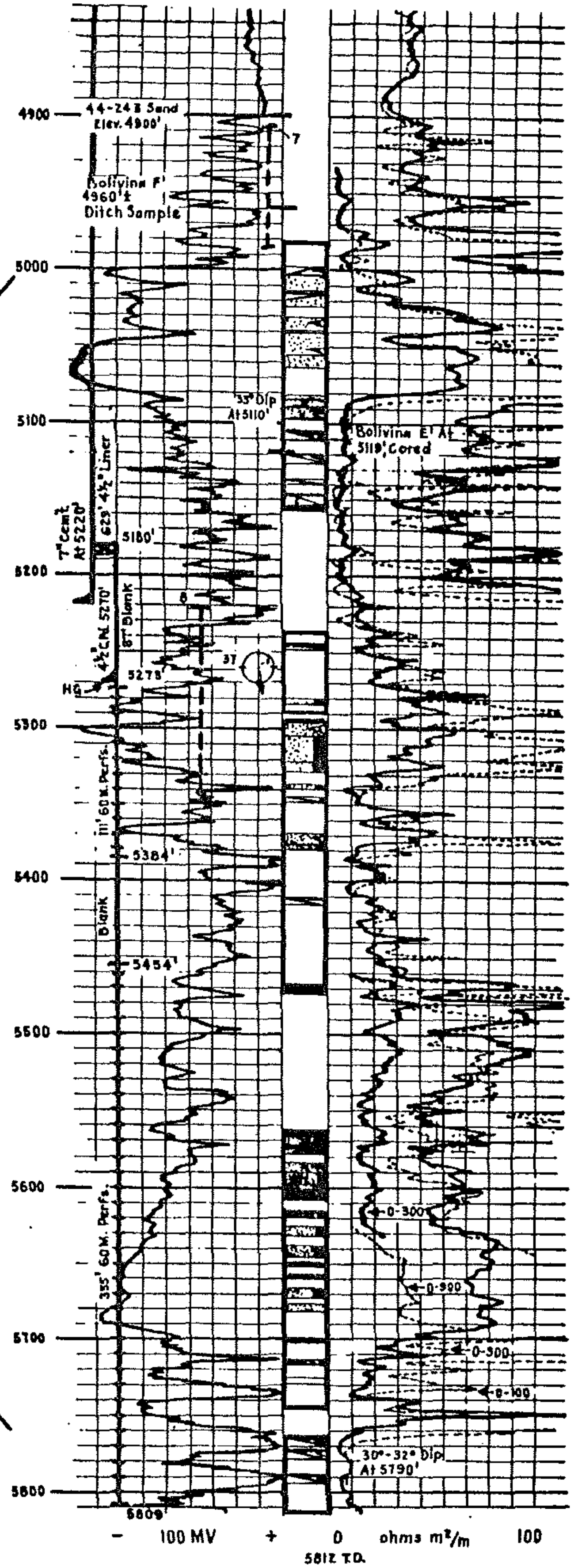

Figure 2-6

CHANNEL SANDS

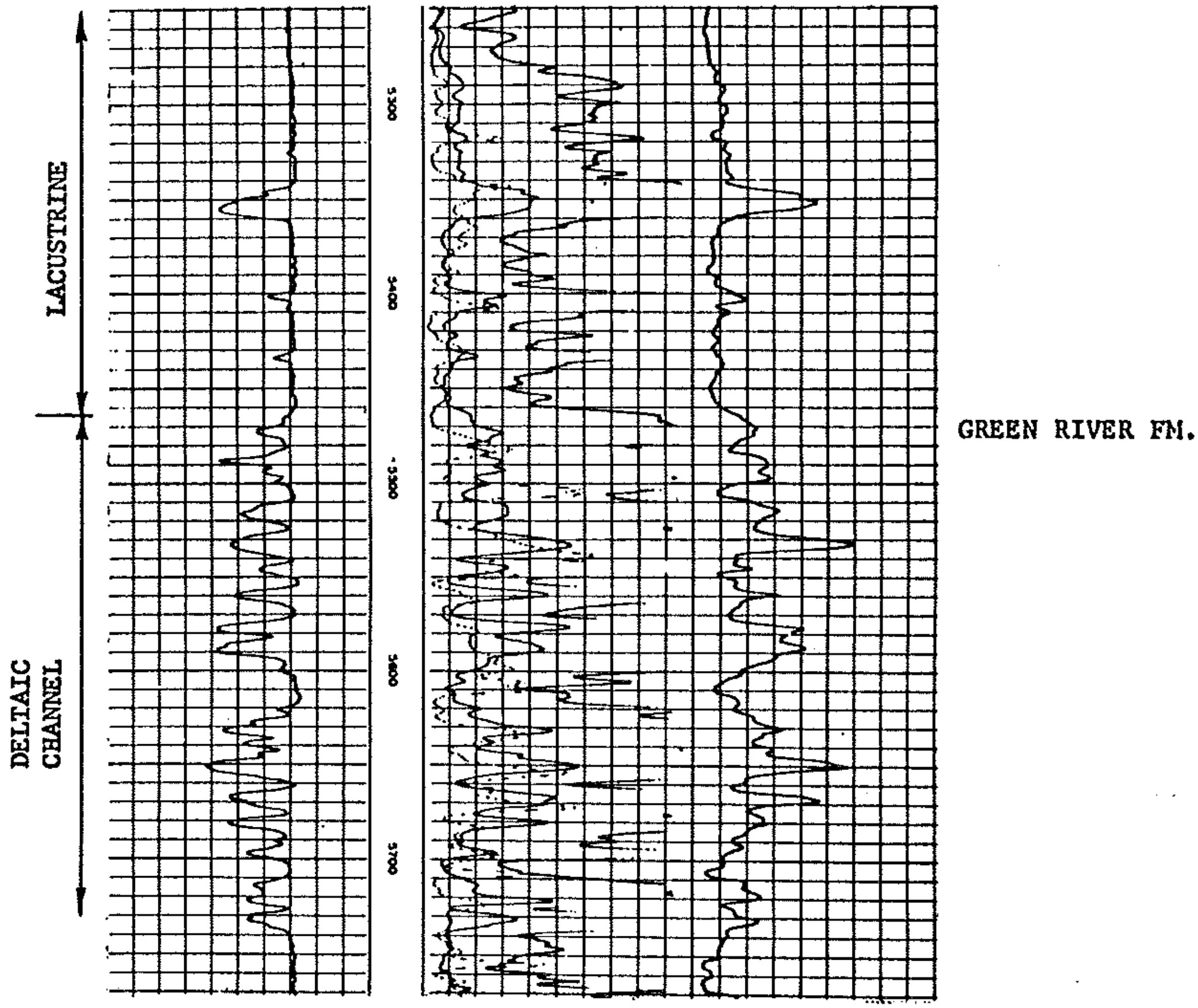

RED WASH FIELD
UINTA BASIN
UTAH

The channel sand environment cannot be conclusively identified from electric logs. The thin sand beds reflecting frequent depositional variation are well shown by electric logs. However, such a pattern characterizes not only channel environments but others as well. Lithologic descriptions of the sands and associated beds plus detailed mapping must support identification here.

Figure 2-7

LAGOONAL DEPOSITIONAL PATTERN

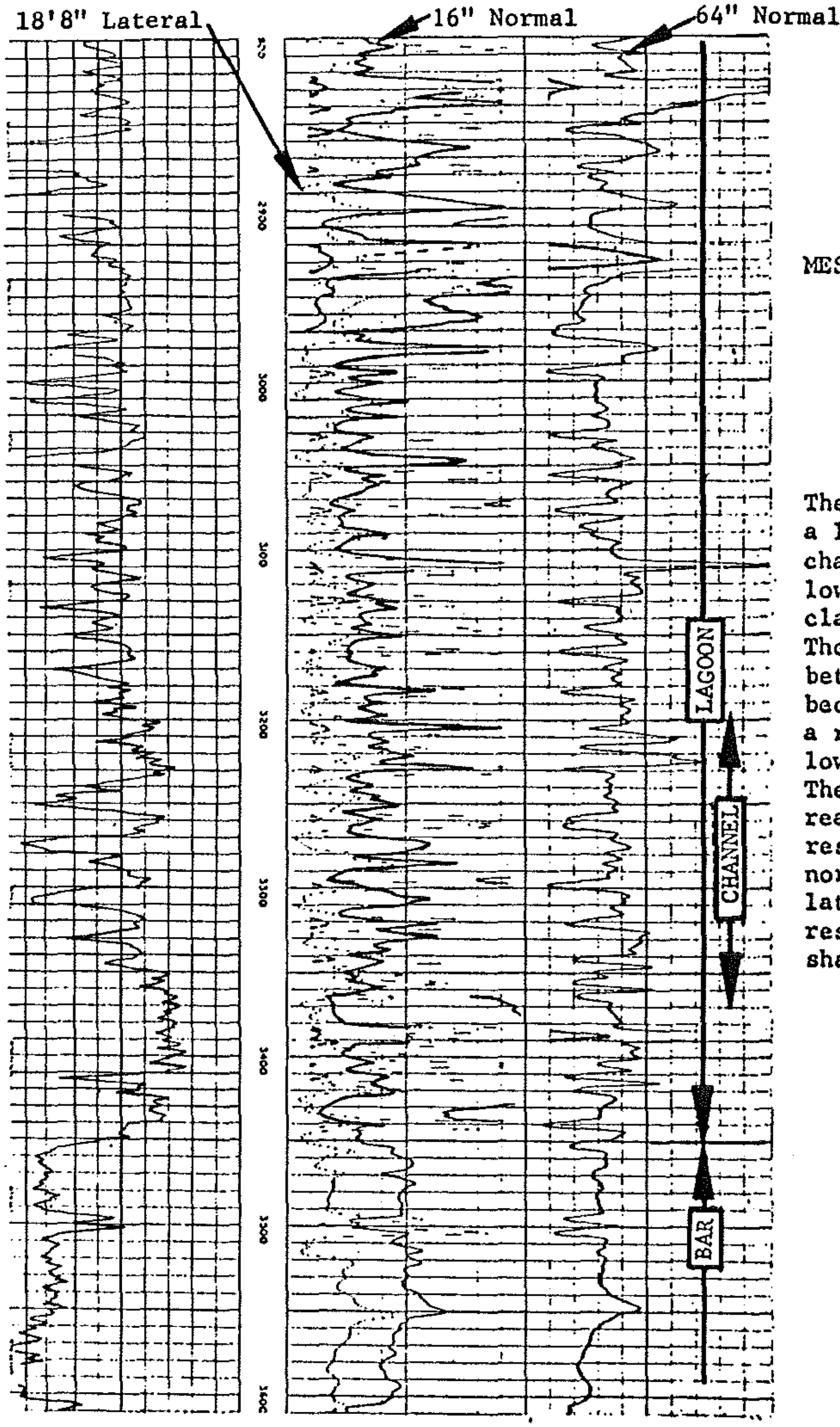

MESAVERDE FORMATION

The sedimentation pattern of a lagoonal environment is characterized by relatively low percentage of coarser clastics, thin beds and coals. The resistivity contrast between thin coal or siltstone beds and shale or sand causes a rapidly alternating high to low resistivity character. The thin resistive beds may reach critical thickness for resistivity reversal in the normal curves, however, the lateral curves reflect the resistive beds except in the shadow zones.

GREEN RIVER BASIN
WYOMING

Figure 2-8

CONTINENTAL CYCLES

Cyclical deposition can sometimes be recognized in continental fresh or brackish water sediments. Figure 2-9 is an example from the west side of the Cook Inlet in Alaska where the Tertiary topography was probably similar to that of today, but the climate was warmer.

The log example shows two cycles which began with the dumping of coarse sand and gravel into coastal marshes at or near sea level. These flood deposits were followed by finer sediments and periods of little or no sedimentation during which thick peat deposits accumulated. The peat has since been converted to soft, lignitic coal beds by burial and compaction.

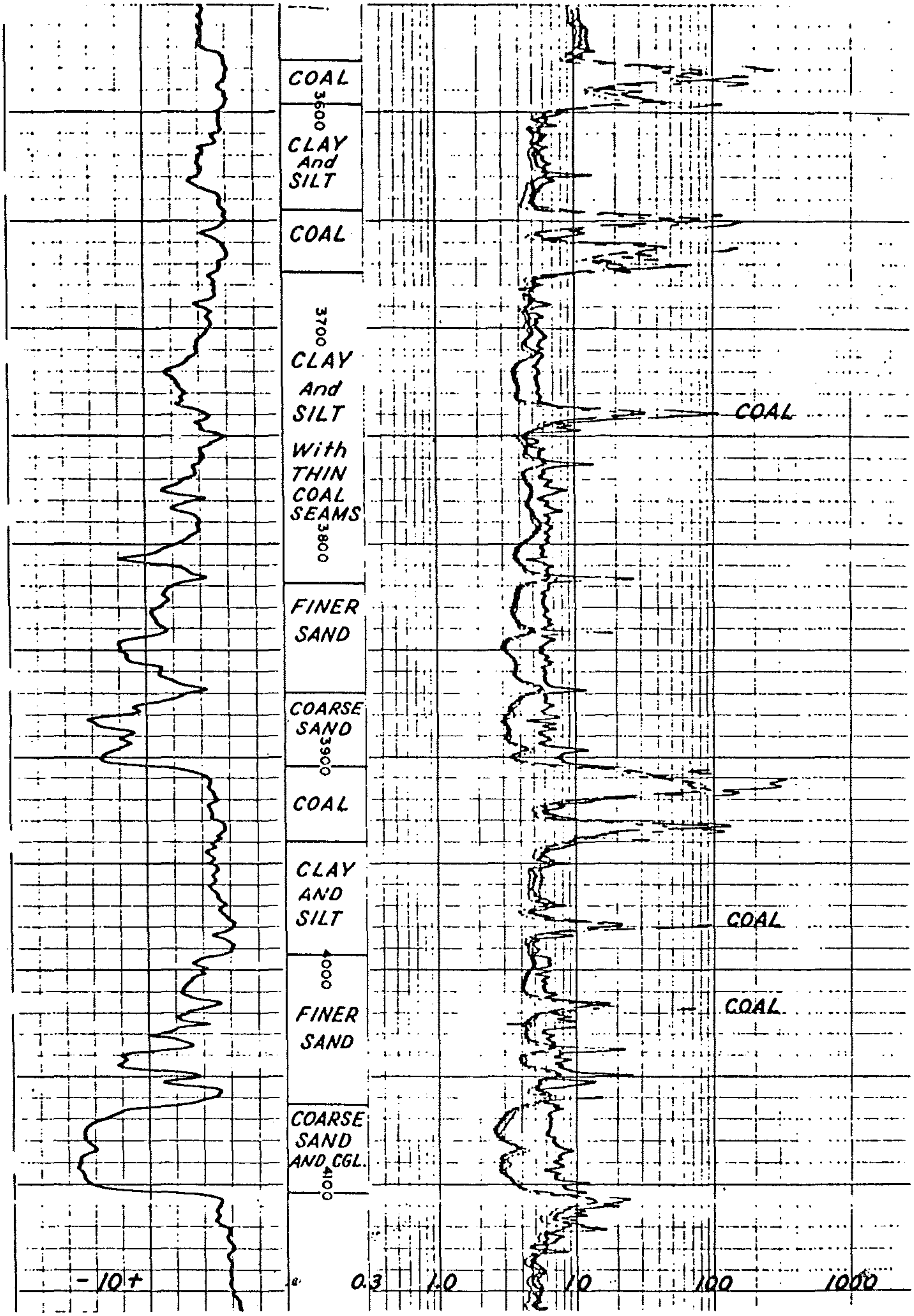
COAL
3600
CLAY And SILT
COAL
3700
CLAY And SILT With THIN COAL SEAMS
3800
FINER SAND
COARSE SAND
3900
COAL
CLAY AND SILT
4000
FINER SAND
COARSE SAND AND CGL.
4100
COAL
COAL
COAL
- 10 +
0.3
1.0
10
100
1000

Figure 2-9

TYPE OF CLAY IN CLAYEY SANDS

The type of interstitial material in sands can often be used to interpret the depositional environment because it is indicative of the source of the sediments. Figure 2-10 shows a continuous sand and conglomerate section with a sharp break in electrical properties and permeability at 12,154'. The only apparent difference from visual examination of the cores was a slight change from gray to white in the pore fillings, but the x-ray spectrograph identified montmorillonite and chlorite in the upper sands and kaolinite and clay-size white mica in the lower. The former identifies a volcanic source whereas the latter is indicative of plutonic rocks.

The "b" factor is proportional to the cation exchange capacity and therefore the surface conductivity of the interstitial material. A "b" factor greater than -0.2 will cause a rock to react like a shale electrically. For further detail on electrical properties of clayey sands refer to C.R.C. Research Report 781 by A. E. Worthington, dated November 9, 1962.

The presence of swelling clays in the upper sands is also indicated by the micro-caliper curve on Figure 2-10. Permeable sands normally stay to gauge because of the protective mud cake whereas impermeable sands are subject to physical and chemical erosion by the drilling fluid.

Another example of sands with electrical properties similar to shale is shown on Figure 2-11. The sands above 2120' are relatively clean, reworked marine sands whereas the lower sands are plugged with montmorillonite clays indicating a continental volcanic source. In this area, the tight, clayey sands are easily distinguished in cores by their characteristic green or brown coloring.

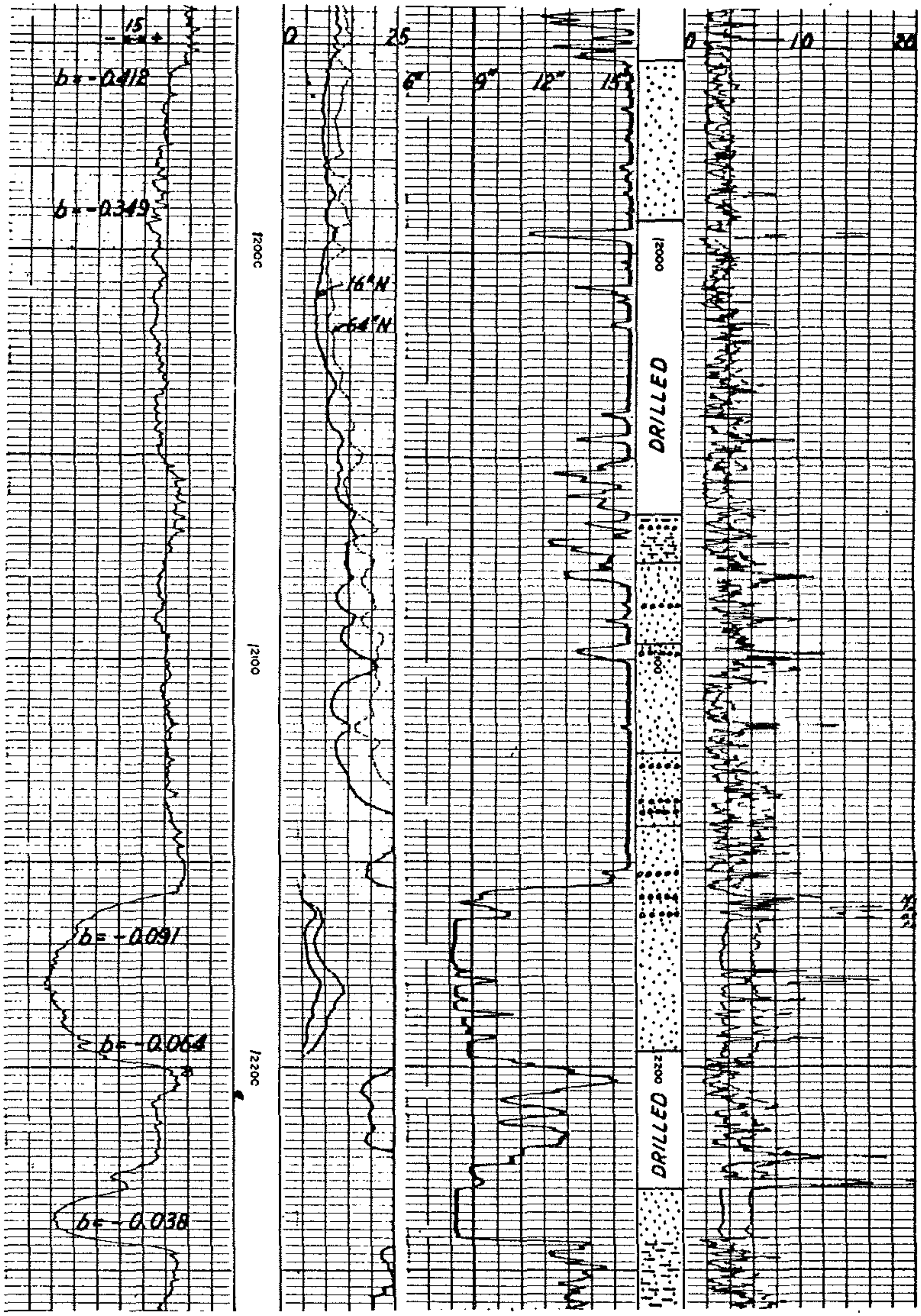
15
b = -0.412
b = -0.349
b = -0.091
b = -0.064
b = -0.038
0
25
16"N
64"N
6"
9"
12"
15"
1200C
1210C
1220C
DRILLED
DRILLED
0
10
20

Figure 2-10

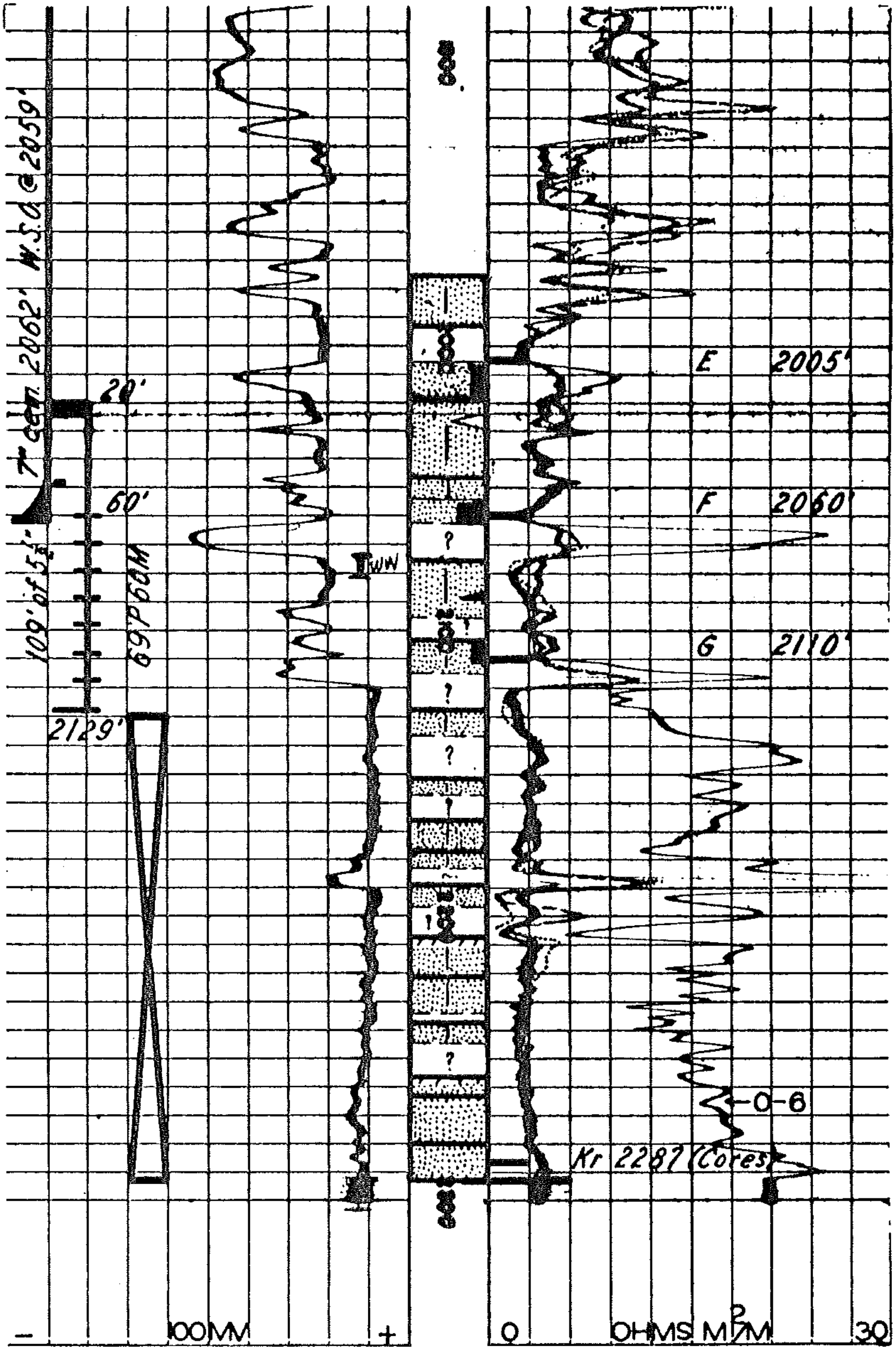

7" cem. 2062' W.S.O.@2059'
20'
60'
109' of 5½"
69P60M
2129'
WW
E
2005'
F
2060'
G
2110'
0-6
Kr 2287 (Cores)
-
100MV
+
0
OHMS M²/M
30

Figure 2-11

SANDSTONE

STREAM CHANNEL CUT AND FILL OF THE CRETACEOUS MUDDY ("GRIEVE") SANDSTONE IN THE WIND RIVER BASIN, WYOMING

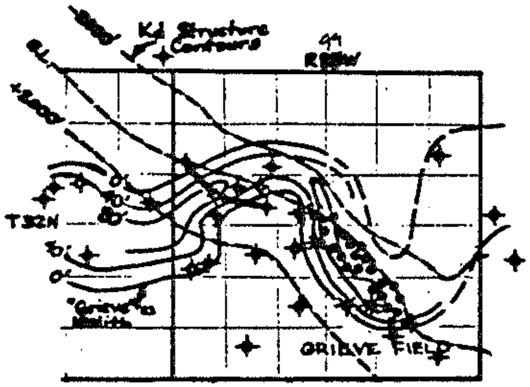

This is a good example of cut into a pre-existing marine shale and silt interval followed by ss fill. This appears to be stream channel deposition on a nearly flat, slightly emergent surface. The width of the channel is less than 2 miles at the line of the cross section. This sand produces from an upstructure meander in the Grieve field. That this is not a marine bar sand may be readily seen from the marine shale and silt found on both sides of the sand development, with widespread silt "markers" found in every well in which the Grieve sandstone is absent. Differential compaction of the shale-sand interval is readily apparent.

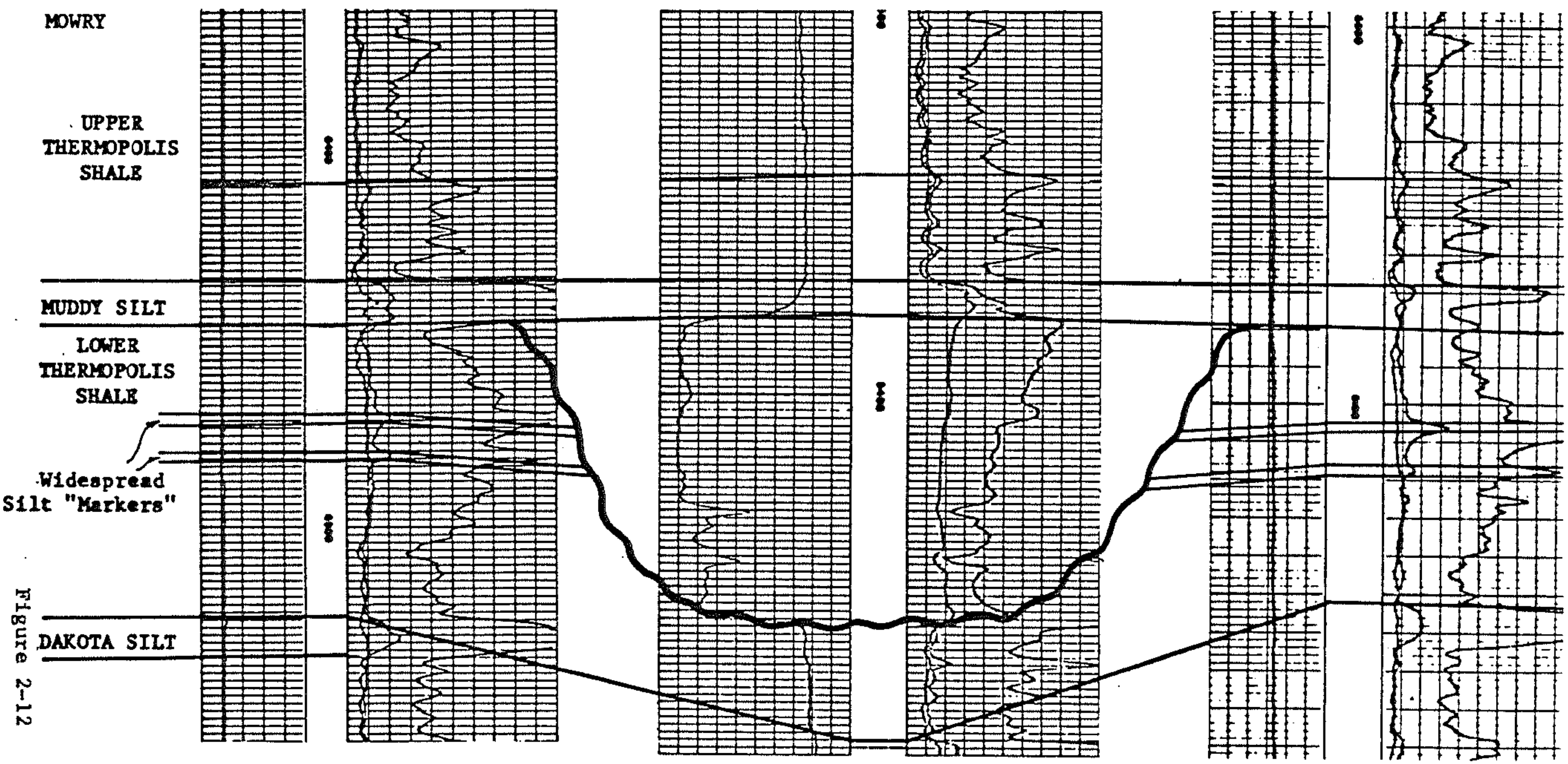

Figure 2-12

SALT SOLUTION AND SAND INFILL

POWDER RIVER BASIN, WYOMING

Campbell County (Pleasant Valley Field)

Detailed log correlations reveal anomalous stratigraphic and structural conditions created by differential solution of salt, and compensating thickening of overlying beds. The time of collapse is dated by the compensating thickening in the part salt beds. In this example, the bulk of the Goose Egg salt was removed from the left well post-Morrison, with the resulting collapse low being infilled with lower Lakota sand. These two wells are 80 acres apart.

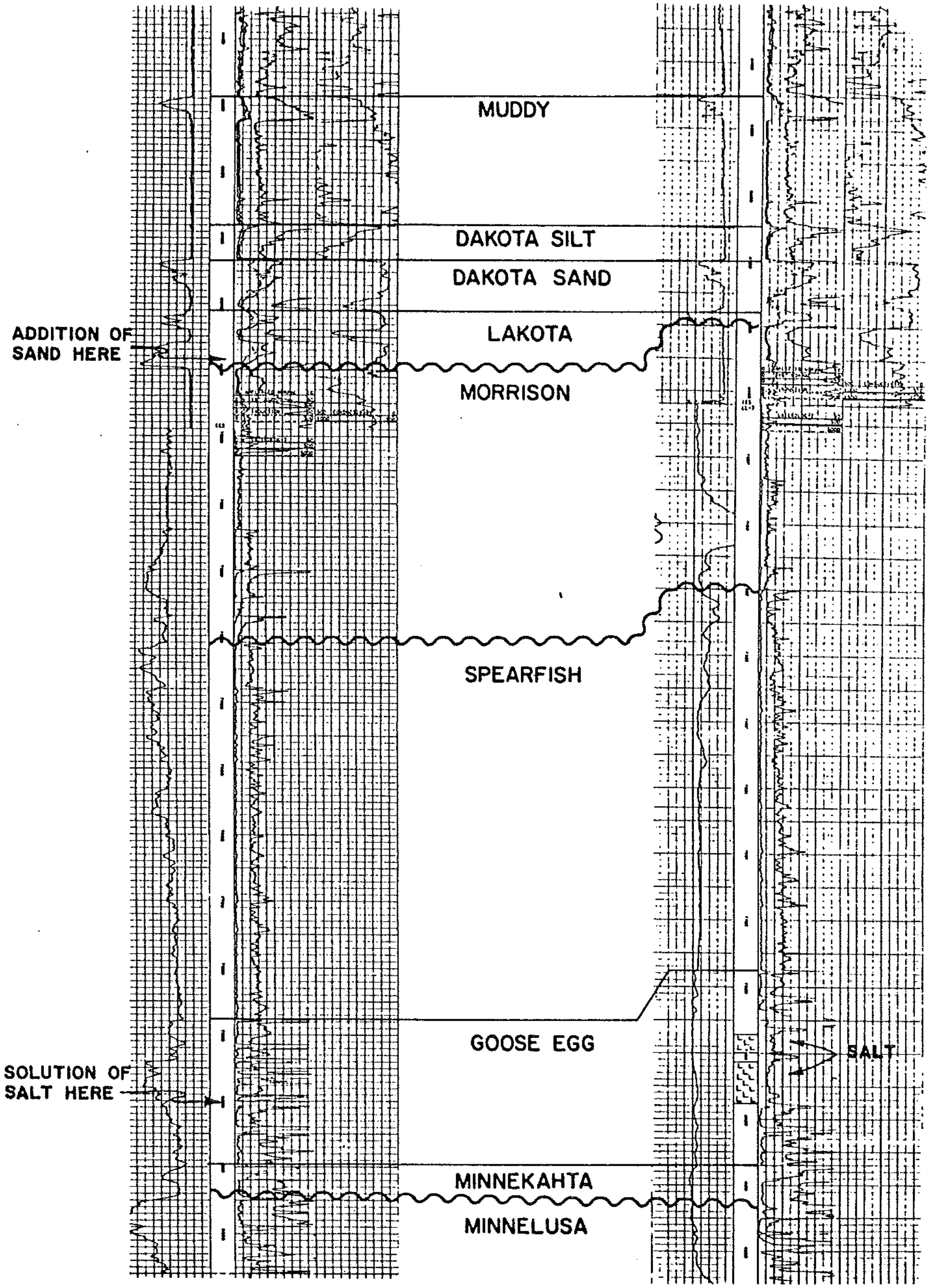
MUDDY
DAKOTA SILT
DAKOTA SAND
ADDITION OF SAND HERE
LAKOTA
MORRISON
SPEARFISH
GOOSE EGG
SOLUTION OF SALT HERE
SALT
MINNEKAHTA
MINNELUSA

Figure 2-13

CARBONATE PATTERNS

A carbonate section is characteristically highly resistive as compared with a sand-shale section, and because of the high resistivity, which causes a high potential drop in the formations with respect to the bore hole, the S.P. curve is sluggish or rounded in appearance and formation discontinuities are poorly defined.

Porous intervals in carbonates are recognized by abrupt decreases in resistivity opposite intervals on the S.P. curve which are convex in the negative direction. If the S.P. curve is concave in the negative direction, the interval is shaley. For the recognition of thin porous intervals, wall resistivity, induction, and focused resistivity logs used with the S.P. or gamma ray curve have been highly successful. For quantitative evaluation of porosity the neutron, Sonic, or density log is used with the gamma ray curve.

Radioactivity logs are preferred for detailed correlation in most carbonate areas. These are supplemented by focused electric logs and continuous velocity logs like the Schlumberger Sonic Log.

CARBONATE
ROCKS

SOUTHEASTERN
IDAHO

NOTE SLUGGISH
S.P. CURVE AND
HIGH RESISTIVITIES.

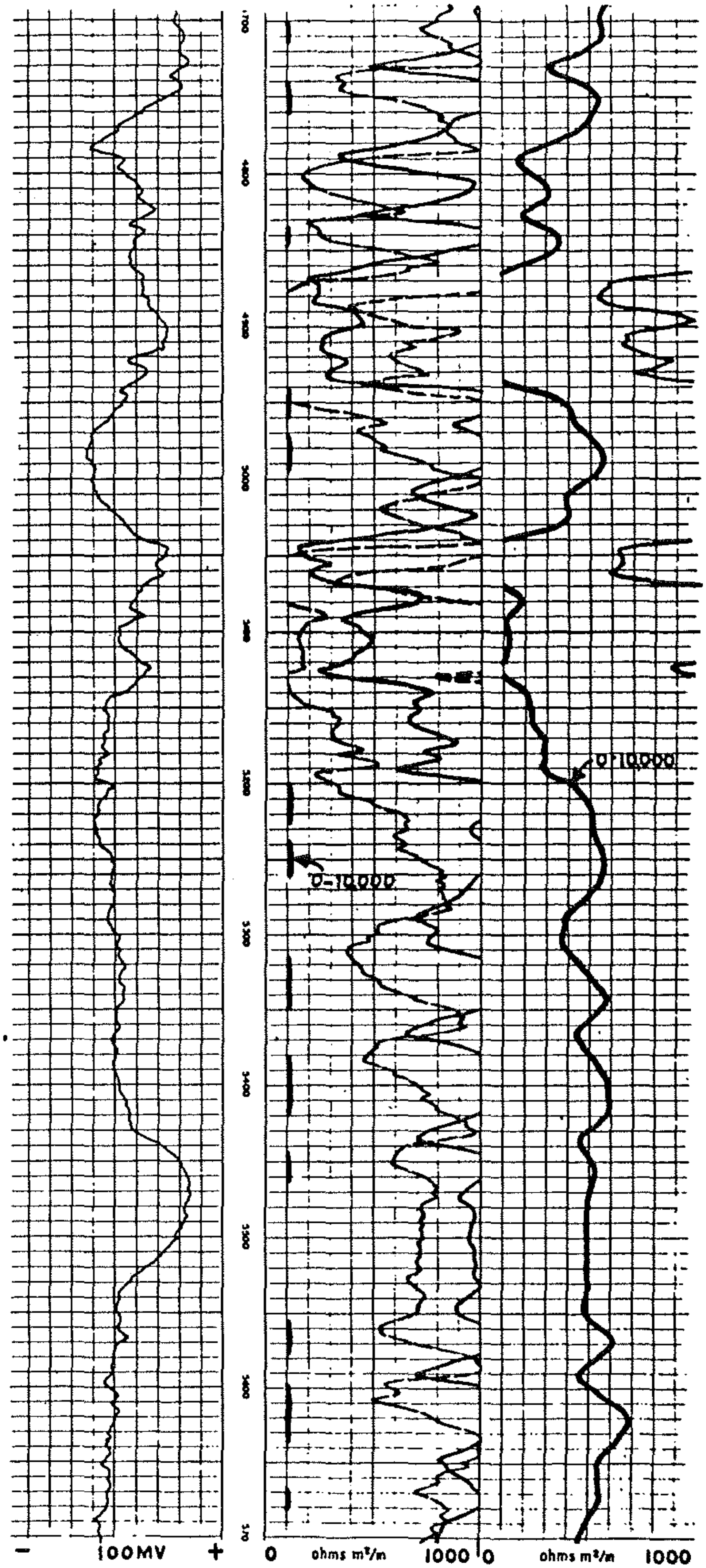

Figure 2-14

RECOGNITION OF DEPOSITIONAL ENVIRONMENTS IN CARBONATES

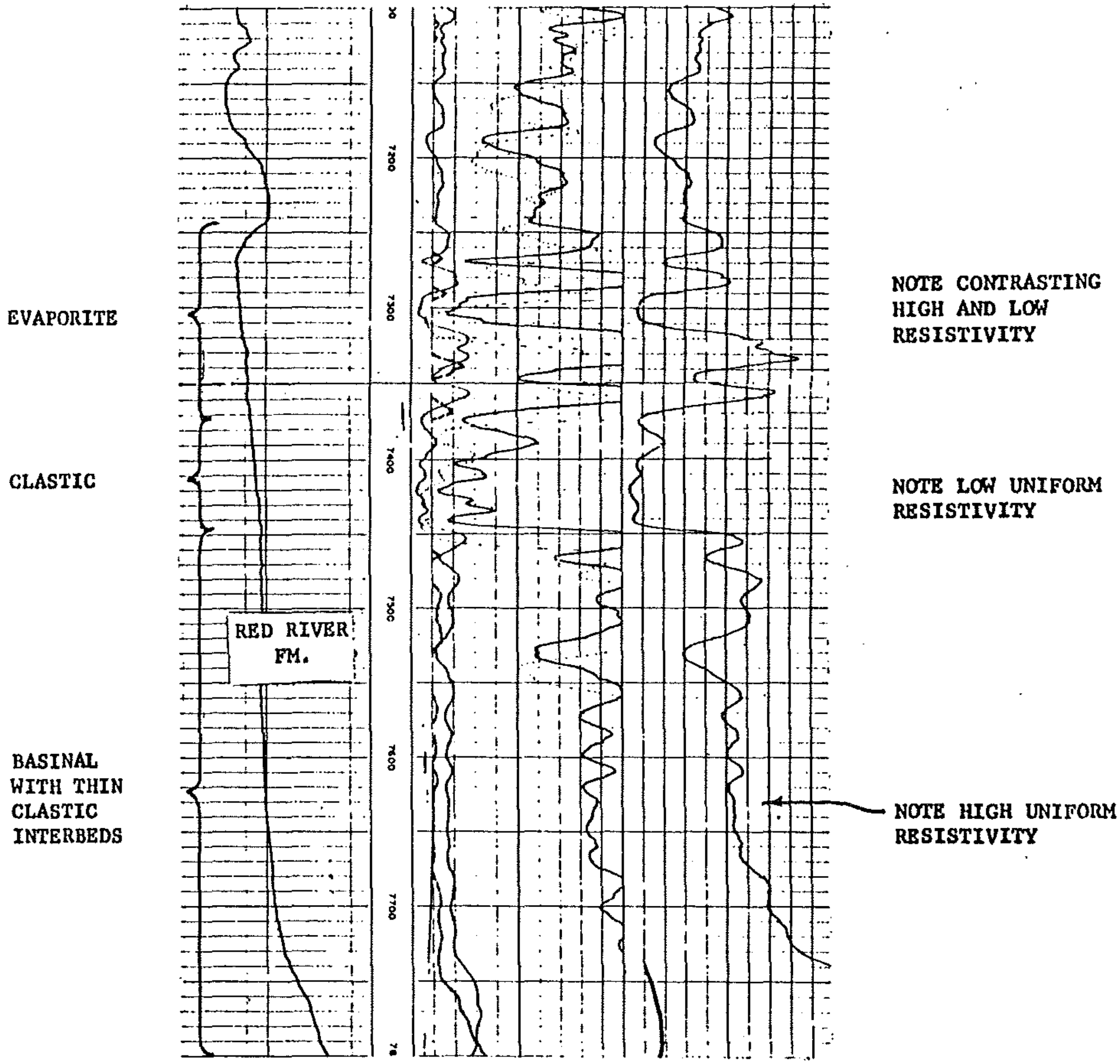

WILLISTON BASIN
NORTH DAKOTA

Three broad carbonate depositional environments can sometimes be recognized by electric logs. The evaporite association is characterized by alternation of very high and low resistivity. The clastic phase may have low resistivity if the porosity is high and formation fluid is saline. The basinal limestones, if not argillaceous, usually show high uniform resistivity.

Figure 2-15

REEF CARBONATE

The log character that distinguishes a reef from other porous carbonates is a complete lack of bedding indication on the gamma ray and S.P. curves. Both curves have a uniform, blocky appearance similar to that shown by thick bar or beach sands. Figure 2-16 shows a true biohermal reef mass from 7234' -7388'.

Depending upon the post-depositional structural history, back-reef sands may enhance or dissipate stratigraphic entrapments. A typical example of the electric log character of back-reef sandstones is shown on Figure 2-17. In this case the reef was built on granite wash covering a granitic basement high. The high radioactivity shown on the gamma ray log indicates these sands were derived from the underlying granite wash which apparently contains a high percentage of potassium feldspar (orthoclase). The radioactive isotope of potassium, K-40, probably accounts for most of the radioactivity.

Proximity to a reef may be recognized from a comparison of well logs by an increase in the calcareous content of shales. Also, a small increase in dip may indicate draping against the side of a reef.

REEF CARBONATE

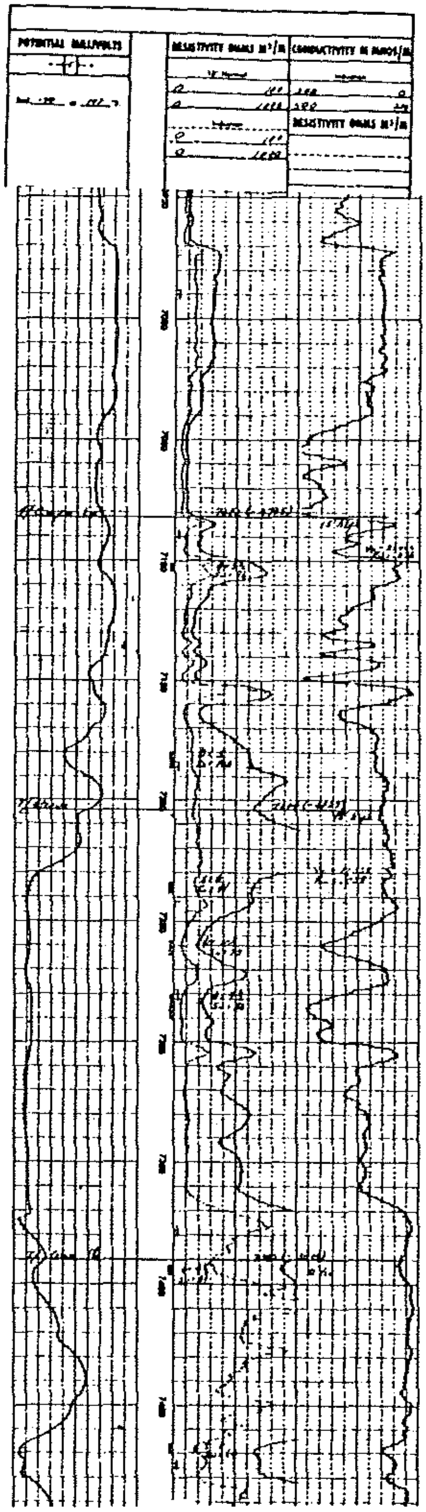

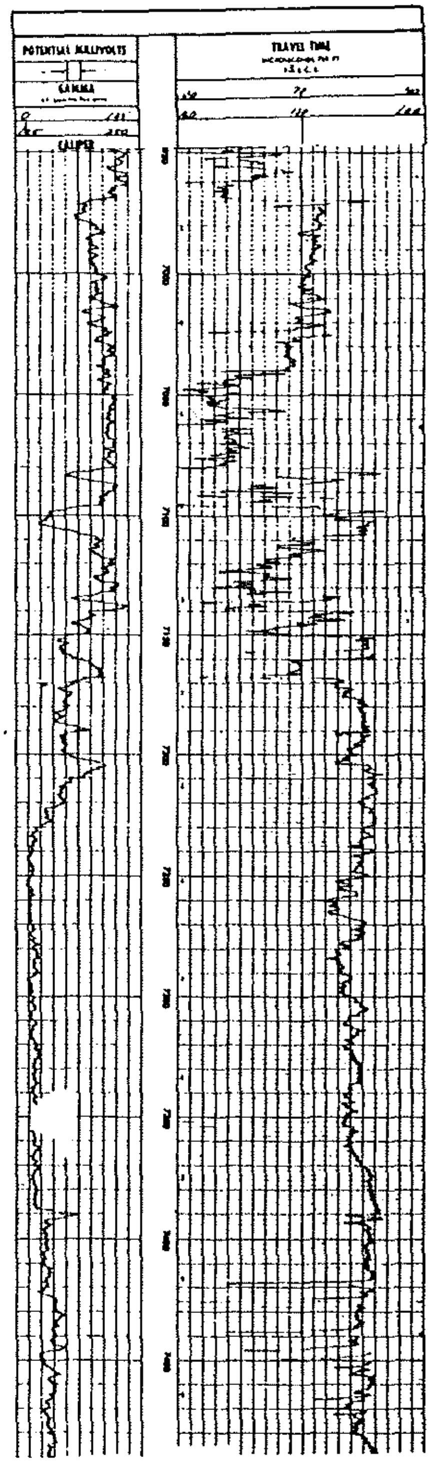

Figure 2-16

BACK REEF SANDSTONE

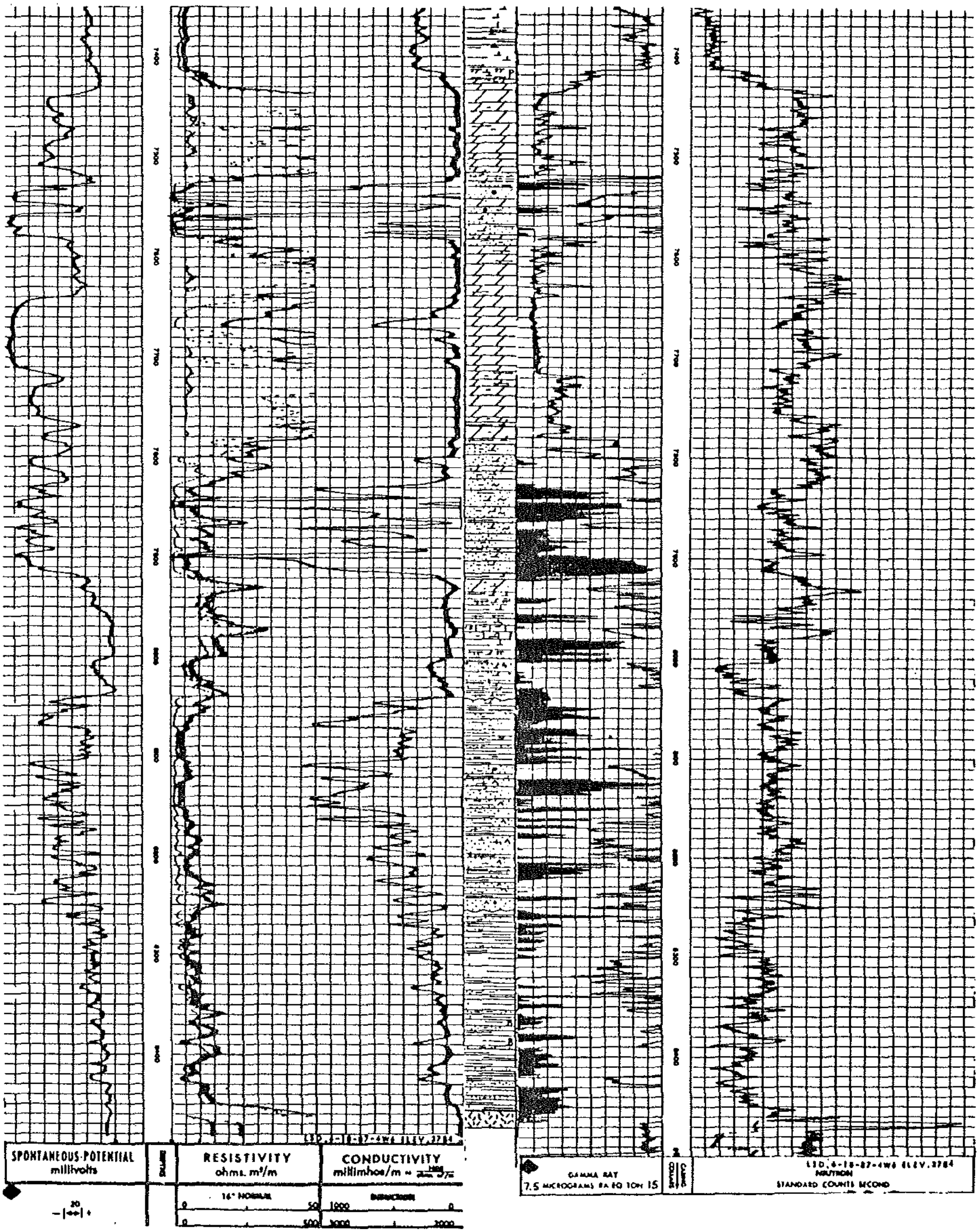

Figure 2-17

CROSS-BEDDING IN UNIT "B" INDICATING
THE SAND TRANSPORT DIRECTION

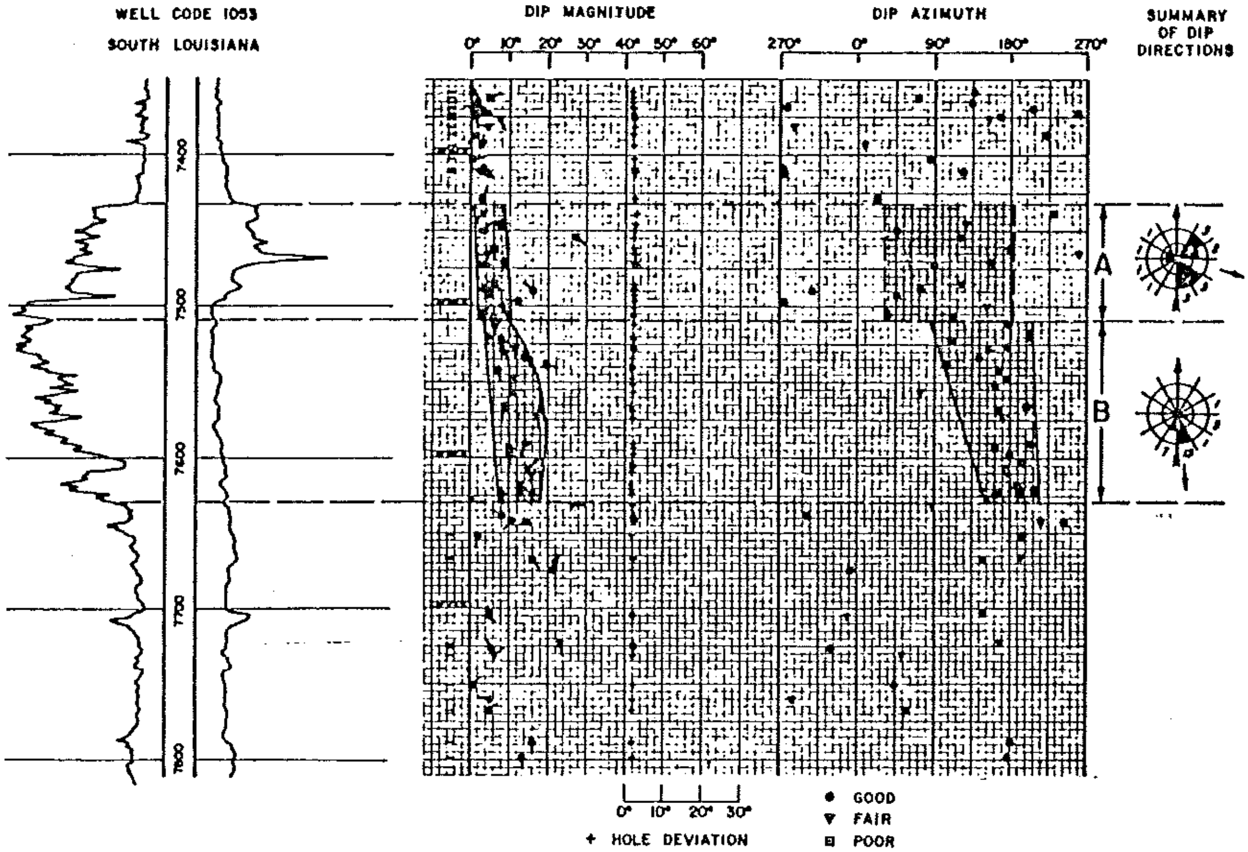

The dips in Sand Unit "B" range in magnitude from about 4° to 20° and form a prominent southerly directional pattern. In contrast, the dips in Sand Unit "A" are generally lower (except for 3), and they form a less consistent directional trend. The structural dip of about 2° southeast at this location was determined from subsurface mapping.

The dips in Unit "B" are interpreted to be cross-bedding, and the directional pattern indicates that the approximate direction of sand transport was S 10° E. The dips in Unit "A" conform more closely to structural dip than do the dips in Unit "B", and cross-bedding appears to be less prominent.

This stratigraphic section is part of a deltaic sequence in the Miocene of South Louisiana. Subsurface mapping has shown that the sand body, composed of both units "A" and "B", is lenticular, and that its axis is oriented approximately north-south. The well in this example is located in the thicker part of the sand body. The combined data indicate that the sand was deposited by paleocurrents flowing southward.

Figure 2-18

CROSS-BEDDING IN UNIT "B" INDICATING THE SAND TRANSPORT DIRECTION

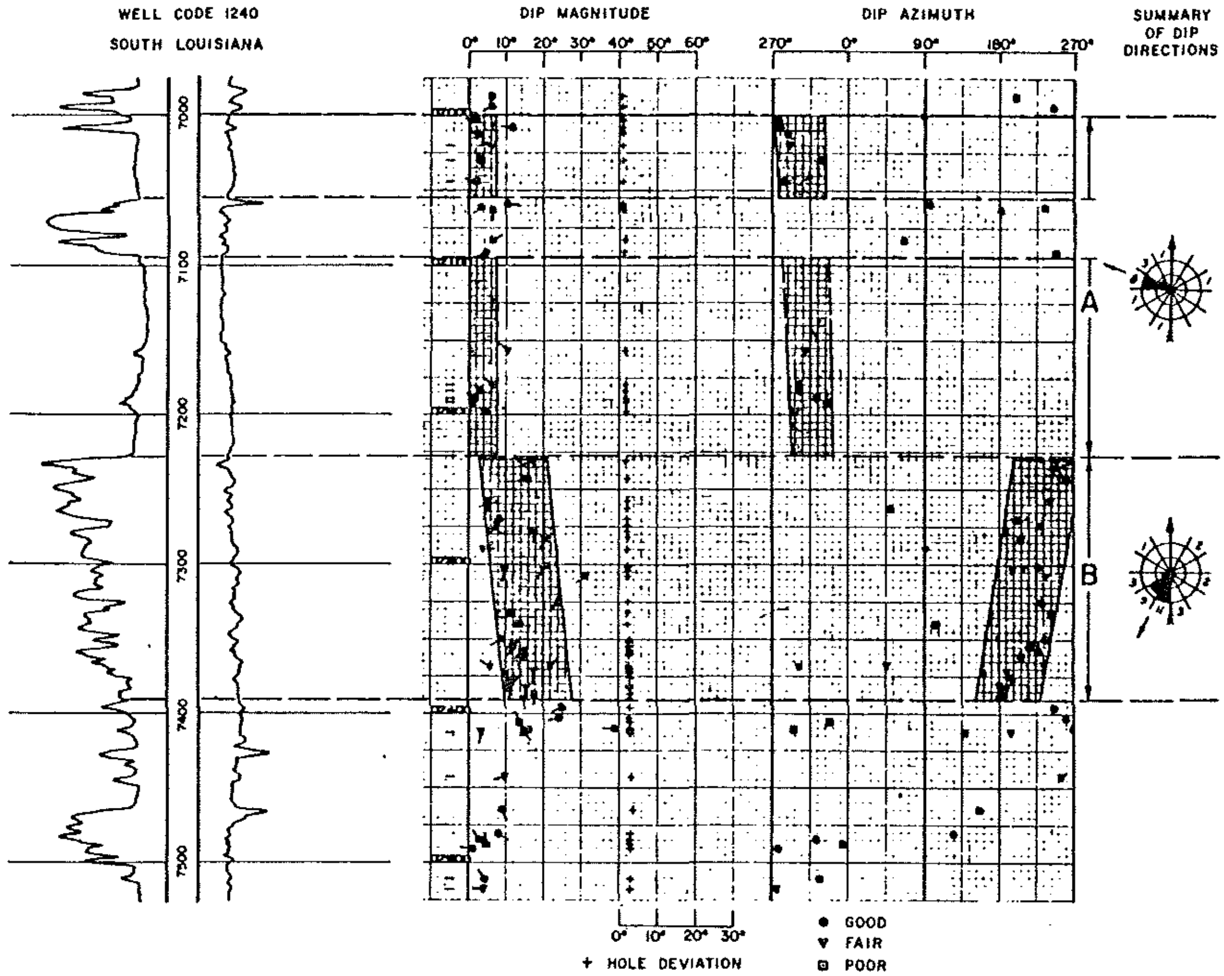

In Sand Unit "B" dips range from about 4° to 32° and are relatively consistent in direction. Structural dip in the vicinity of this well is no more than 1°, based on subsurface mapping. The dips in the shale, Unit "A", and in the sand and shale below Unit "B" indicate that locally the structural dip direction is slightly north of west. The dips in Sand Unit "B" are interpreted as cross-bedding and indicate an average sand transport direction of about S 25° W.

This stratigraphic section is part of a deltaic sequence in the Miocene of South Louisiana. Sand Unit "B" is a lenticular sand body that trends generally west-southwest. This well is located in the thicker part of the sand body. These data suggest that this sand unit was deposited by paleocurrents flowing in a south-southwesterly direction at this location.

Figure 2-19

CROSS-BEDDING IN UNIT "B" INDICATES NORTHWARD THICKENING AND AN EAST-WEST TRENDING LINEAR SAND

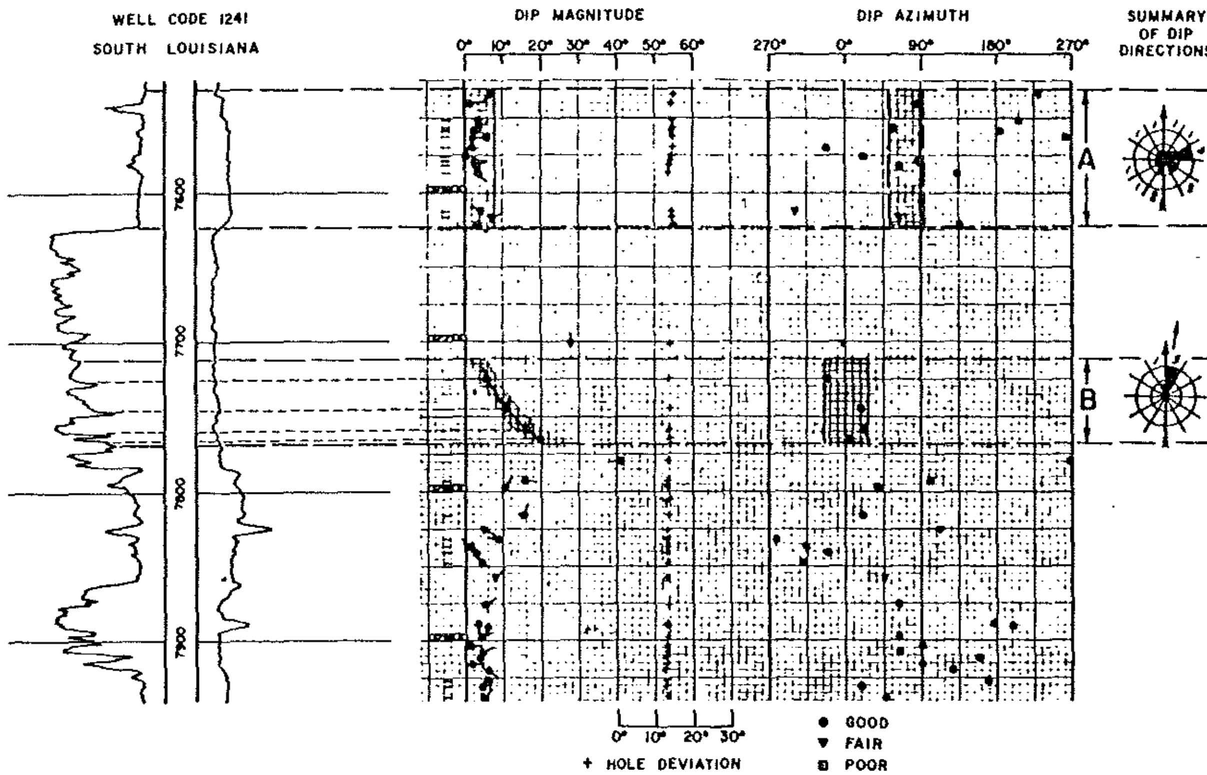

The four dips in the basal part (Unit "B") of the thick sand in this example illustrate a special type of cross-bedding. These dips are consistently toward the north, but become progressively steeper near the base of the sand. Notice that each of the four dips is measured near the base of a separate sand lobe, as shown by the S.P. curve. These dips define a series of sand wedges or lenses that become thicker to the north in the direction of dip, or, conversely, that are thinning to the south. The southward thinning is inferred to be stratigraphic convergence within the basal part of the sand body.

Subsurface maps show that the northeasterly structural dip is less than 2°. The dips in the shale, Unit "A", approximate structural dip.

The sand is part of a deltaic sequence in the Miocene of South Louisiana. The dip pattern in the basal part of the sand suggests that this well is located on the south side of a lenticular sand body. The trend of the sand body is interpreted to be nearly east-west, perpendicular to the direction of maximum thickening. Subsurface maps support the interpretation made from the dipmeter log.

CROSS-BEDDING IN UNITS "B", "C" AND "D" INDICATES A MAJOR CHANGE IN SAND TRANSPORT DIRECTION BETWEEN UNITS "B" AND "C"

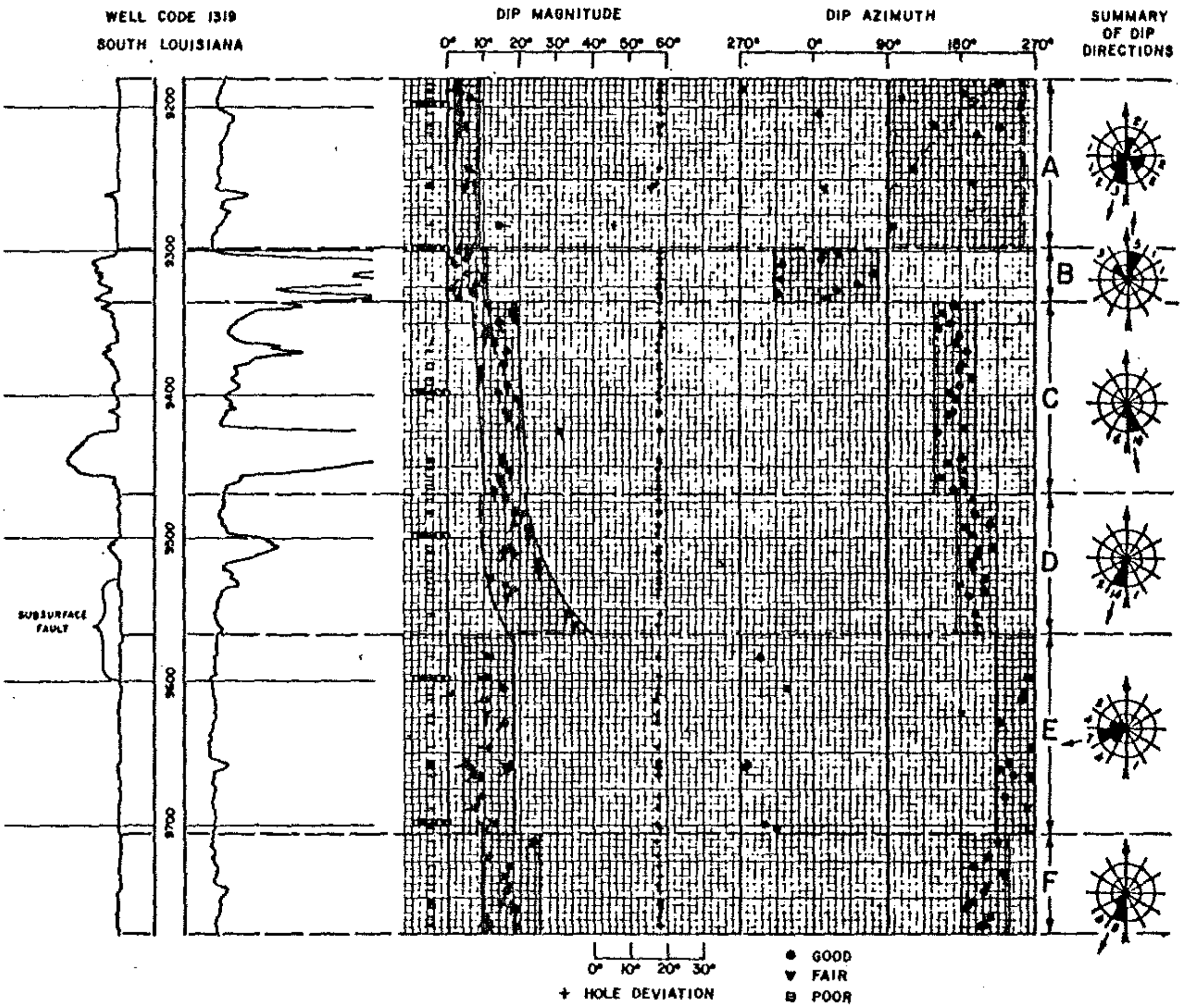

When dipmeter logs show varying dip patterns in both magnitude and direction in areas of low structural dip, as in this example, it is generally difficult to separate structural from stratigraphic dips. In many cases accurate interpretation is possible only if the interpreter is extremely familiar with the area or has recourse to other subsurface information.

In this example, a fault has been picked in the well between the depths of 9530 and 9600 feet, based on E-log correlations. The change in dip between units "D" and "E", therefore, is the result of a fault which can be localized at about 9570 feet by means of the dipmeter log. No faults can be picked above this zone in an area of closely-spaced well control and good correlations. Therefore, the shallower anomalies are probably of stratigraphic origin.

The structural dip on the top of the sand in Unit "B" is locally about 5°-7° south, based on closely-spaced well control. The dips in Unit "A" may approximate structural dip, but the rate of dip is only 2°-3° in this interval. The dips in Unit "E" are assumed to represent structural dip in the lower fault block, although this cannot be completely verified. The origin of the dips in Unit "F" is not known.

In order to evaluate accurately the dip patterns in Units "B", "C" and "D", the effects of structural tilting must be removed by rotation. The dips have been rotated, and the results have been plotted on Figure 2-21A.

Figure 2-21

DIPS IN FIGURE 4 AFTER ELIMINATING STRUCTURAL TILTING BY ROTATION. THESE DIPS INDICATE SOUTHWARD TRANSPORT IN UNITS "C" AND "D" AND NORTHWARD TRANSPORT IN UNIT "B".

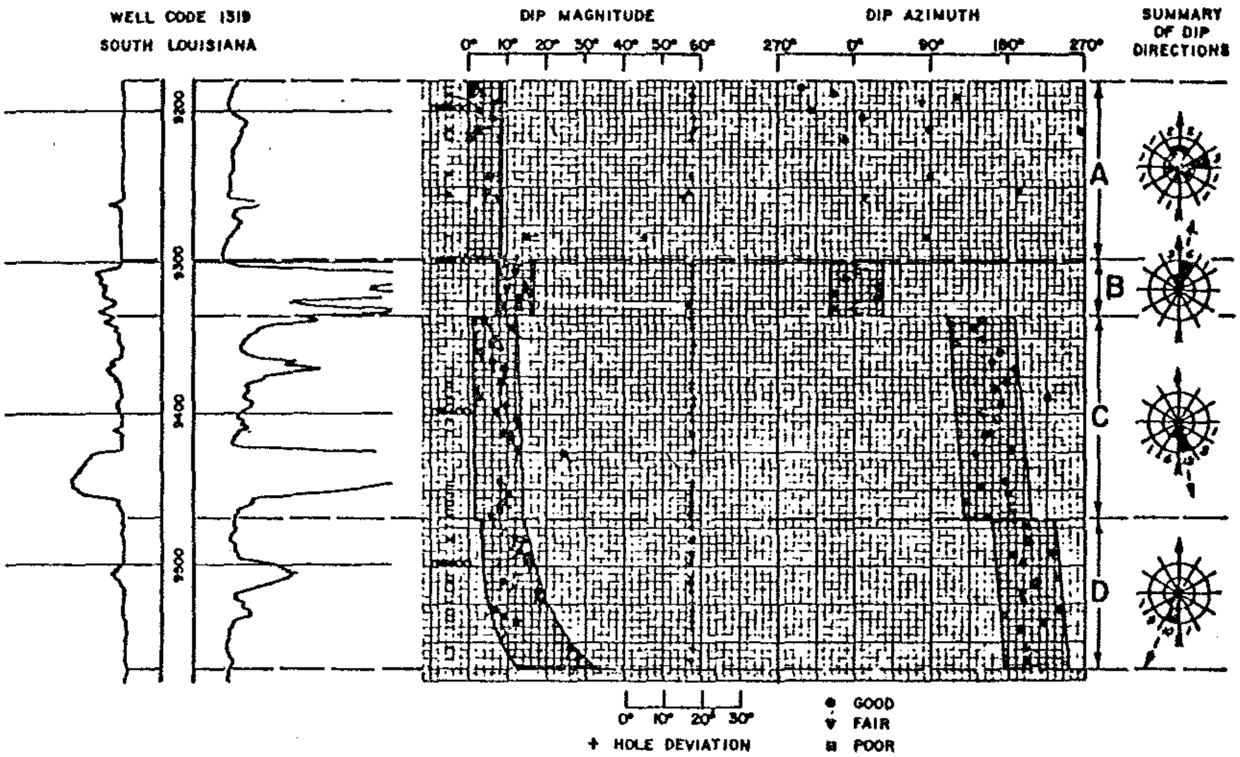

The dips in Units "A" through "D" on Figure 2-21 have been replotted after removal of the effects of structural tilting. The structural dip in Unit "A" was assumed to be 3° S 15° W. The dip in Units "B", "C" and "D" was assumed to be 7° south.

The northward rotation has increased the north dip in Unit "B" and decreased the south dip in Units "C" and "D". Also notice that the rotation has reduced the width of the azimuth pattern in Unit "B" and broadened it in Units "C" and "D".

If it is assumed that all structural tilting has been eliminated, the remaining dip would be only cross-bedding. The original dips in Units "C" and "D" suggest that the sediment transport direction was southward for these units. The sand transport direction in Unit "B" was northward. This indicates a 180° shift in the direction of paleocurrents, or a change in the agent of sediment transport.

Figure 2-21A

TWO SEPARATE AND DISTINCT SAND BODIES, UNITS "B" AND "C", RECOGNIZED BY THE CHANGE IN DIP PATTERN WITHIN THE SAND

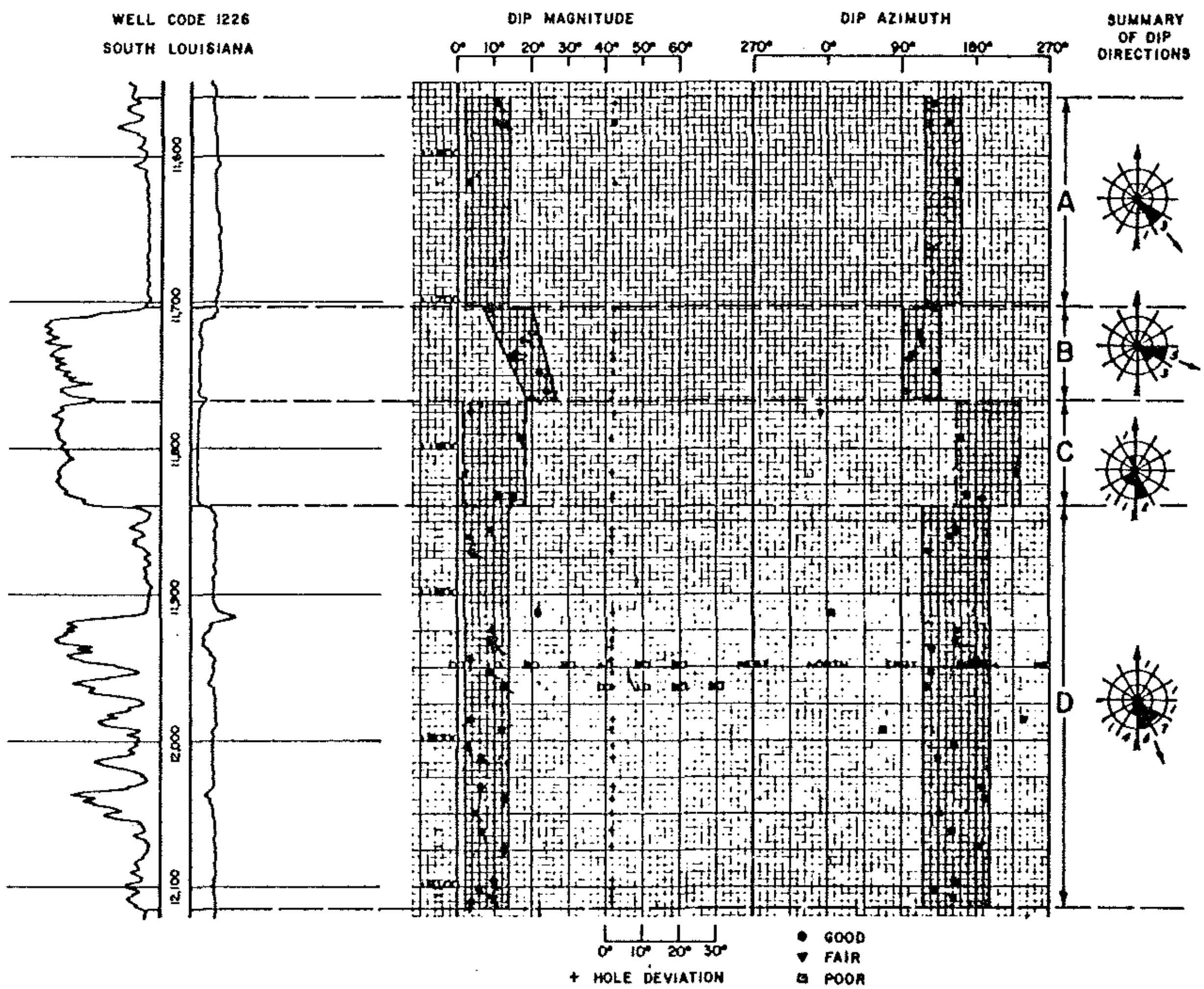

The massive sand below 11,700 feet on the log appears to be a single thick sand unit on casual inspection of the E-log. The dipmeter log, however, shows a distinct change in the dip pattern between Units "B" and "C". This change in dip pattern is evidence that Sand Units "B" and "C" are two separate and distinct sand bodies. A re-evaluation of the E-log shows slight differences in log character between the upper and lower parts of the sand.

The dips in Sand Unit "B" are interpreted as cross-bedding, which in turn can be used to determine the sand transport direction, after the effects of structural tilting have been removed. Sand Unit "C" appears to be more massive, and since there is no distinct cross-bedding pattern, the dips in Units "A" and "D" represent structural dip. Notice that nearly all of the dips in the sand below 11,900 feet reflect structure and not cross-bedding.

Other wells have been drilled in the vicinity of the well in this example. All have penetrated a sand that correlates with Sand Unit "B". No sand has been found that correlates with Sand Unit "C". Apparently Unit "C" is a separate sand body of small areal extent.

Figure 2-22

DIPS IN FIGURE 5 AFTER ELIMINATING STRUCTURAL TILTING BY ROTATION. THESE DIPS INDICATE AN EASTWARD TRANSPORT DIRECTION FOR UNIT "B".

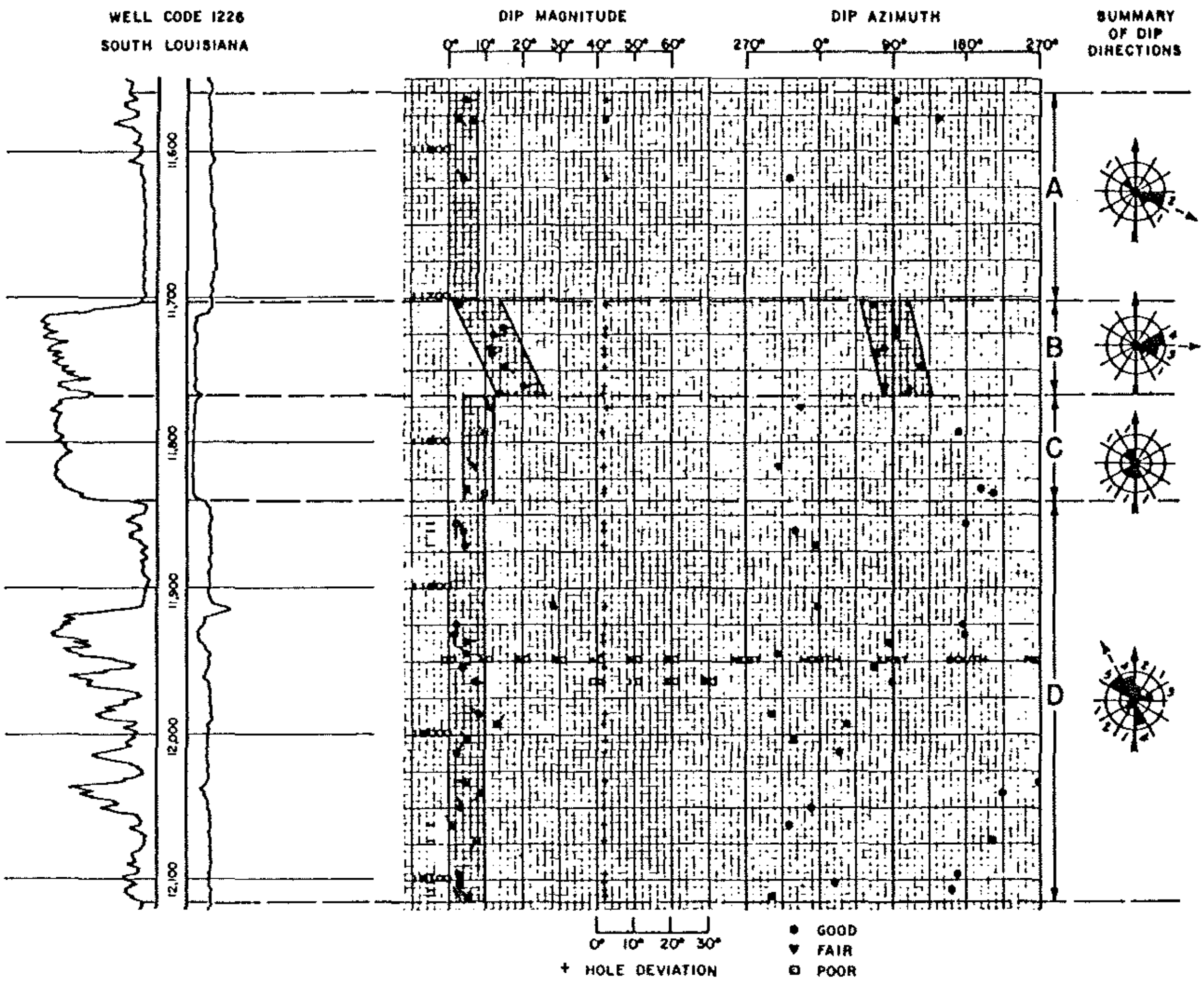

The dips from the well on Figure 2-22 were replotted after removing the effects of structural tilting. The structural dip assumed was 7° S 30° E, from interpretation of the dips in Units "A" and "D" on the dipmeter log on Figure 2-22. This dip corresponds closely to that determined by subsurface mapping in this area.

The results plotted in Unit "D" after rotation have a small northwesterly component, indicating that the dip probably does not exceed 6°. After removing structural dip, the dip directions should be random.

The original dips in Sand Unit "B" (determined by the process of rotation) range from 3° to 20°, and they are interpreted as cross-bedding. They indicate an easterly sand transport direction. This direction differs at least 20° from the direction indicated prior to rotation.

Figure 2-22A

PART 3

LITHOLOGY FROM LOGS

CONGLOMERATES

Conglomerates present some of the most difficult problems in quantitative interpretation of fluid content from electric logs. Even when fully wet, they usually show a similar character to that of good oil and gas sands. The S.P. curve usually shows values ranging from those shown by clayey sands to those shown by clean, highly porous sands, and the resistivity values are always higher than those shown by porous wet sands containing water of comparable salinity.

Two factors are responsible for this characteristic appearance of conglomerates on electric logs. First, because of the irregular porosity caused by extreme variations in particle size, invasion of mud filtrate and sometimes whole mud is usually deep. Secondly, the formation factor is higher than in sands of comparable porosity because the tortuosity factor is higher. In a conglomerate, the current paths must bend around pebbles and sometimes boulders composed largely of highly resistive material. The result is an increase in the bulk resistivity analogous to that resulting from an increase in the length of conductors in a metallic circuit.

Conglomerates can often be distinguished from oil or gas sands by their vertical patterns. In a conglomerate the resistivity usually increases toward the base of the bed due to increase in the size and number of pebbles, whereas in an oil or gas sand the resistivity may decrease in the downward direction if the bed is penetrated near the oil-water contact.

If there is any doubt about the interpretation, the electric log should be compared with the mud and cuttings log, the drilling rate should be checked, and core and cuttings samples examined.

CONGLOMERATE

NEWHALL AREA

CALIFORNIA

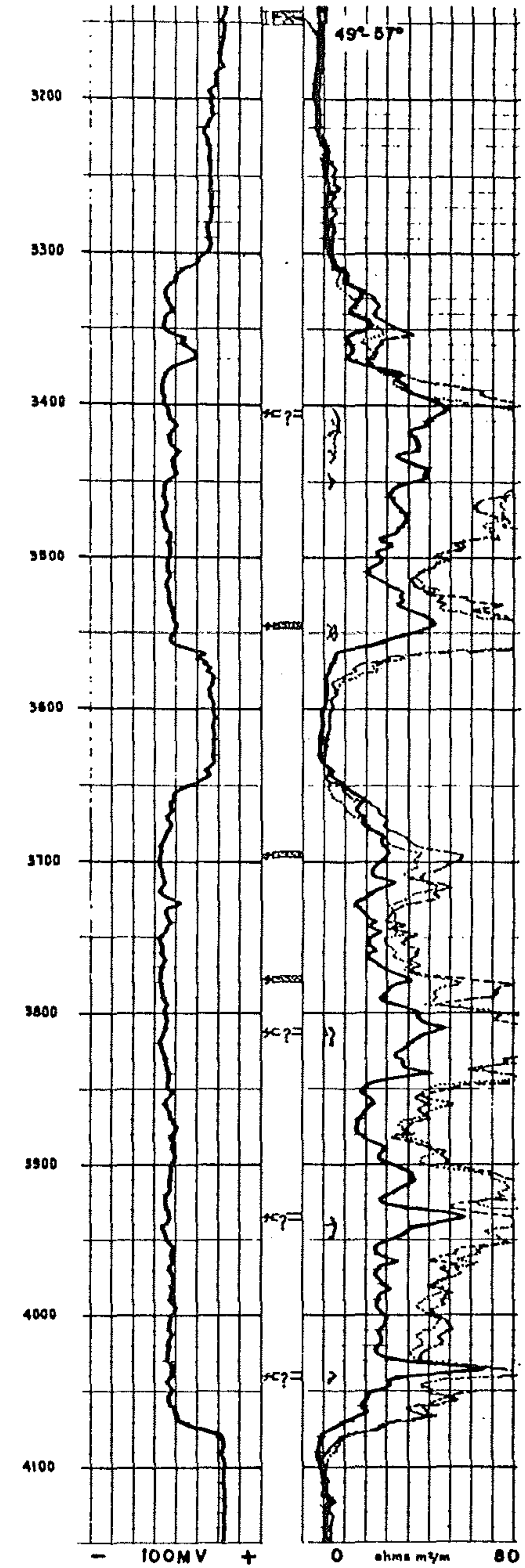

Figure 3-1

SILICEOUS SHALES

DIATOMITES

The characteristic electric log pattern through a diatomite bed is as shown on Figure 3-2. The resistivity curves show low values and approximately coincide, as they do in porous argillaceous shales, but the S.P. curve looks similar to the curve obtained opposite a uniform sand.

The reasons for this behavior become readily apparent when we consider the factors controlling resistivity and self-potential. Diatomites are very porous but have little or no permeability because of their fine grain size. Consequently they contain a large amount of formation water which cannot be readily displaced by oil or gas or by mud filtrate from the bore hole. This accounts for the low values shown by all three resistivity curves. The uniform negative departure shown by the S.P. curve results from the uniformly high porosity and siliceous composition of diatomites. The S.P. current circulation at a diatomite - argillaceous shale contact is, therefore, similar to that at a sand-shale contact.

An electric log pattern of this type should always be checked by cuttings, sidewall samples, or cores, however, because a uniform, non-argillaceous siltstone shows a similar pattern, but siltstones usually do not maintain the same uniformity through thick beds. Another check, which should be made if cuttings or cores are not available, is the time interval between penetration of the bed and the logging run. A permeable salt water sand will quite often show little or no invasion effects on an electric log run a few hours after penetration, and will, therefore, show an electric log pattern similar to that of a diatomite.

Figure 3-3 shows an interesting example of diatomite interbedded with clayey oil sand. The thicker diatomite beds are easily identified by their distinctive electric log patterns similar to that shown on Figure 3-2. The thinner beds would be difficult to distinguish, however, were it not for the density log. The unusually low bulk density of the diatomite is ascribed to the low grain density of the diatom shells and the high porosity. Diatom shells are composed of hydrous silica which has a grain density of 2.0-2.2 gm./cc. compared with an average sand grain density of 2.65 gm./cc.

DIATOMITE BED

R_M = 2.4 OHM-M

AT 84°F

SOUTH BELRIDGE

CALIFORNIA

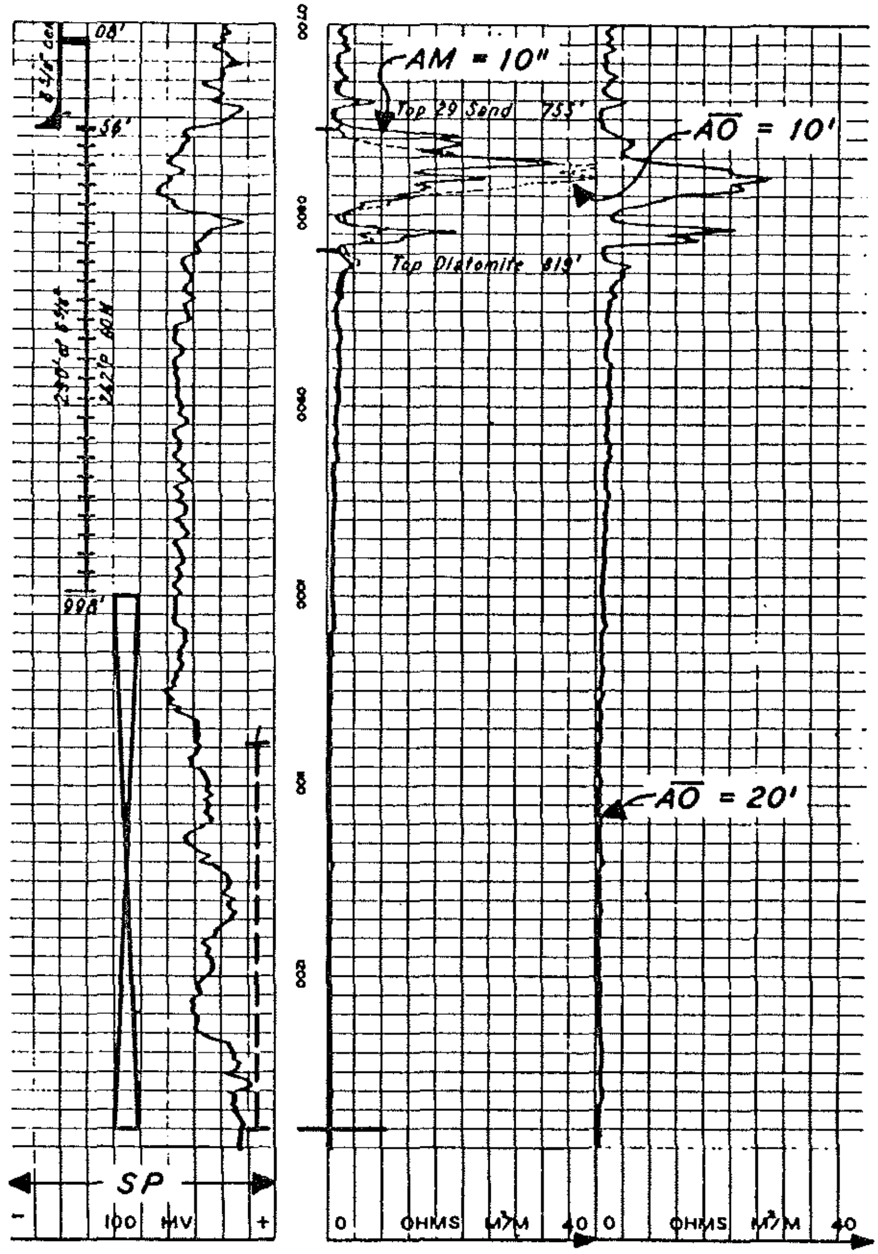

Figure 3-2

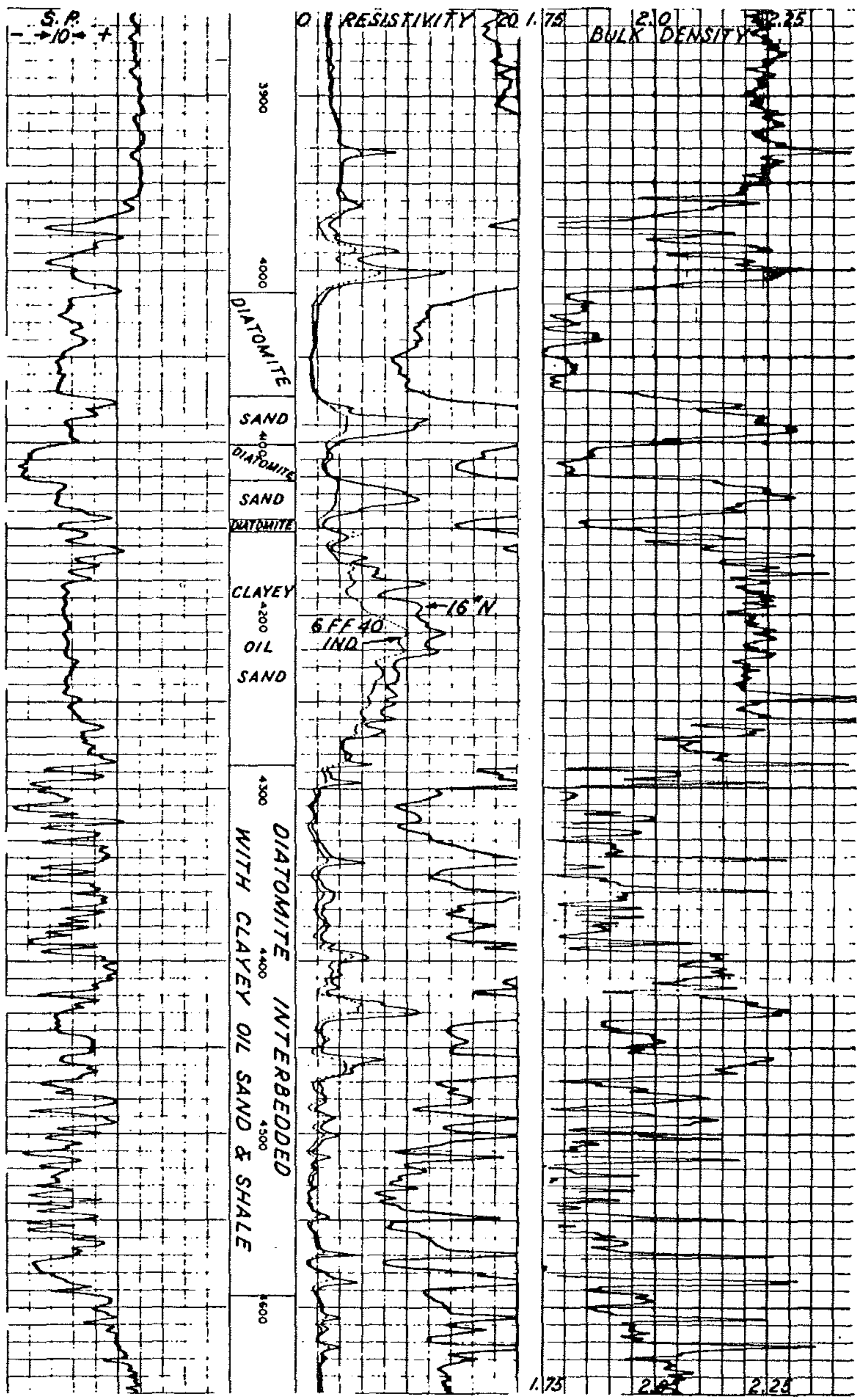
S.P.
- 10 +
0 RESISTIVITY 20
1.75 2.0 2.25
BULK DENSITY
3900
4000
DIATOMITE
SAND
DIATOMITE
SAND
DIATOMITE
CLAYEY
4200
OIL
SAND
16"N
6FF40
IND
4300
DIATOMITE INTERBEDDED
WITH CLAYEY OIL SAND & SHALE
4400
4500
4600
1.75 2.0 2.25

Figure 3-3

OPALINE SHALE

Upper Miocene siliceous shales in California developed in large part from diatomite which is still preserved in some localities near the basin edges where subsequent deposition was minimal. Deeper burial and solution progressively changed the diatomite to opal and finally chert as the end product. Recent grain density determinations from cores(1) and density logs from wells(2,3) have shown the opaline stage to be more widespread than was previously recognized. The reservoir quality of these shales in some areas was undoubtedly enhanced by the microfracturing in the opaline stage of alteration.

Figure 3-4 shows how these opaline shales can be distinguished from sands or chert by comparing the density log with the S.P. curve. Normal sand response is apparent in the top 120'. The caliper shows mud cake, the S.P. indicates sand, and the bulk density averages about 2.2 gm./cc. Assuming an average sand grain density of 2.65, the average porosity would be 27%, which is a reasonable figure for that sand. The next 200' looks like normal silty shale on the IES log and the bulk density averages about 2.15, which is a reasonable figure for silty shale at that depth. Below 4650', the top of the siliceous shale section, comparison of the S.P. curve with the bulk density shows that the negative deflections on the S.P. correlate with abnormally low bulk densities except for a few high resistivity - high density streaks which are either hard sandstone or dense chert. The abnormally low bulk densities are now known to result from opal in the shale. If we assume an average grain density of 2.2 for opal, the total porosity of the more porous intervals would be in the range of 25% to 33% which is confirmed by core analysis. The effective porosity, however, is considerably lower because the matrix porosity of the shale probably accounts for more than half of the total.

(1) Chevron Research Project 14,706, Dec. 31, 1962.

(2) Geological Item of Interest No. 94, Producing Item of Interest No. 38, "Formation Evaluation of Fractured Shales - San Joaquin Valley, California," R. R. Johnston, W.O.I., 1964.

(3) "Application of the Density Log to Fractured Shale Evaluation," J. C. Wells, Formation Evaluation Committee Report, April, 1964.

OPALINE SHALE

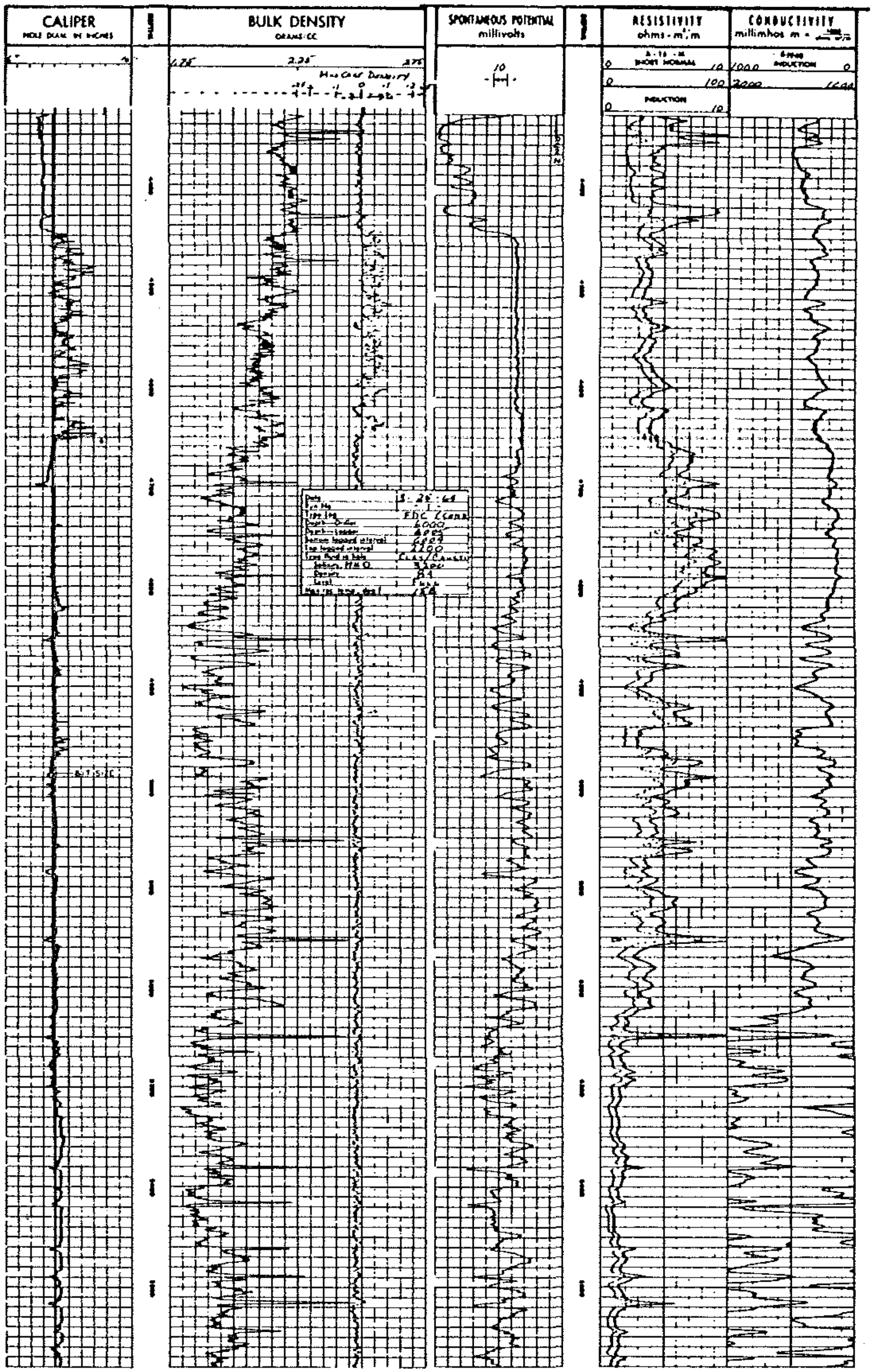

Figure 3-4

FRACTURED SHALE RESERVOIRS

The characteristic electric log pattern of fractured shale reservoirs in California is as shown on Figure 3-5. The S.P. curve resembles that produced by a finely interbedded sequence of argillaceous shales and sands of varying porosity or clay content, and for the same reasons. Given similar relationships between mud resistivity, formation water resistivity, and streaming potential, the resultant S.P. curve will primarily reflect differences in porosity and concentration of clay minerals. In the case of the fractured shale, the more siliceous or cherty beds will also be more brittle resulting in greater fracture porosity.

Resistivity curves in fractured shales are usually very erratic showing extremes of contrast opposite what appear to be similar beds from the S.P. curve and lithology determinations. Unfortunately, for quantitative evaluation, these variations more often reflect erratic changes in formation factor over short intervals, because of the irregular nature of fracture porosity, rather than changes in type and concentration of formation fluids.

Wet sands interbedded with siliceous shales can sometimes be distinguished by comparing the resistivity curves for invasion if the sand beds are more than three or four feet thick. For thinner sands and oil sands, a wall resistivity log is useful if the hole is to gauge because mud cake does not form on fractured shale unless the shale is pulverized sufficiently to approximate intergranular porosity.

Figure 3-6 shows a contact between siliceous shale and dolomitic shale. The dolomitic shale has a lower matrix porosity and is not as brittle as the siliceous shale. Consequently it shows an electric log pattern intermediate between that of siliceous and argillaceous shale. The density log, however, shows the contact quite sharply because of the high grain density of dolomite compared to that of silica or opal.

FRACTURED SHALE

ELK HILLS CALIFORNIA

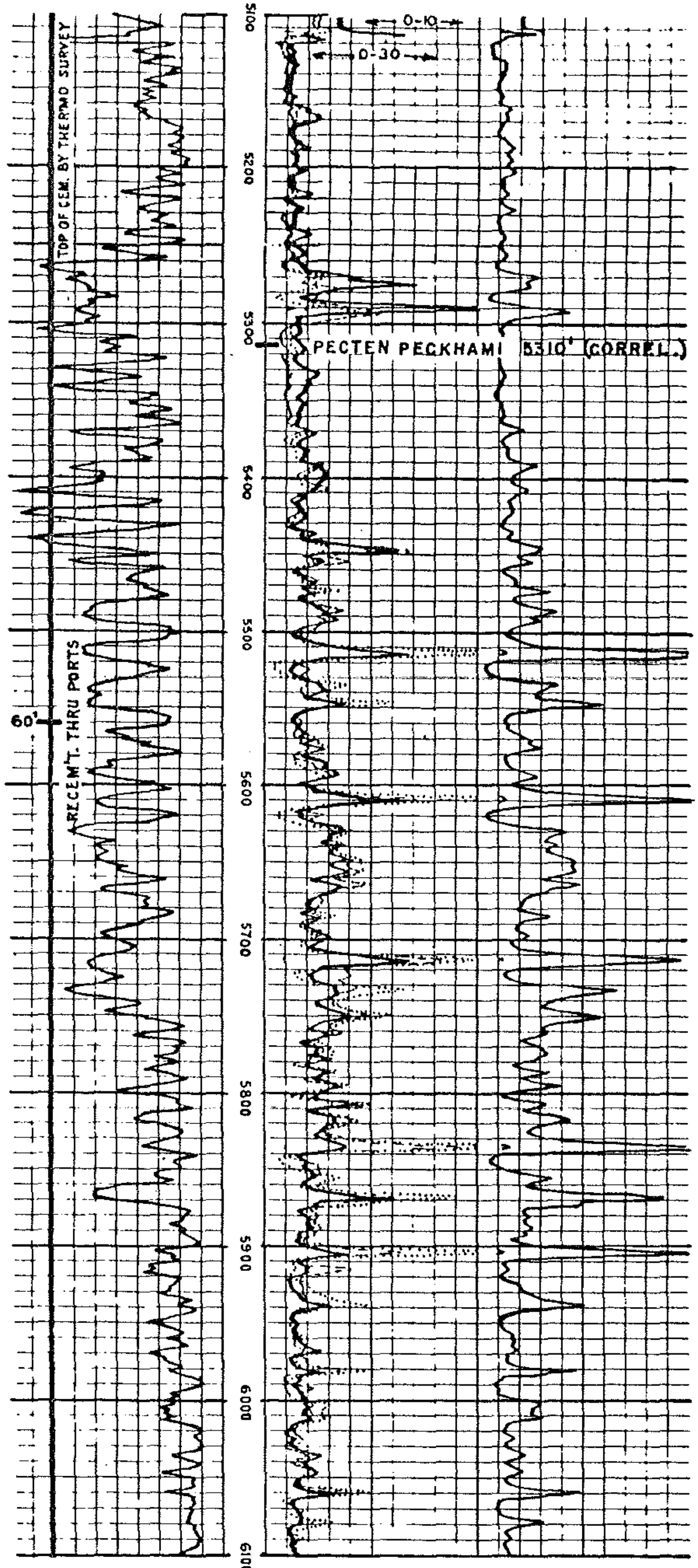

Figure 3-5

SILICEOUS AND DOLOMITIC SHALE

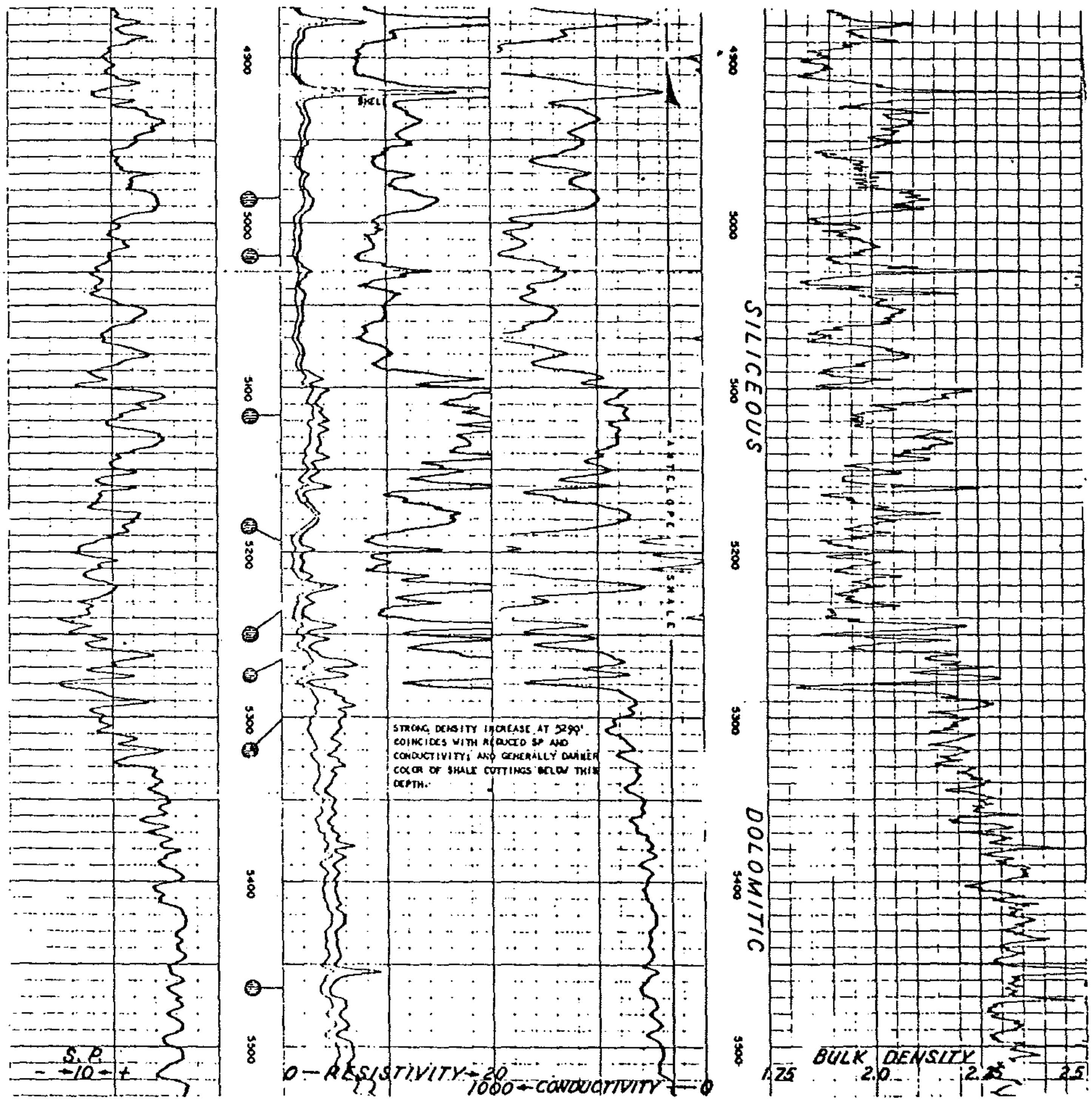

Figure 3-6

SILTSTONE

In some areas, siltstones may be sufficiently clean to show electric log patterns similar to thick sand sections or even diatomites if the log is run soon after penetration. (Figure 3-7). Cuttings, sidewall samples, or cores are necessary to distinguish this siltstone from sand. If the log is not checked against samples, serious errors in sand counts will result.

Note that the resistivity recorded by the 16' Lateral curve is lower through the siltstone than through the shale below. This indicates either a much higher porosity in the clean siltstone or saltier formation water.

SILTSTONE
FILLMORE AREA
CALIFORNIA

CLEAN
SILTSTONE

ARGILLACEOUS
SILTSTONE
AND
SILTY
SHALE

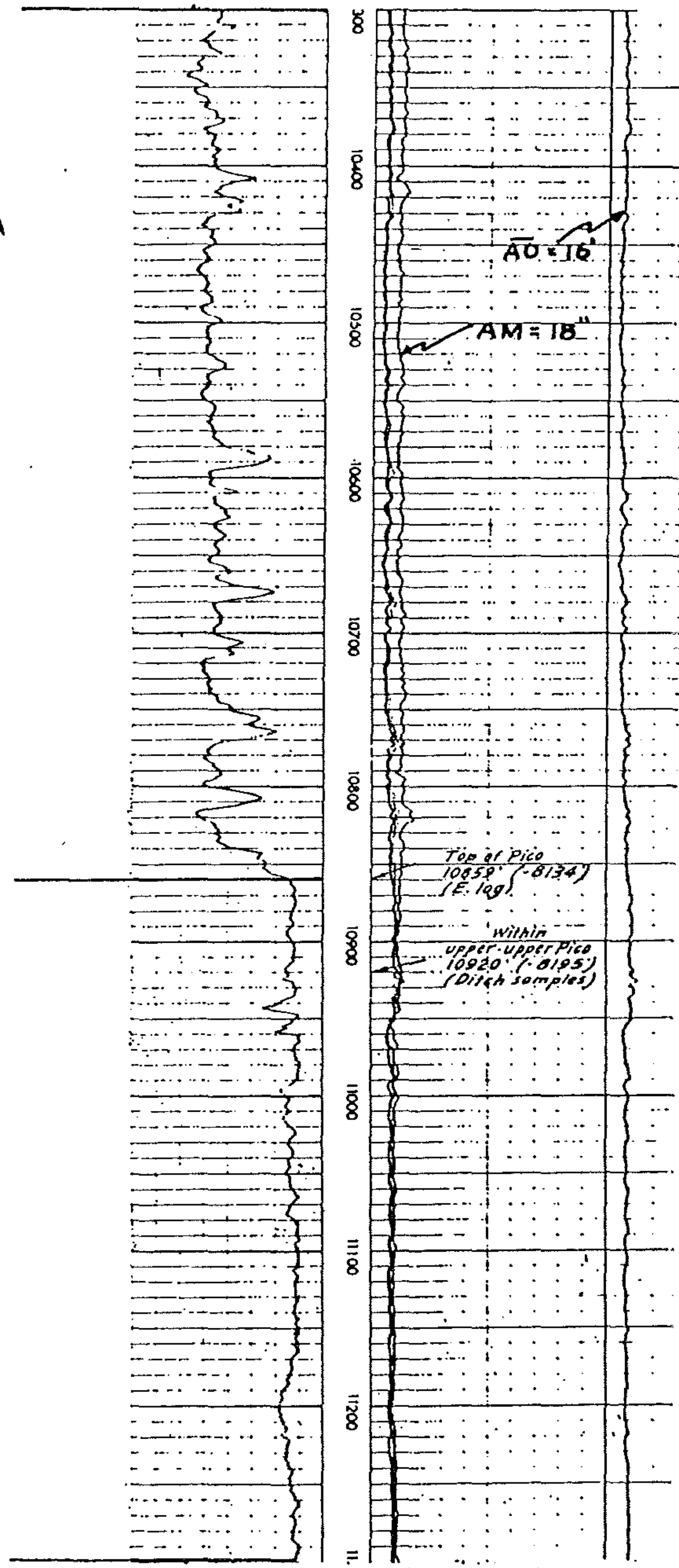

Figure 3-7

BENTONITES

A pure bentonite always shows a positive departure on the S.P. curve (i.e., to the right of the shale line on the hour glass type log), and a resistivity value lower than the average shale value on all three curves. (Figure 3-8).

The reason for this behavior is the super clay effect of the montmorillonite group of clay minerals. The minerals of this group absorb more water than the kaolinites and illites and are even more selective to the passage of ions.

The modern induction-electric log combination now enables us to identify bentonite beds in sandy intervals as shown on Figure 3-9. The high contrast in conductive (low resistivity) formations on the conductivity curve causes bentonites to stand out from ordinary shales even when interbedded with sand, provided that the sands do not contain super saline waters. Maximum water salinities in California are about 3000 G/G or 50,000 P.P.M. Consequently, sand conductivities do not approach the conductivity of bentonite.

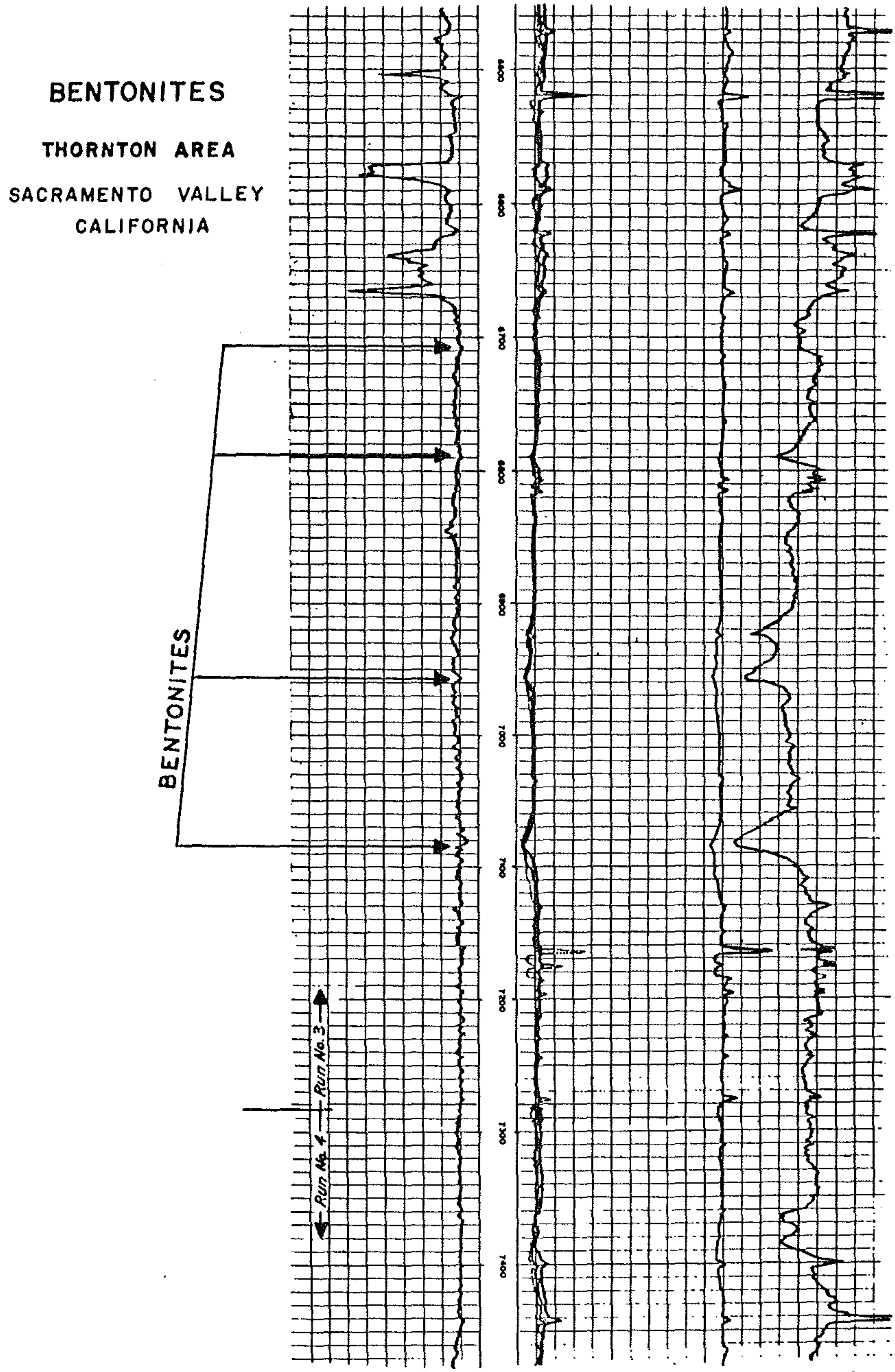
BENTONITES
THORNTON AREA
SACRAMENTO VALLEY
CALIFORNIA
BENTONITES
Run No. 4
Run No. 3

Figure 3-8

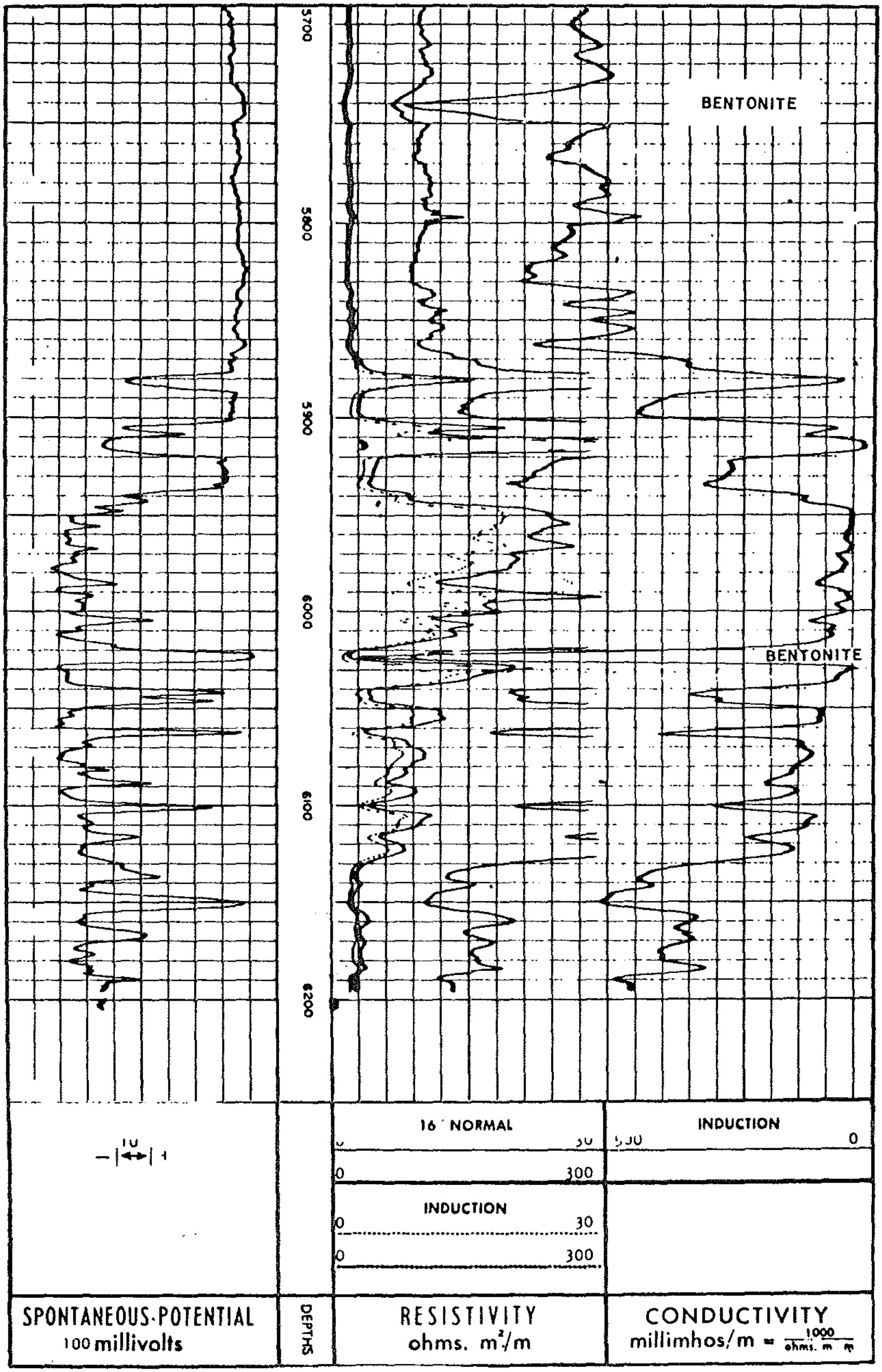

BENTONITE
5700
5800
5900
6000
6100
6200
BENTONITE
16' NORMAL
0
300
INDUCTION
0
INDUCTION
0 30
0 300
SPONTANEOUS-POTENTIAL
100 millivolts
DEPTHS
RESISTIVITY
ohms. m²/m
CONDUCTIVITY
millimhos/m = 1000/ohms. m m

Figure 3-9

BENTONITE

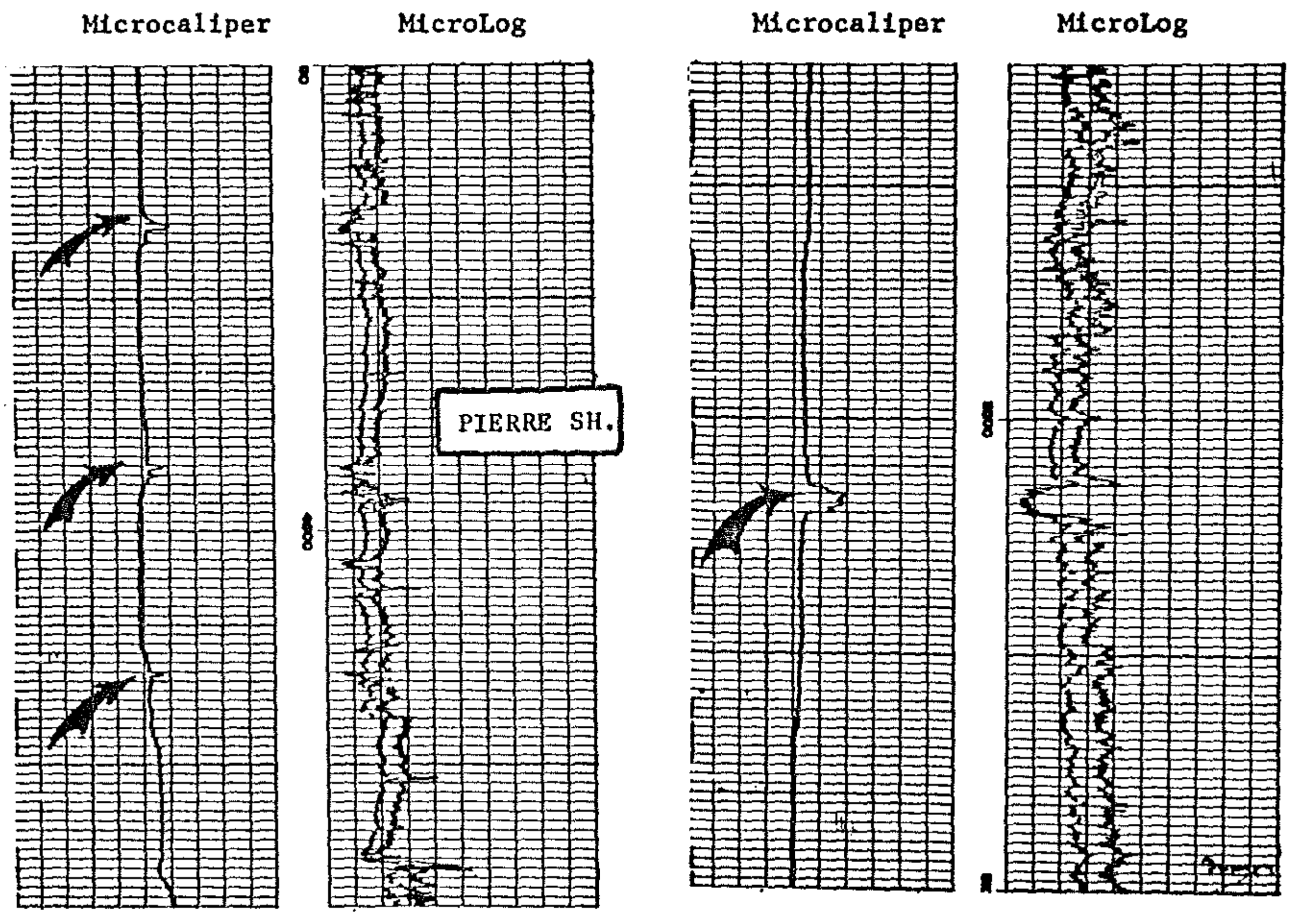

DENVER BASIN (probably from Pierce
COLORADO Field area)

Bentonites can often be recognized by observing hole enlargement with corresponding low resistivities. The Microcaliper-MicroLog or MicroLaterolog surveys make good logs for this use.

Figure 3-10

SANDWICH BEDS
(Finely Interbedded Sand and Shale)

Finely interbedded clean sands and shale, where the individual beds are less than two feet thick, show an electric log pattern similar to that of siltstone regardless of the fluid content of the sand. Figure 3-11 shows an electric log example where, in the cored interval, the individual oil sands are less than six inches thick. The interval was completed for an initial production of 80 B/D oil. Figure 3-12 shows an induction-electric log example where the individual gas sands are probably one to two feet thick. This interval made a good gas producer.

Quantitative evaluation is not possible where bed thickness is less than three feet because the true resistivity of the sands cannot be determined with our present tools. However, we can detect thin, permeable sands with wall resistivity devices and short spacing velocity logs. Then, if mud logging or sidewall sampling indicates hydrocarbon saturation, and the sand count appears to be sufficient, the interval is further evaluated by a drill stem test or a production test.

SANDWICH BEDS
WHEELER RIDGE, CALIFORNIA

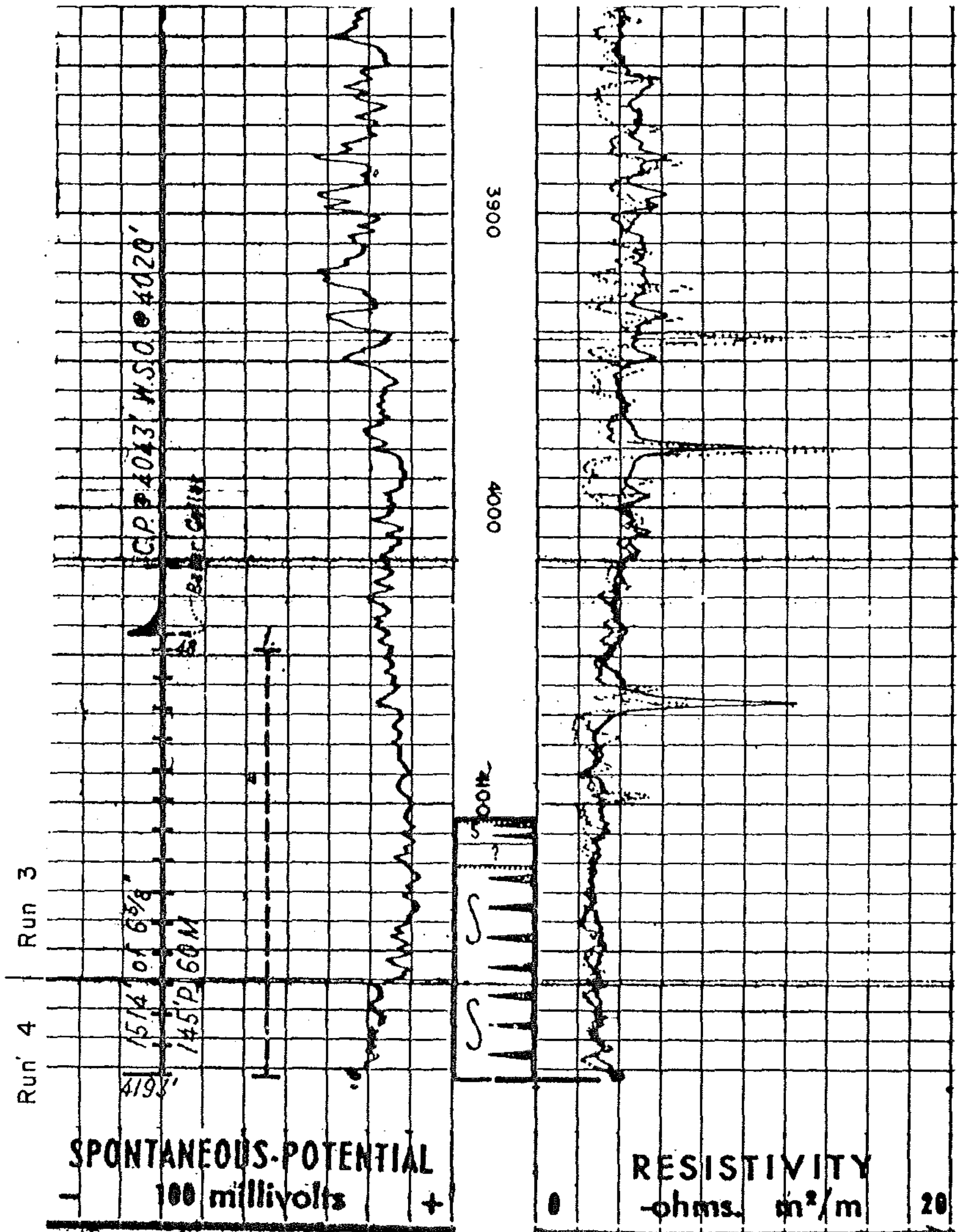

Figure 3-11

SANDWICH BEDS
SOUTH TEXAS

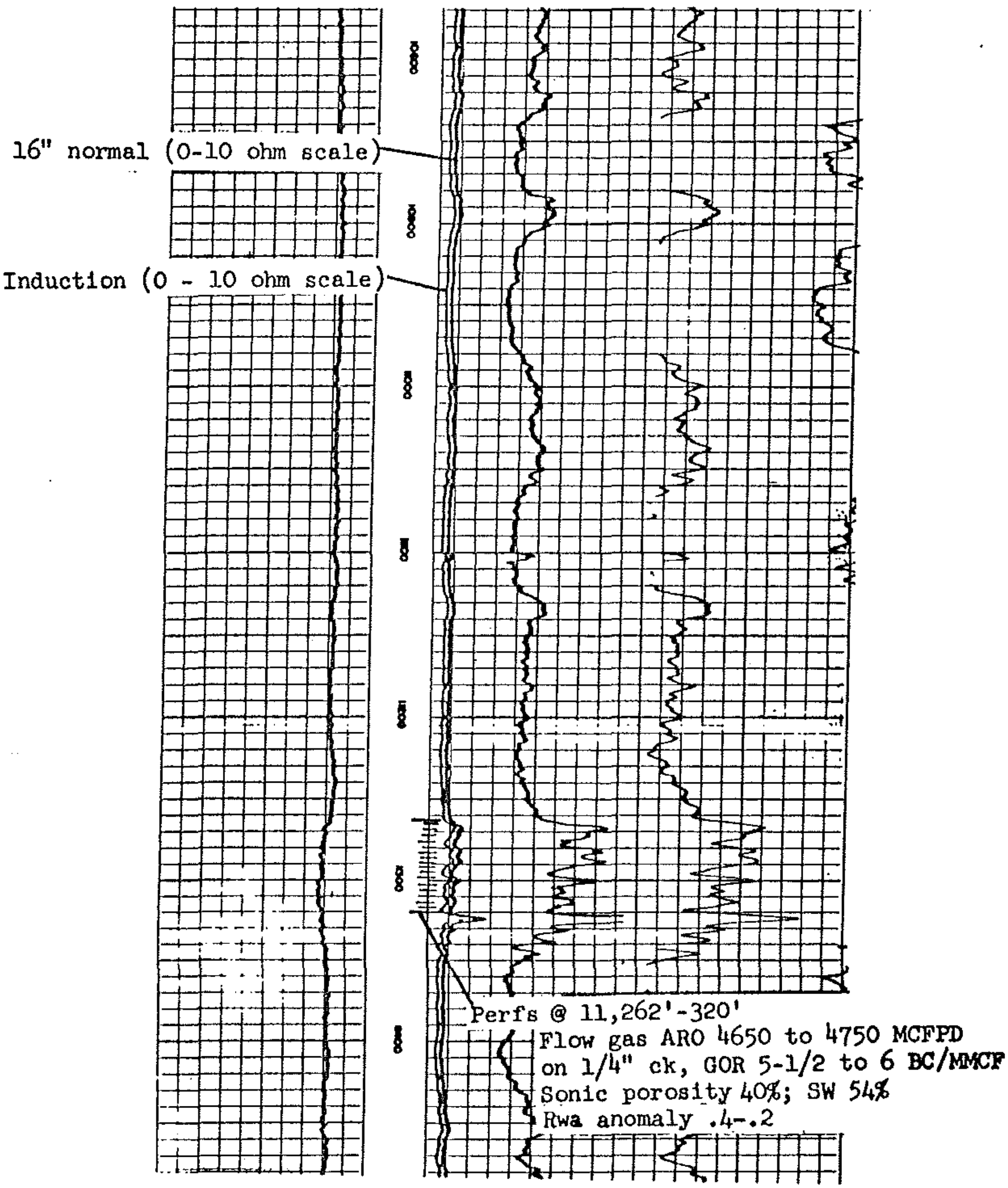

Figure 3-12

GLAUCONITIC SANDS

On electric logs, glauconitic sands cannot be distinguished from other sands with like permeability and porosity, but can be easily recognized on gamma ray logs because of their high natural radioactivity. The high radioactivity value results from the presence of radioactive potassium, K-40, in the mineral glauconite. Figure 3-13 shows a typical example from the Lower Tertiary in California.

RADIOACTIVE EXPRESSION OF GLAUCONITIC GREEN SANDS

RIO VISTA AREA

CALIFORNIA

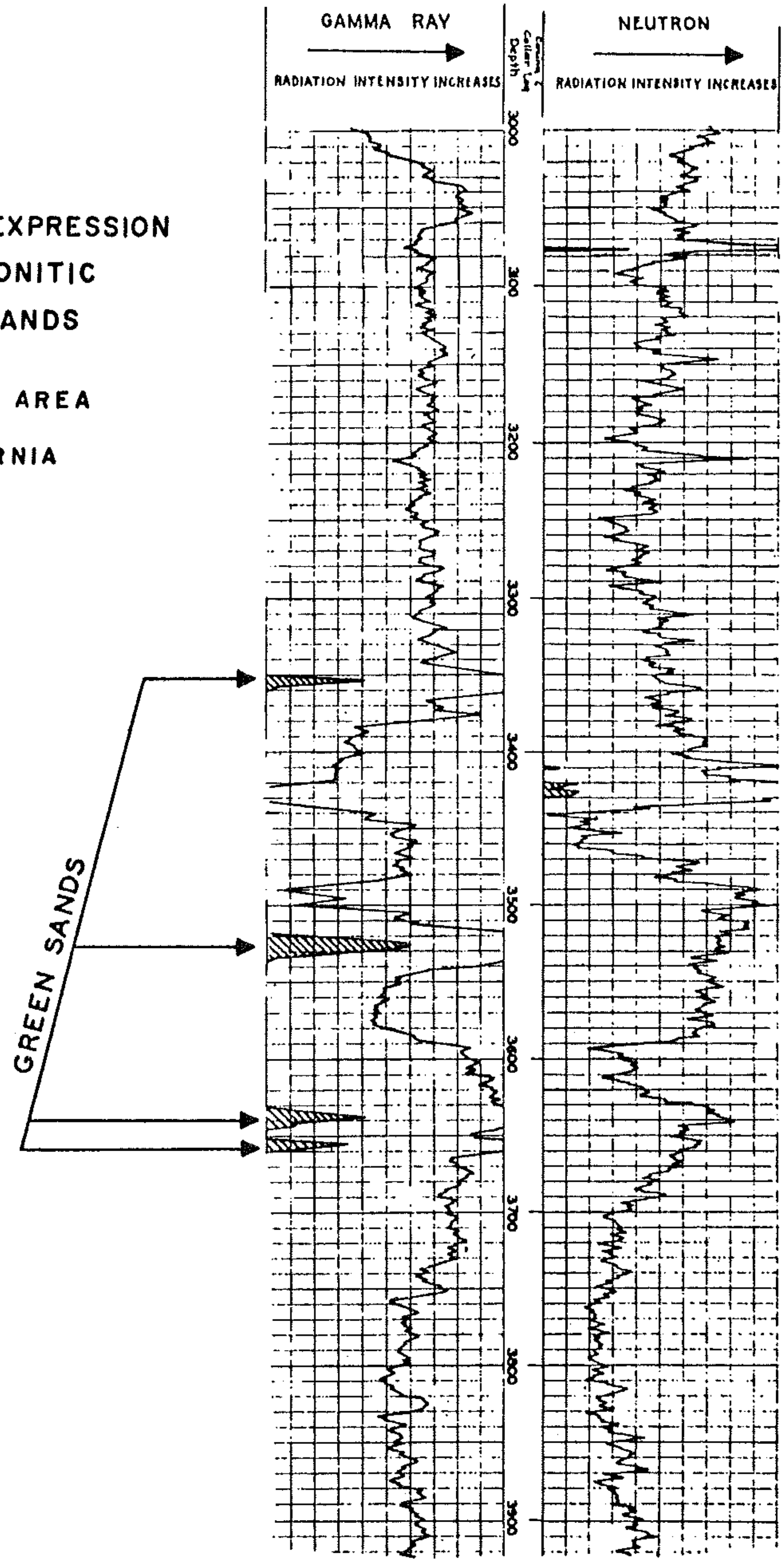

Figure 3-13

ORGANIC SHALES

NODULAR SHALE

The Nodular Shale is a subsurface term for an organic, phosphatic shale that overlies an unconformity at the top of the middle Miocene in many parts of the Los Angeles Basin in Southern California. Where the middle and lower Miocene are absent, the Nodular Shale rests directly on schist basement or is separated from the schist by a thin basal sand or conglomerate. (Figure 3-14).

The Nodular Shale is a black, hard, fissile shale. It is highly organic (up to 10% organic carbon by weight) and contains bands or nodules of brown phosphatic material. The phosphate mineral is predominantly apatite. Carbonate, usually dolomitic, is associated with the apatite and is also present in the non-phosphatic portions of the shale. Core analyses yield a range of 1 to 18 per cent carbonate by weight.

The high resistivities of the Nodular Shale (20 to 1000 ohmmeters) are attributed to its high organic carbon content as are the low densities and velocities. The S.P. expression varies from that of a normal shale to a siliceous shale with irregular negative departures. Comparative properties of intervals with differing S.P. are as follows:

	Negative S.P.	Shale-type S.P.
Resistivity	Very high	Moderate to high
Organic carbon content	Very high (12+%)	High (5-9%)
Density	Very low (2.1 gm./cc.)	Low (2.2-2.4 gm./cc.)
Velocity	Low (7300-11,000 ft./sec.)	High (13,000-15,400)
Drilling rate	Fast	Slow
Clay content	Low	Moderate

For additional detail on the Nodular Shale, please refer to W.O.I. geological report, "Sentous Study - Inglewood Field, California," by W. J. Plumley and T. L. Wright, dated August 1964. The above description was taken from this report.

NODULAR SHALE

LOS ANGELES BASIN, CALIFORNIA

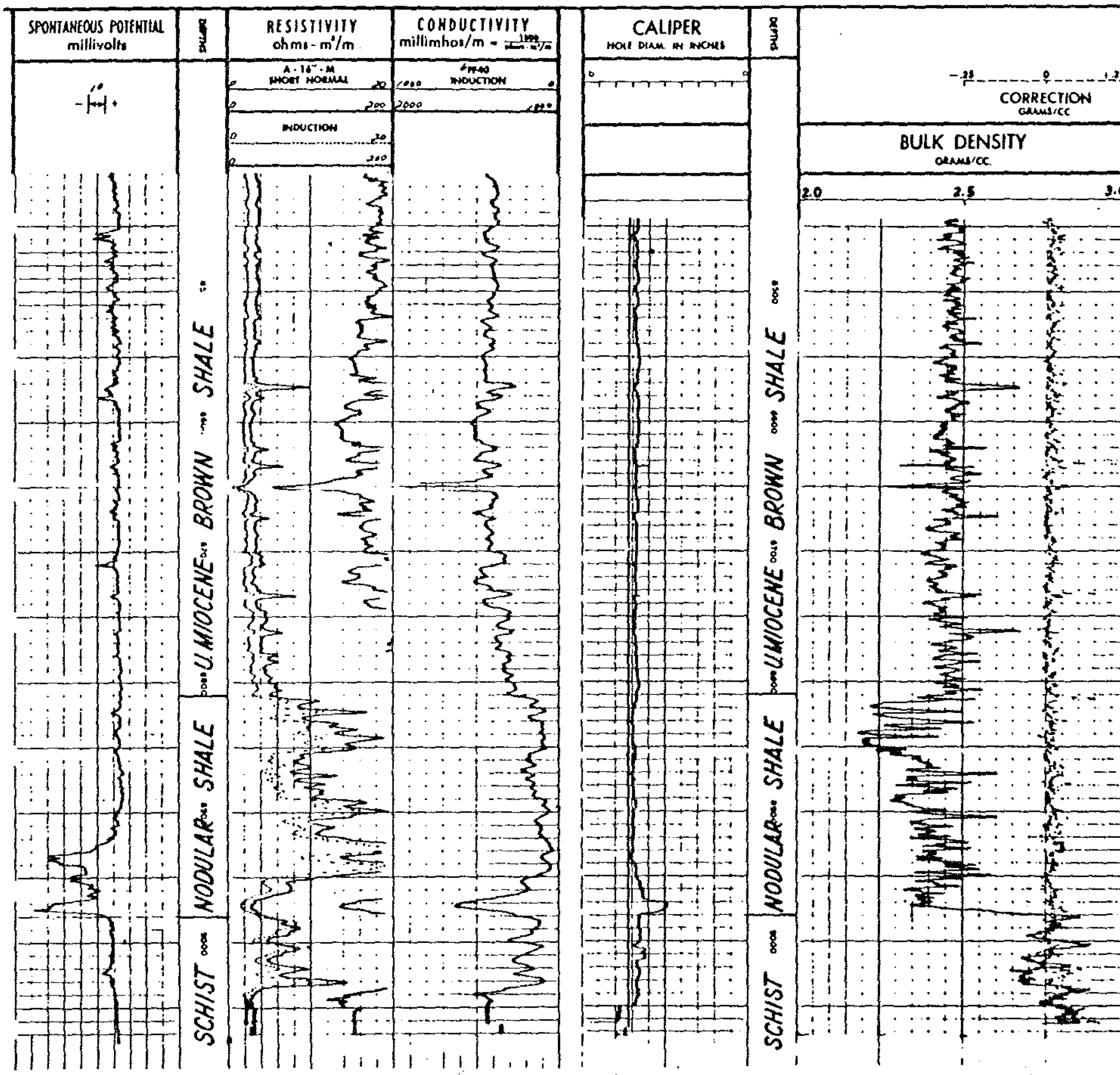

Figure 3-14

CARBONACEOUS SHALE

C/NW/NE, 13-T148N R98W, California Company, Rough Creek #1, McKenzie County

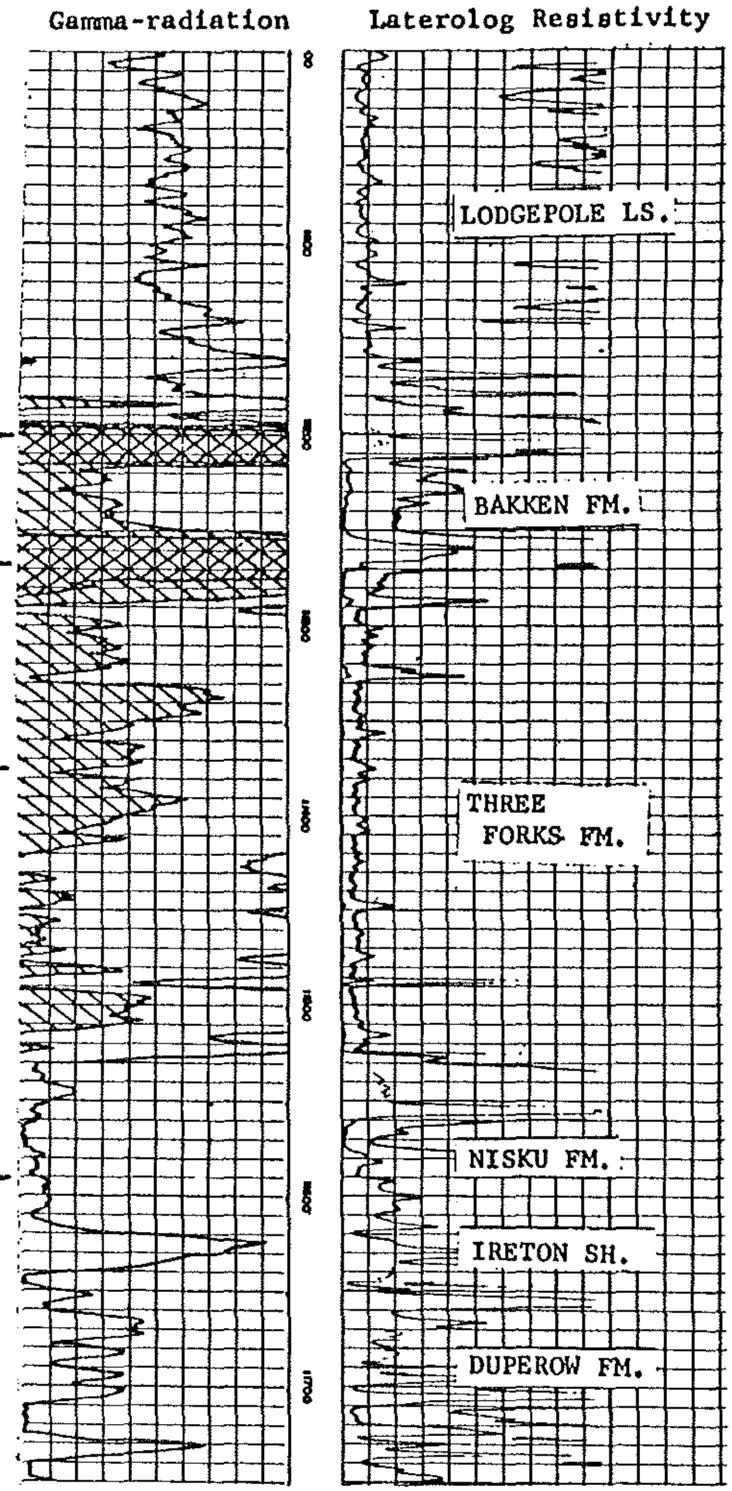

Carbonaceous shales can be recognized by the abnormally high gamma ray activity. Laterolog to right also shows higher resistivity in carbonaceous shale interval than in the other shale sections.

WILLISTON BASIN
NORTH DAKOTA

Figure 3-15

COAL BEDS

Coal beds are normally highly resistive with little or no S.P. development on electric logs. The electrical expression is, therefore, similar to other nonporous rocks such as dense basalt, cemented sandstone, dense carbonates, and evaporites. They can be easily recognized, however, if a velocity log or density log is available for comparison.

Unlike other nonporous sediments, coal has a low velocity, about 7,100 feet per second or a travel time of about 140 microseconds per foot. The density of coal is 1.0-1.8 gm./cc.

The accompanying example, Figure 3-16, shows the comparison of the electric log and Sonic log opposite a relatively thick coal bed. The density log can also be used to distinguish coal from other high resistivity rocks if the hole is not badly eroded.

Fractured coal may look like a good oil sand on an electric log, and if fractured sufficiently to form a mud cake, it will look like a sand on the microlog. (Figure 3-17). A velocity or density log is therefore essential for proper identification.

COAL BED
ELECTRIC LOG AND VELOCITY LOG
POWDER RIVER BASIN, WYOMING

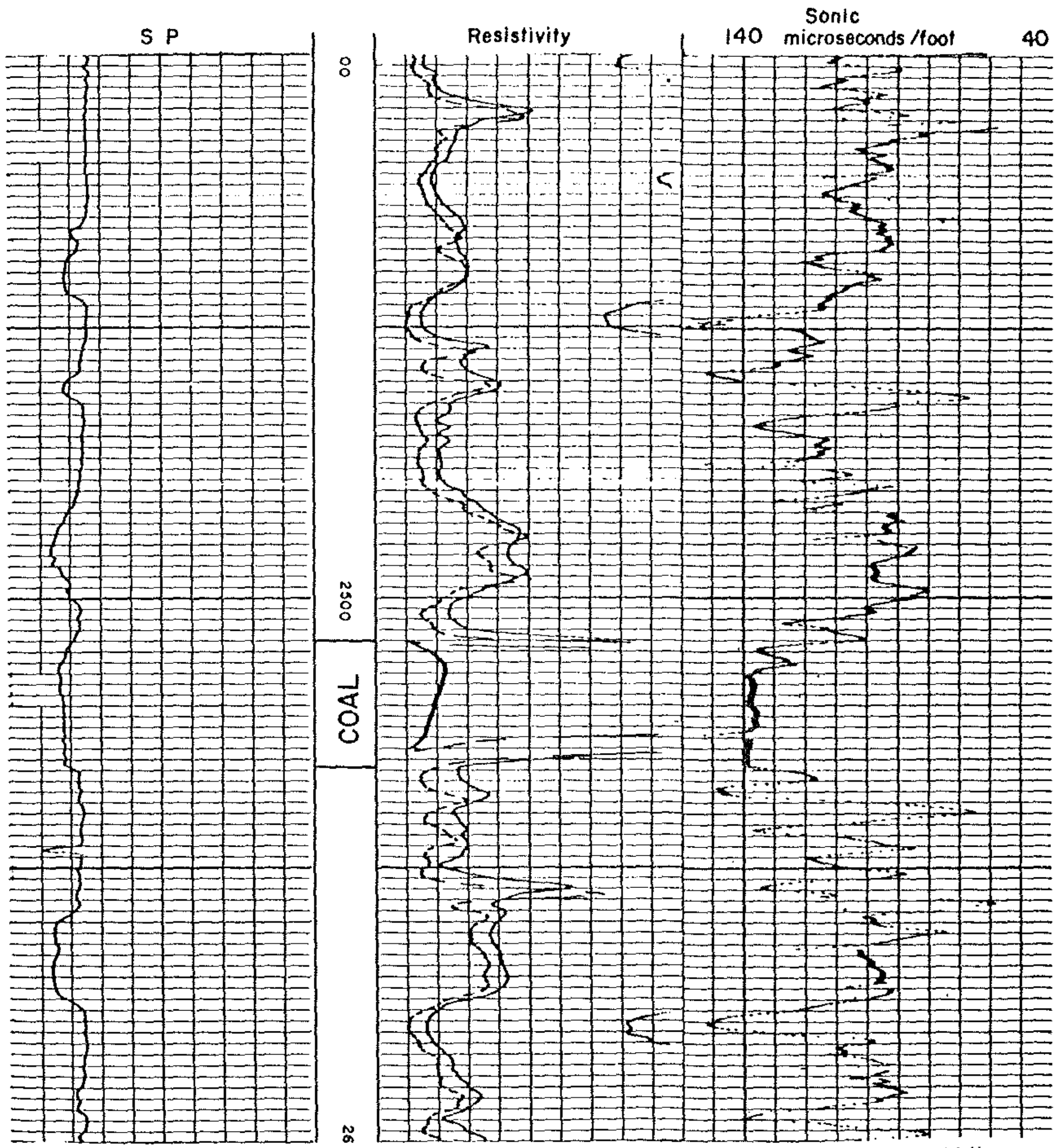

Figure 3-16

COAL
TERTIARY FORT UNION FM OF THE POWDER RIVER BASIN
BIG HORN CO., MONTANA

This is an example of a fractured coal bed displaying SP development, filter cake buildup, and positive ML Separation, all of which are similar to overlying and underlying sandstones. Lack of a velocity log to differentiate this coal from sandstones, and lack of good sample quality, could lead to the misinterpretation as an oil bearing sand in view of the very high accompanying resistivity. A good methane gas kick accompanied the drilling of this coal.

nelse 22-9s-43E
Hose Austin #1 Kendrick

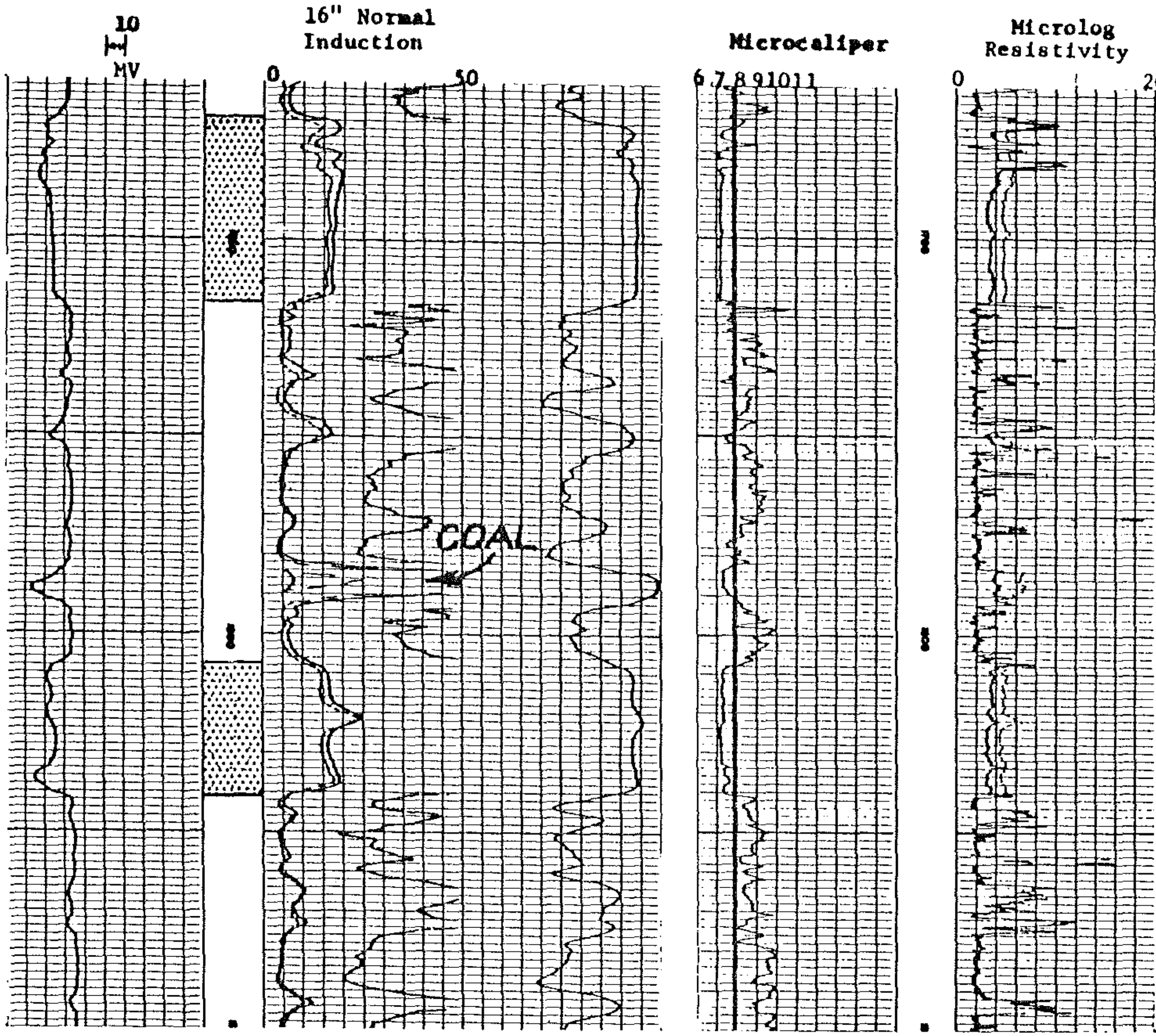

Figure 3-17

SANDSTONE REEFS

A high resistivity interval in a sand-shale section with low resistivities above and below may indicate hydrocarbons, a fresh water aquifer, a coal bed, or unusually low porosity. Figure 3-18 is a good example of the latter case, and shows why porosity logs are now run in all exploratory wells.

Aside from quantitative evaluation there may be geological significance to a porosity change such as that shown on Figure 3-18. In this case we are looking at a calcareous sandstone member of the upper Miocene Santa Margarita formation which is probably the cliff-forming Ostrea titan-Pecten estrellanus reef exposed in canyons north of Coalinga, California.

SANDSTONE REEF

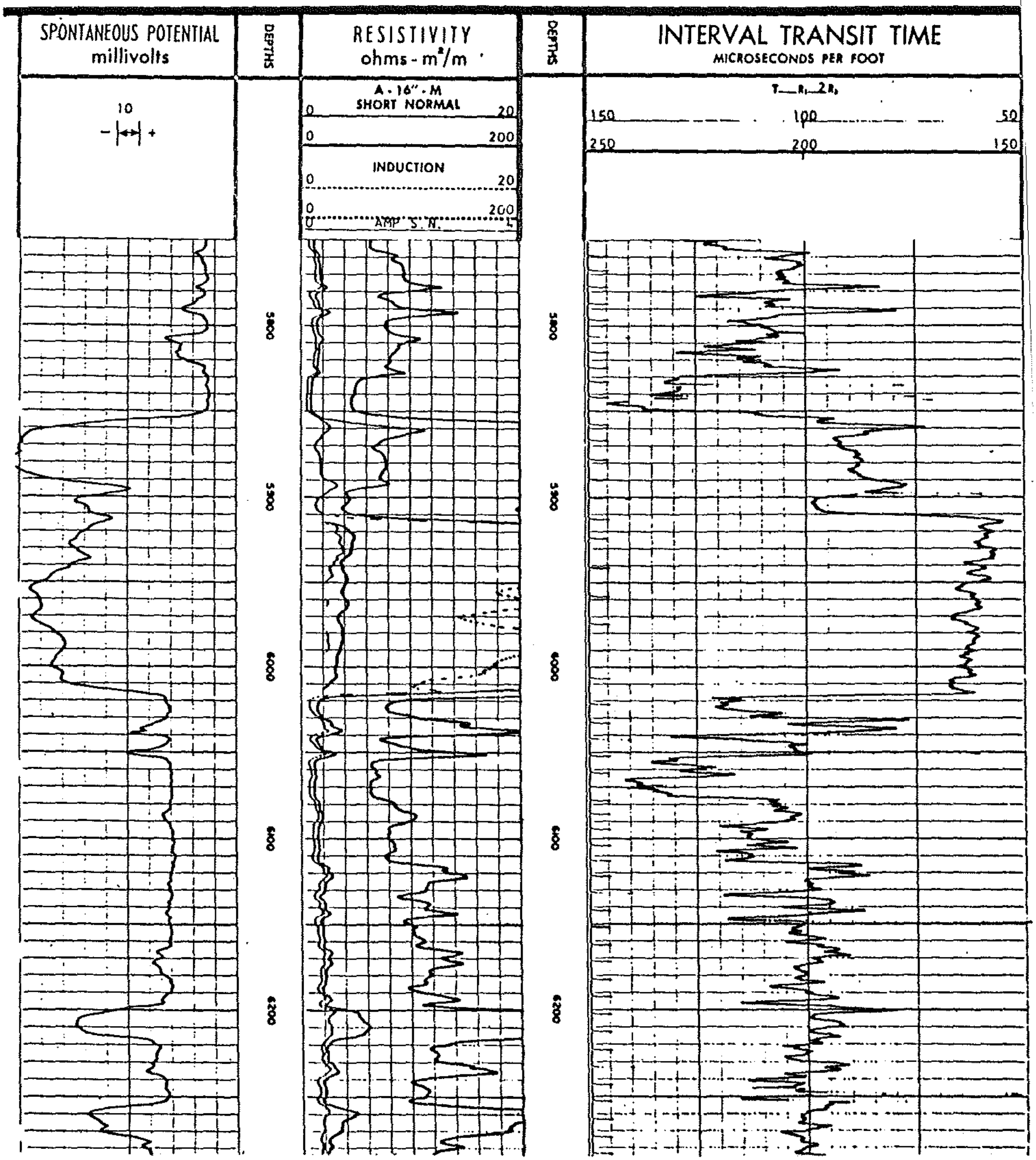

Figure 3-18

CARBONATES AND EVAPORITES

LIMESTONE VS. DOLOMITE

With the advent of the continuous velocity log and the density log we can now distinguish clean limestone from clean dolomite by comparison with the neutron log. In a carbonate section the velocity log and the density log are affected by both lithology and fluid in the pore spaces whereas the neutron log responds primarily to the amount of hydrogen in the rock. In pure carbonates all of the hydrogen will be in the pore spaces. Consequently, the lithology does not affect the neutron log.

Figure 3-19 shows a comparison between the neutron log and the Sonic log in the "B" zone of the Aneth Field. Two intervals, 5491'-95' and 5537'-44', appear to have the same maximum porosity on the neutron log but show much different values on the Sonic log. The upper interval is limestone with a matrix velocity of about 21,000 feet per second, whereas the lower interval is dolomite with a matrix velocity of about 24,000 feet per second.

c/sw/nw, 9-T41S-R24E, Standard Oil, #12-9 Navajo

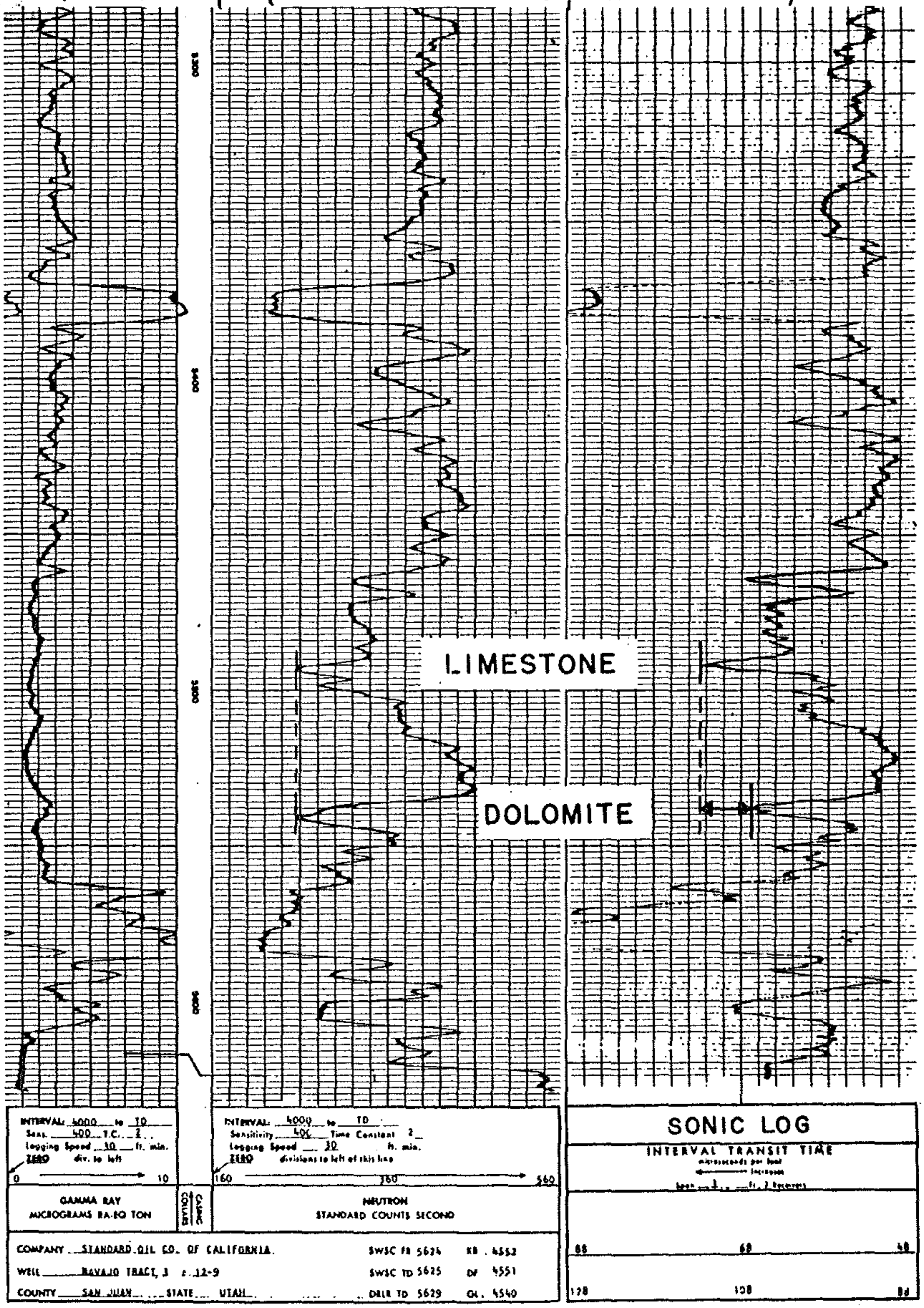

Figure 3-19

DOLOMITE CAVERN
ANADARKO BASIN, OKLAHOMA

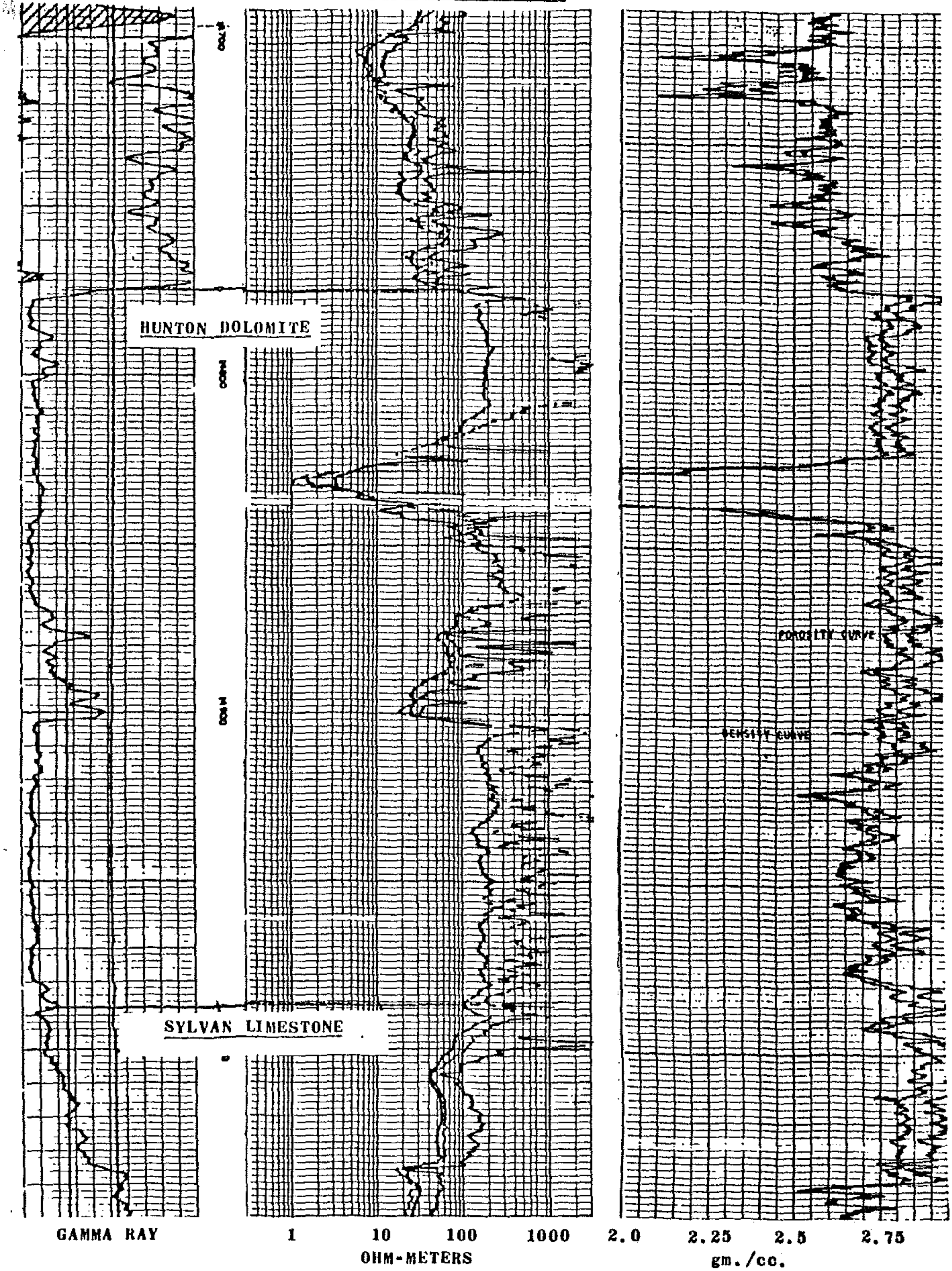

Figure 3-20

VERTICAL FRACTURES

Vertical fracturing in carbonates may be detected by comparing different types of resistivity curves with acoustic velocity and amplitude logs as on Figure 3-21.

The formation is Ellenburger dolomite in the Texas Panhandle. The Sonic log shows the consistent low porosity of the matrix throughout this interval. However, from 12,210-12,324 feet the ILd is reading higher than the LL8 whereas above and below this interval the relationships are normal. This is believed to be due to near vertical fracturing in this interval where the LL8 current is somewhat short-circuited by the mud in the fractures whereas the LLd current cannot be short-circuited in this manner.

It will be noted that the ILm also reads higher than the LL8 in the upper part of this interval but in the lower part, the two curves average about the same. This might be interpreted as an inconsistency in the thesis. However, there is considerably more difference in the ILd and LL8 resistivities in the upper part of the interval than the lower. The failure of the ILm to conform to the theory is believed due to the poorer resolution at higher resistivities of the ILm.

The fact that the Proximity log sometimes reads higher and sometimes reads lower than the other logs is believed due to the directionality and sampling volume of the device. If a fracture(s) is within the sampling volume (i.e., more or less parallel to it), the "short-circuiting" occurs and the reading is low. If the sampling volume consists of matrix only, the reading is high.

This thesis is confirmed by the shear wave amplitude log and by DST. Substantially more permeability was indicated by the test of this zone than would normally be inferred from the low porosity shown by the Sonic log.

VERTICAL FRACTURES

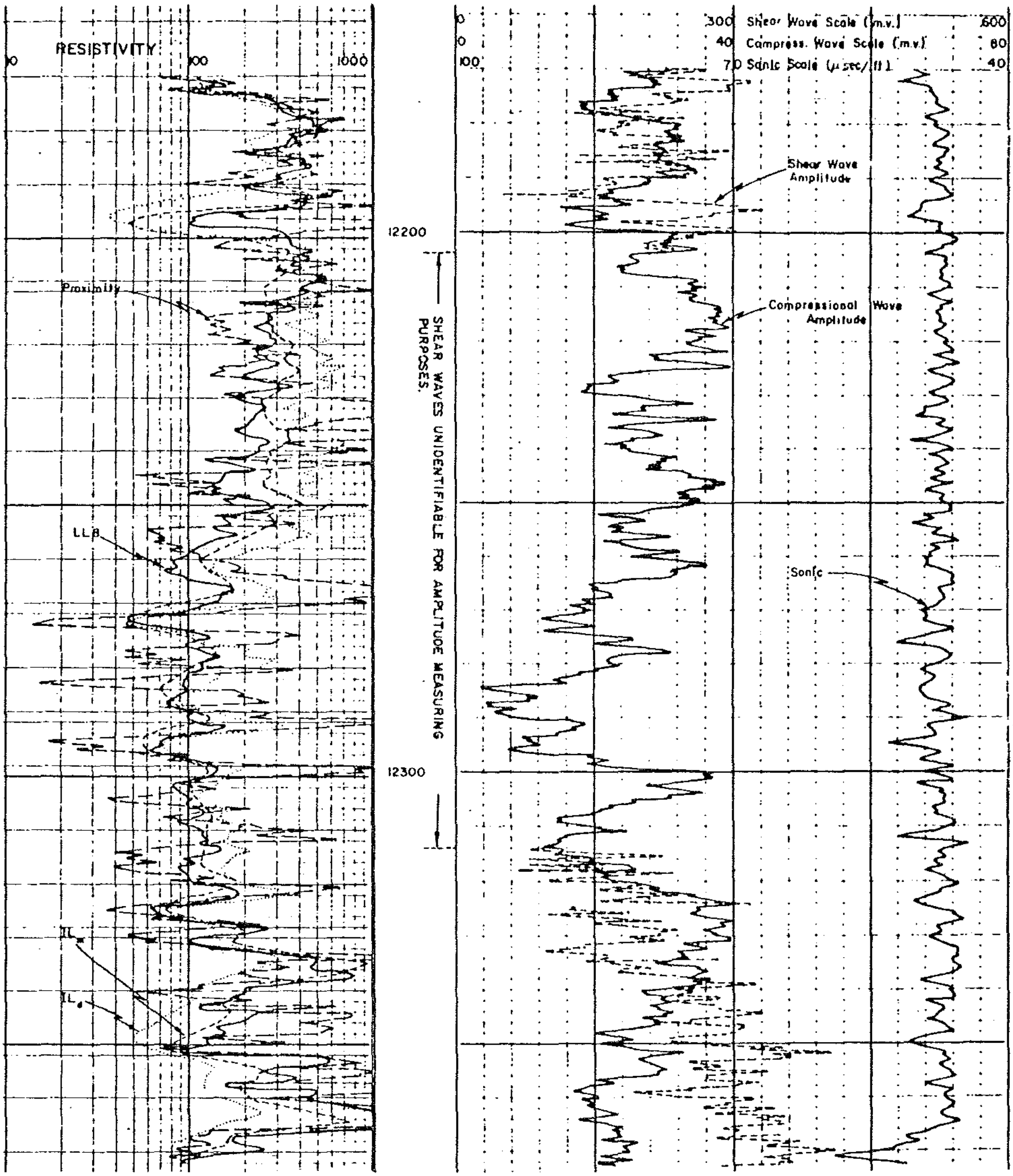

Figure 3-21

ANHYDRITE

Anhydrite is a dense rock which cannot be distinguished from other nonporous rocks on electric logs. Its velocity (20,000 feet per second) is similar to that of low porosity limestone. The gamma ray log shows it to be nonargillaceous with an expression similar to that of pure carbonates.

The density log, however, distinguishes anhydrite from all other common sediments. As shown on Figure 3-22, the bulk density is the same as the grain density, 2.95 gm./cc. The dotted line on the density log shows bulk density from core analysis. Although the anhydrites were partially cored, no analyses were run.

The example is from a well in the Paradox Basin near Blanding, Utah. The formation is upper Paradox of Pennsylvanian age.

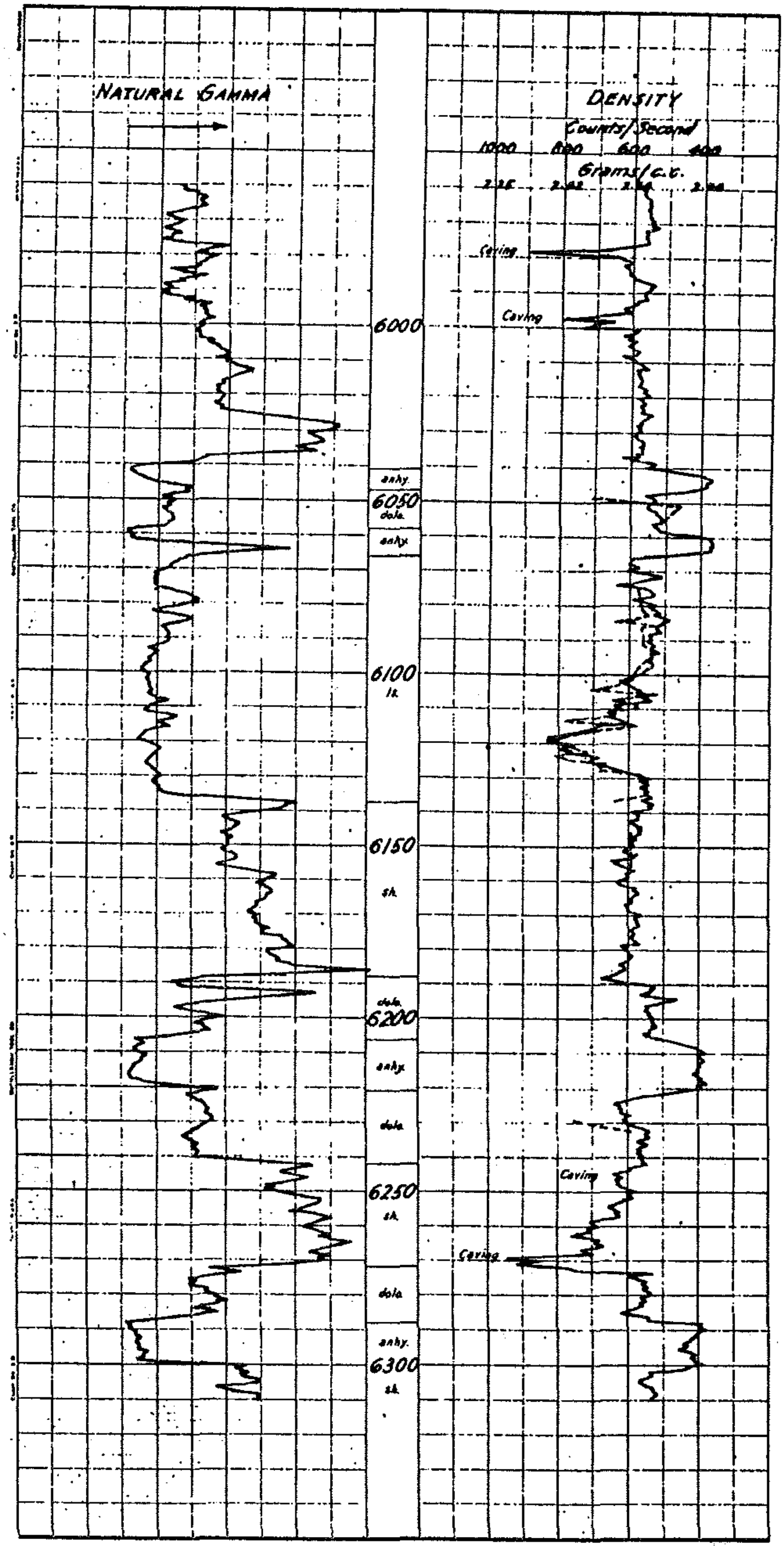
NATURAL GAMMA
DENSITY
Counts/Second
1000 800 600 400
Grams/c.c.
Caving
Caving
6000
anhy.
6050
dolo.
anhy.
6100
ls.
6150
sh.
dolo.
6200
anhy.
dolo.
Caving
6250
sh.
Caving
dolo.
anhy.
6300
sh.

Figure 3-22

SALT AND ANHYDRITE

Distinguishing between salt and anhydrite in an evaporite sequence can be a difficult problem with nothing but regular electric logs, radioactivity logs and cuttings. Salt and anhydrite are both dense rocks which show similar characteristics on electric and radioactivity logs, i.e., high resistivity, no S.P., low gamma, and high or low neutron depending upon hole effect and hydration. Anhydrite can be recognized in cuttings, but salt (halite) is seldom recovered because of its solubility. If salt muds are used, as is customary in evaporite section, the effect of salt beds on the mud is negligible.

Until the development of velocity logs, the caliper log was the most definitive tool for locating salt beds. Figure 3-23 shows how salt and anhydrite can be distinguished on the Sonic log by their velocities. Rock salt has a velocity of 15,000 feet per second compared with 20,000 for anhydrite or a transit time of 66.7 micro-seconds per foot compared with 50 for anhydrite.

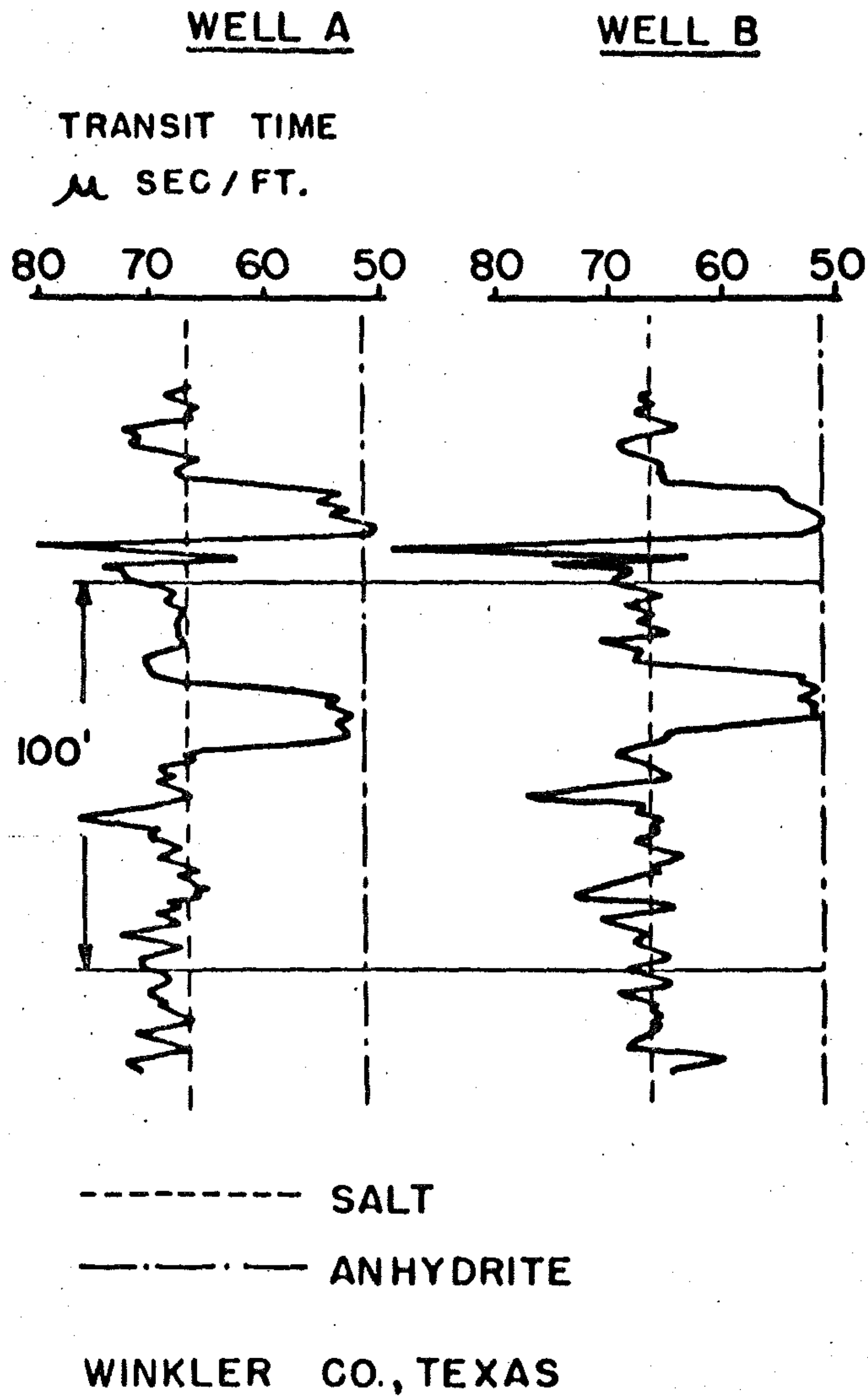

WELL A
WELL B
TRANSIT TIME
μ SEC / FT.
80 70 60 50
80 70 60 50
100'
SALT
ANHYDRITE
WINKLER CO., TEXAS

Figure 3-23

[redacted]

SALT (NaCl) IDENTIFICATION

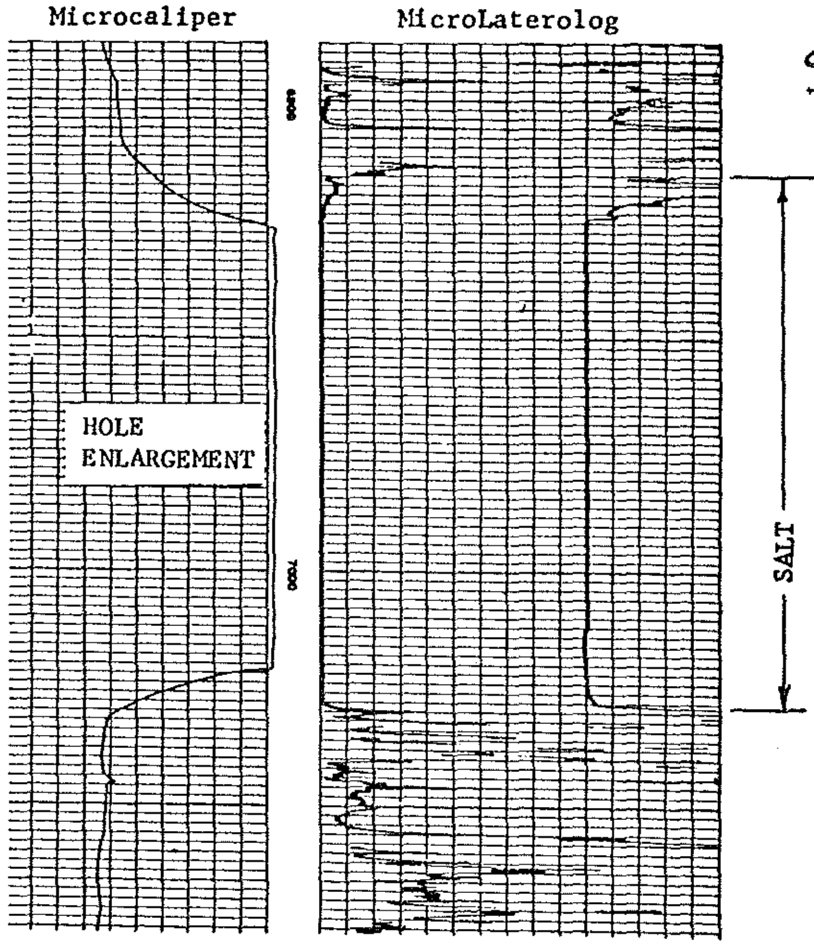

PARADOX BASIN COLORADO

c/nw/nw, 22-33N - 19W, The California Company, #1 Ute Tribal, Montezuma, County

Sodium chloride has the logging properties of low gamma radiation, high neutron and high resistivity. However, all of these properties may not be apparent on many logs. The solubility of salt in drilling fluid may result in considerable hole enlargement. If the hole enlargement is greater than the depth of investigation of the survey, the drilling fluid becomes the investigated medium. The MicroLog, MicroLaterolog, Neutron and E.S. normal surveys may be affected by hole enlargement.

The upper example is a typical case where hole enlargement results in the log reading mud resistivity. The lower example shows very little hole enlargement by the caliper measurements and the high salt resistivity is recorded. The well with small hole enlargement was drilled with mud saturated with salt prior to drilling the interval shown.

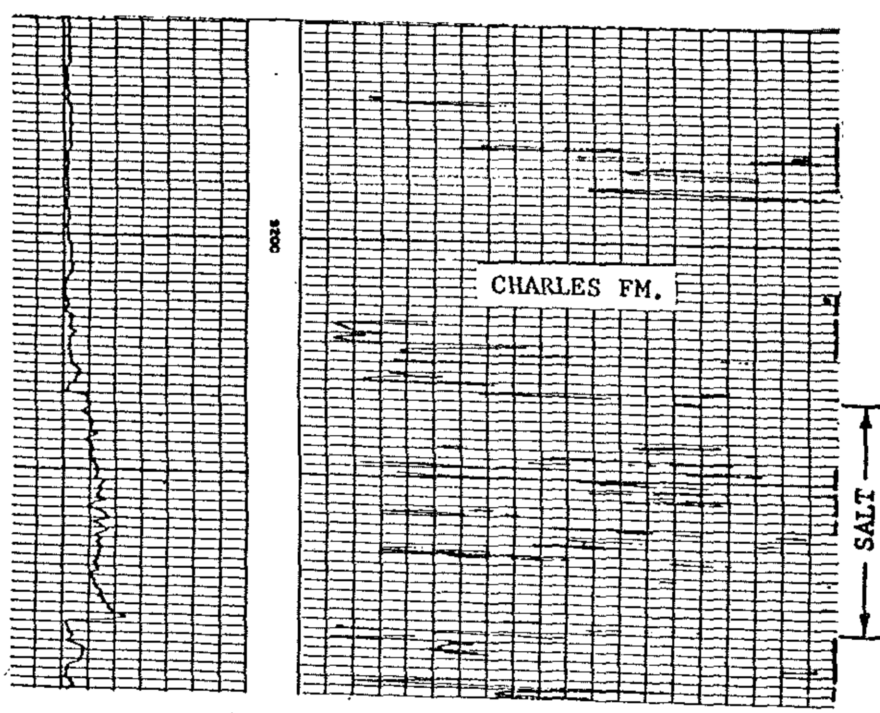

WILLISTON BASIN
NORTH DAKOTA

nw/sw 20-T148N-R97W, California Company, #1 Danielson Dunn County, North Dakota

Figure 3-24

SALT BED IDENTIFICATION

The following is summarized from "Salt Bed Identification from Unfocused Resistivity Logs," by J. R. Lishman, 1960, and for more detailed information the reader is referred to the original work.

ABSTRACT

Salt beds are almost infinitely resistive. They differ from other infinitely resistive beds in that they are usually soluble in the drilling fluid, and give rise to enlarged boreholes. An infinitely resistive bed, lying between shales, may be recognized from the characteristic shape of the electric log resistivity curves, and the ratios of the apparent resistivities which they show. Any one of the curves may then be used to compute the hole diameter, and hence decide whether the bed is salt.

When a washed out salt bed lies adjacent to another infinitely resistive bed in which the hole is to gauge, the configuration of the curves is characteristic. Apparent resistivity ratios again help to identify the salt.

* * * * *

Unless the hole diameter is known, the reading of any one curve cannot be used to determine whether a bed is of infinite resistivity. Ratios between curve readings, however, can be used. In beds of low to moderate resistivity, the reading of the 64" normal curve is never more than four times the reading of the 16" normal. However, in thick beds of high resistivity, the ratio is generally much higher than four. The R64"/R16" ratio is approximately 5 for an infinitely resistive bed 80' thick and ratio increases with increasing bed thickness. For beds thinner than 80', the R64"/R16" ratio is less than 5, but for these beds the ratio of the 18' 8" lateral curve to the 16" normal curve ranges between 12 and 15.2.

BEHAVIOR OF ELECTRIC LOG RESISTIVITY CURVES IN SINGLE INFINITELY RESISTIVE BEDS

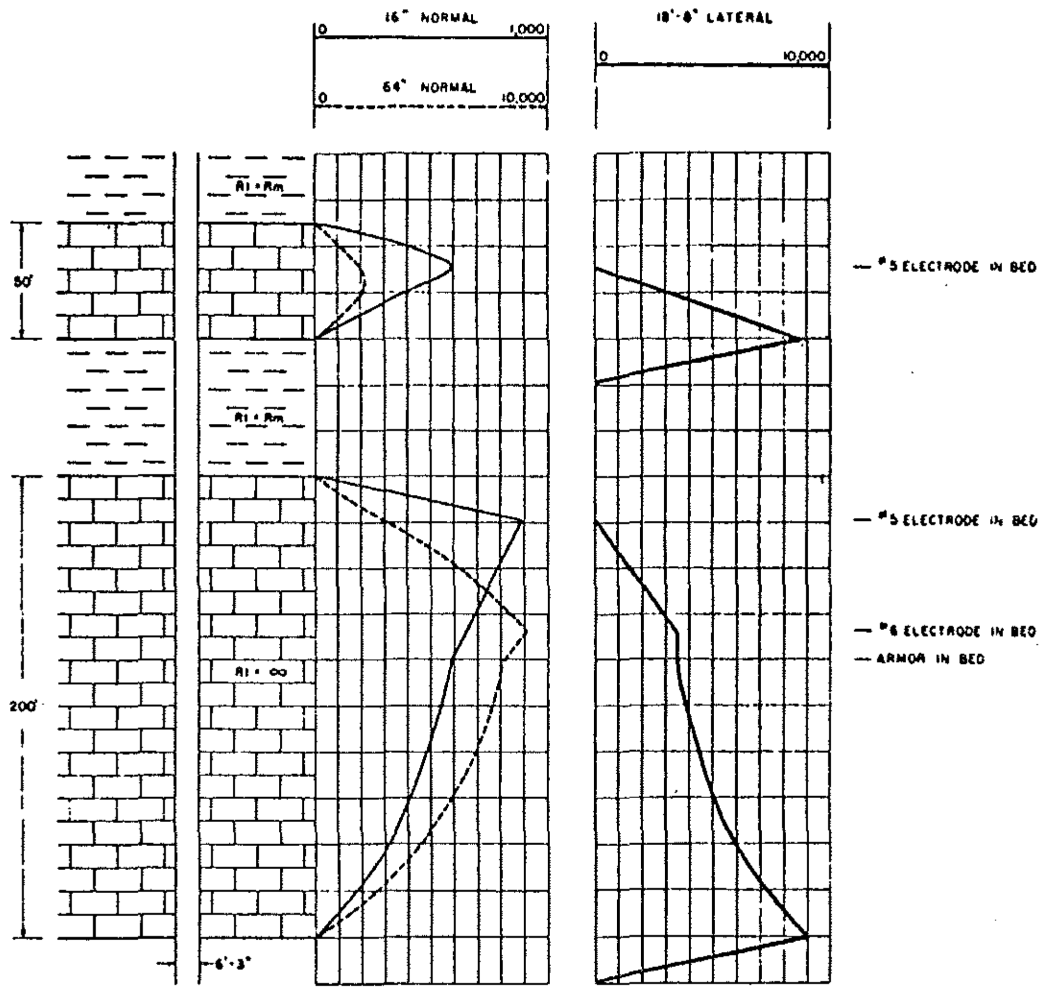

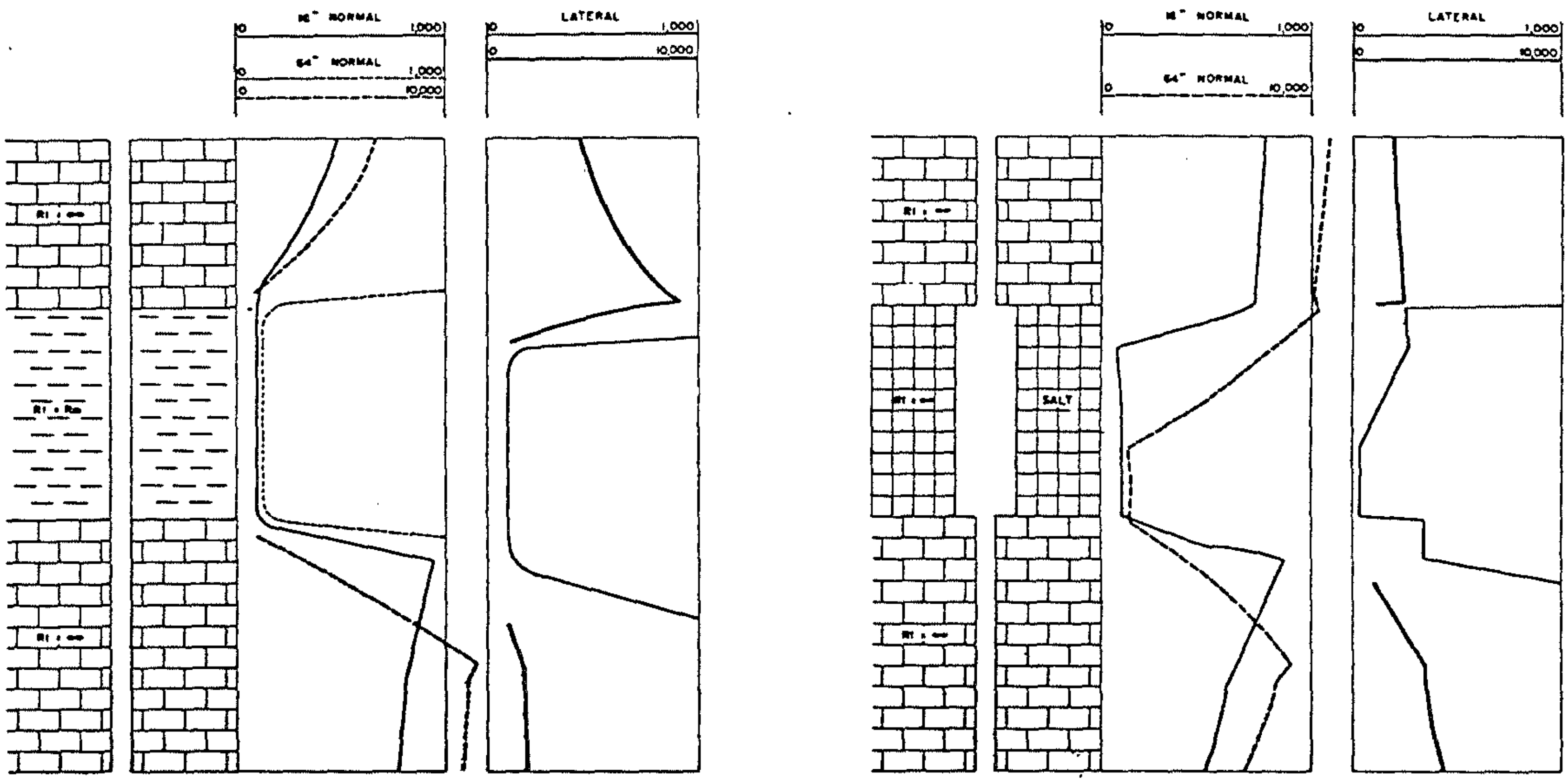

COMPARISON OF ELECTRIC LOG CURVES THROUGH A SHALE & A WASHED OUT ZONE
LYING BETWEEN BEDS OF INFINITE RESISTIVITY

Figure 3-26

COMPARISON OF THEORETICAL ELECTRIC LOG CURVES
THROUGH A SALT BED WITH AN ACTUAL LOG
RM FOR THEORETICAL CURVES = .05

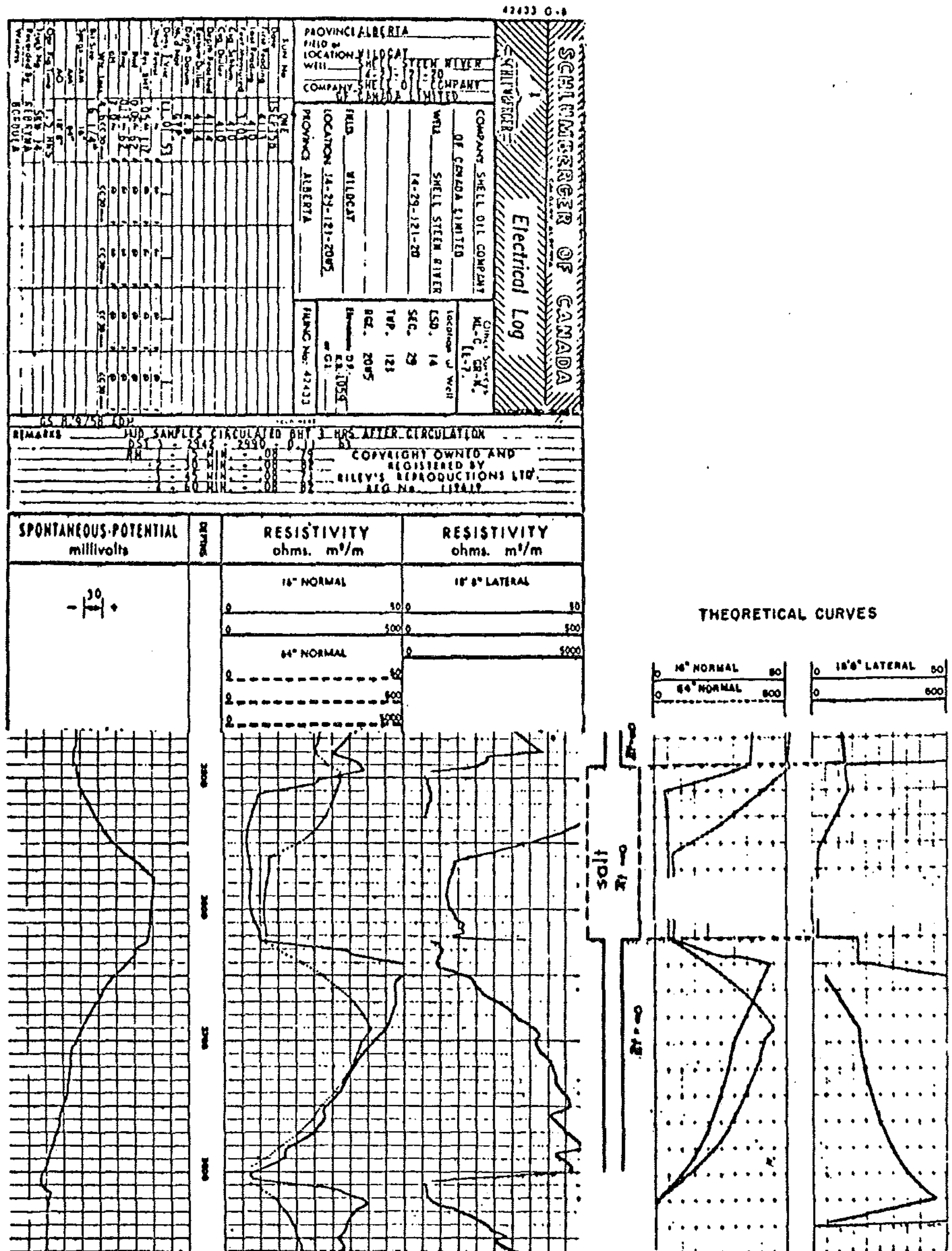

Figure 3-27

POTASH

Potash (sylvite) can easily be distinguished from salt (halite) on gamma ray logs and used as marker beds in saline basins (Figure 3-28). These logs are from two wells in the northern part of the Paradox Basin, Grand County, Utah.

As in glauconite, the radioactive isotope of potassium, K-40, accounts for the high gamma response. The average K-40 content in naturally occurring potassium is 0.0119% as compared with 93.08% K-39 and 6.9% K-41, the stable isotopes.

Sylvite, being a dense rock like halite, shows a similar response to other dense rocks on the neutron log. Potash beds, therefore, cannot be confused with radioactive shales or porous glauconitic sands when gamma ray and neutron logs are used together.

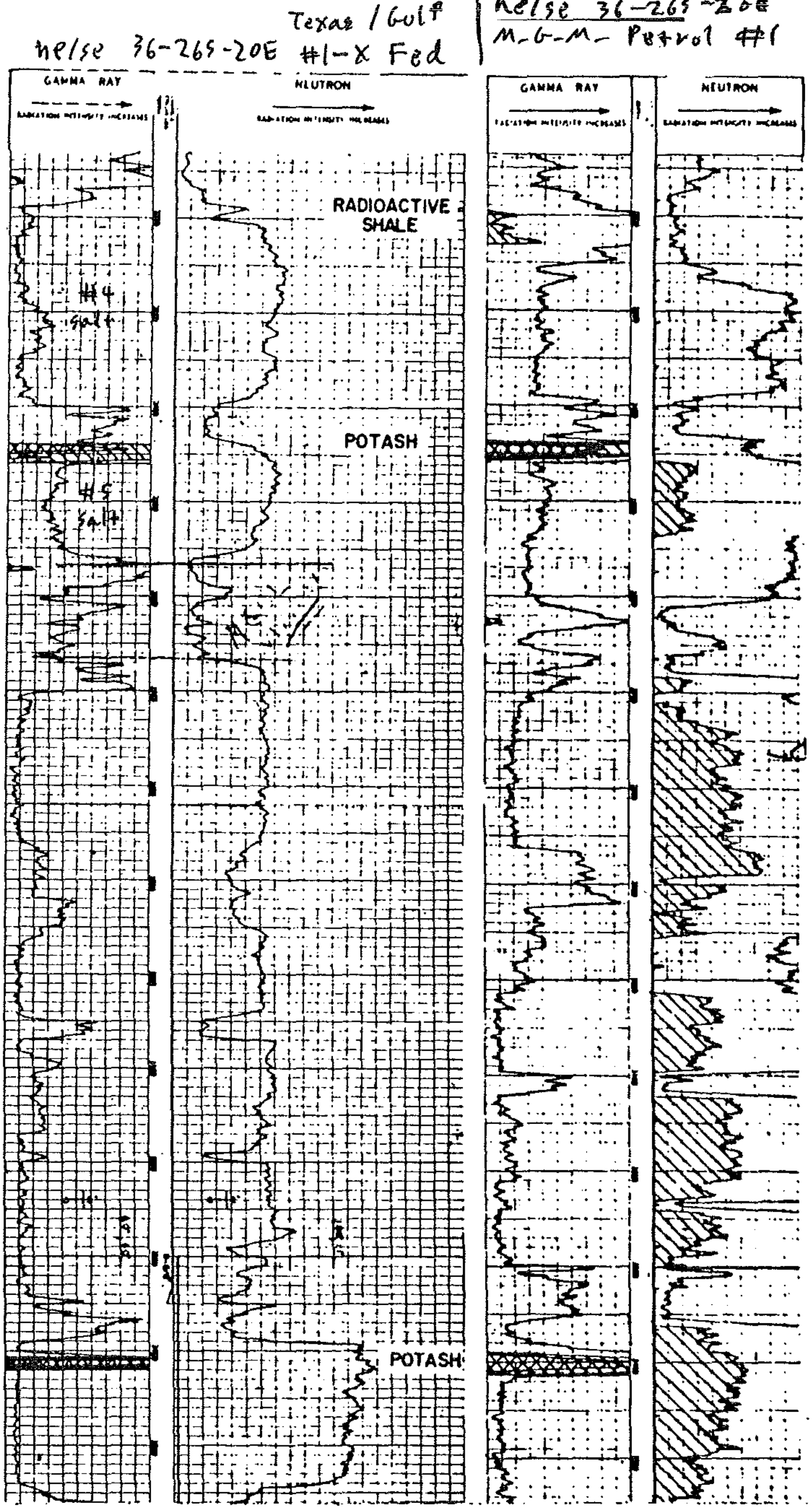
Texas / Gulf
ne/se 36-26s-20E #1-X Fed
M-G-M- Petrol #1
GAMMA RAY
NEUTRON
RADIOACTIVE SHALE
#4 salt
POTASH
#5 salt
POTASH

Figure 3-28

VOLCANICS

Figure 3-29 shows the typical appearance of dense nonfractured basalt on an electric log. The resistivity is very high and the S.P. departure low. The S.P. curve also has the rounded, sluggish appearance which is a characteristic of dense rocks.

Unfortunately, however, dense, nonfractured basalt represents but a small portion of the total section of volcanics in many areas, and it is difficult, if not impossible, to recognize most volcanic rocks by the electric log alone. Pyroclastic deposits may run the whole gamut from dense rocks to sands and shales depending upon size of particles, alteration and cementation, and flows may be sufficiently fractured or vesicular as to approximate the appearance of fractured cherty shales, fractured or vugular limestone, or conglomerates.

Consequently, unless the volcanics in a particular area are known to be solid flows, cuttings and core samples are essential for electric log interpretation. A gamma ray log, if available, may also help considerably because volcanic sediments normally show higher natural radioactivity than other sediments. Hydrous silica or opal in vitric tuff may be identified from the density log. (Figure 3-30).

Figure 3-31 shows an electric log very similar in character to Figure 3-29. In this case, however, two of the highly resistive intervals are tar sands. As explained on Page 19 and illustrated on Figure 3-32, a velocity log will distinguish tar sands from dense basalt.

VITRIC TUFF AND VOLCANIC SANDS
WEST SIDE COOK INLET, ALASKA

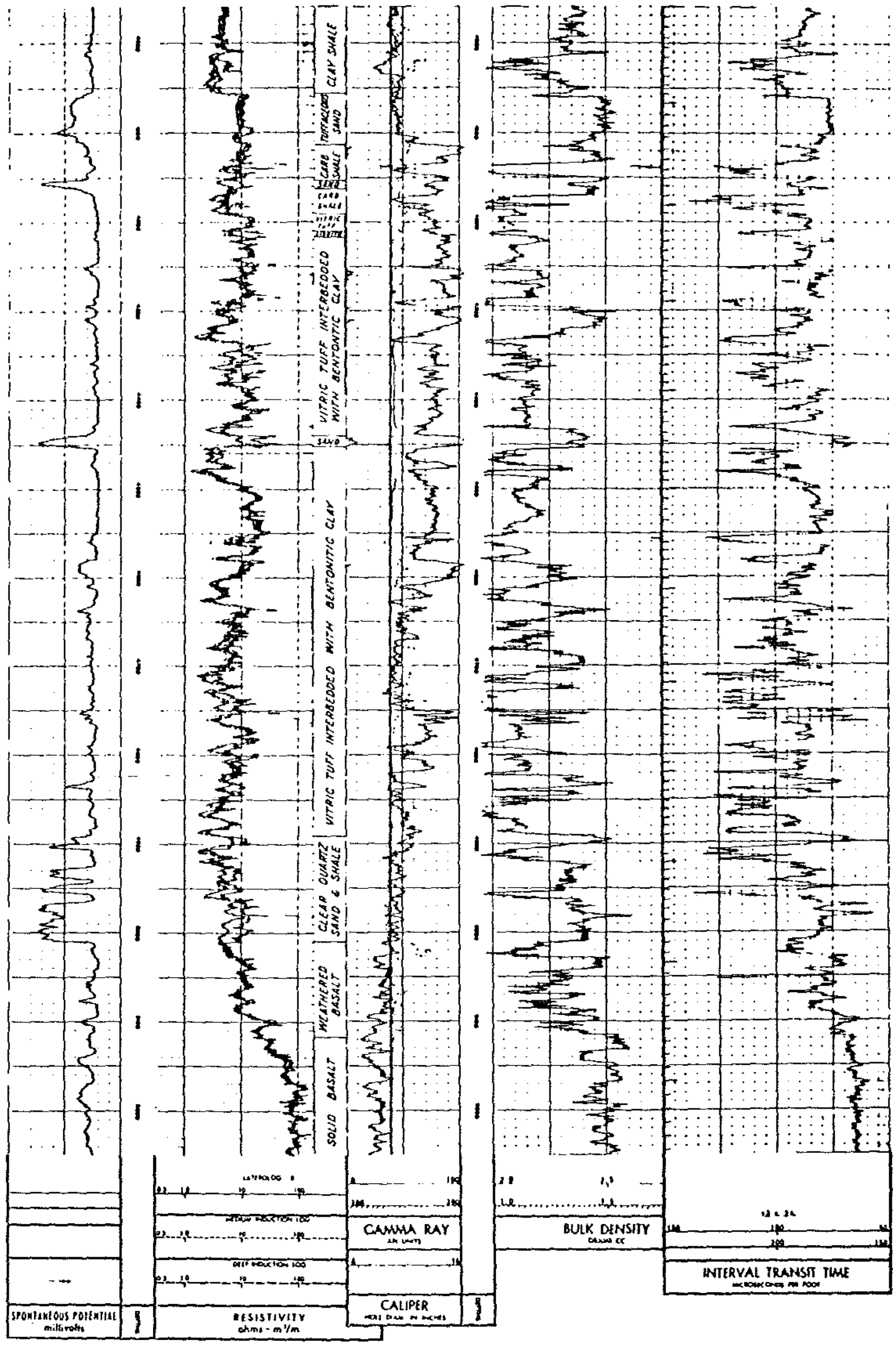

Figure 3-30

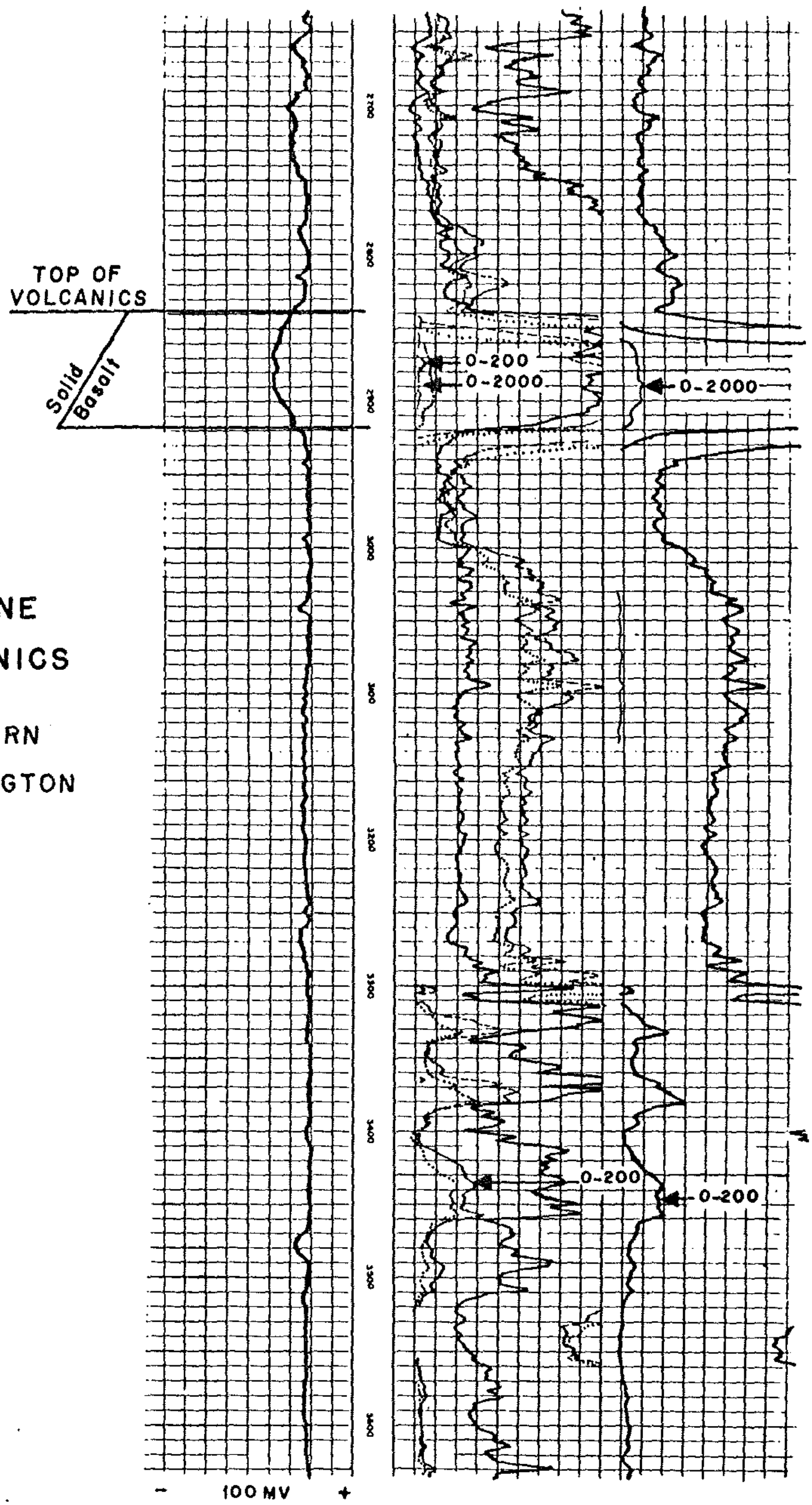

EOCENE VOLCANICS

WESTERN WASHINGTON

Figure 3-29

SHALLOW, UNCONSOLIDATED TAR AND GAS SANDS

As shown on Figure 3-32, continuous velocity logs are excellent for identifying shallow tar sands and gas sands because of their abnormally low velocities. In the tar sands the velocity approaches that of tar itself as the sand grains in these loose sands are literally floating in tar. In the unconsolidated gas sands, the low velocity is attributed to a combination of compaction and the attenuation effect of gas bubbles in the pore spaces.

On the example, which is from Huntington Beach, California, A-C are shown by the mud log to be tar sands and D-K are probably low productivity gas sands.

Similar low velocities have been noted in partially aerated sands at shallow depths.

TAR SANDS AND VOLCANICS

OXNARD AREA CALIFORNIA

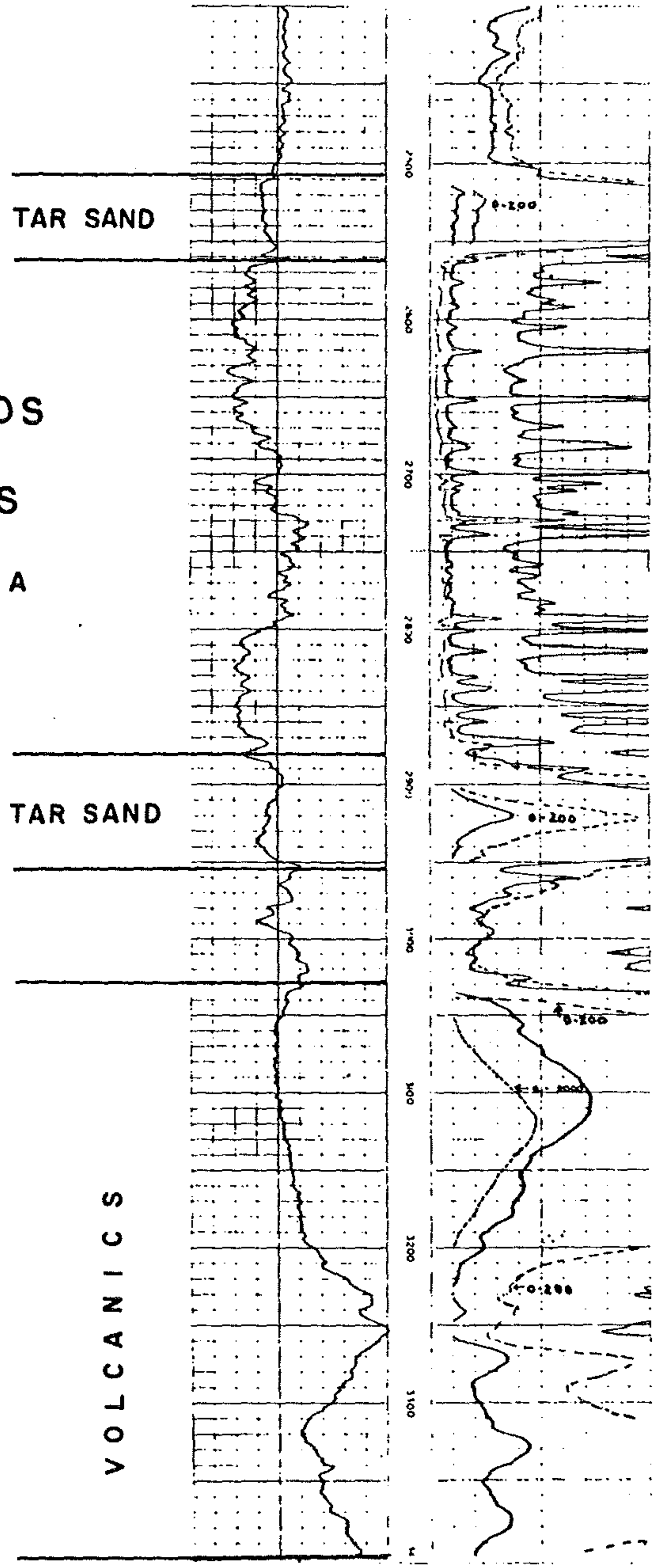

Figure 3-31

[redacted]

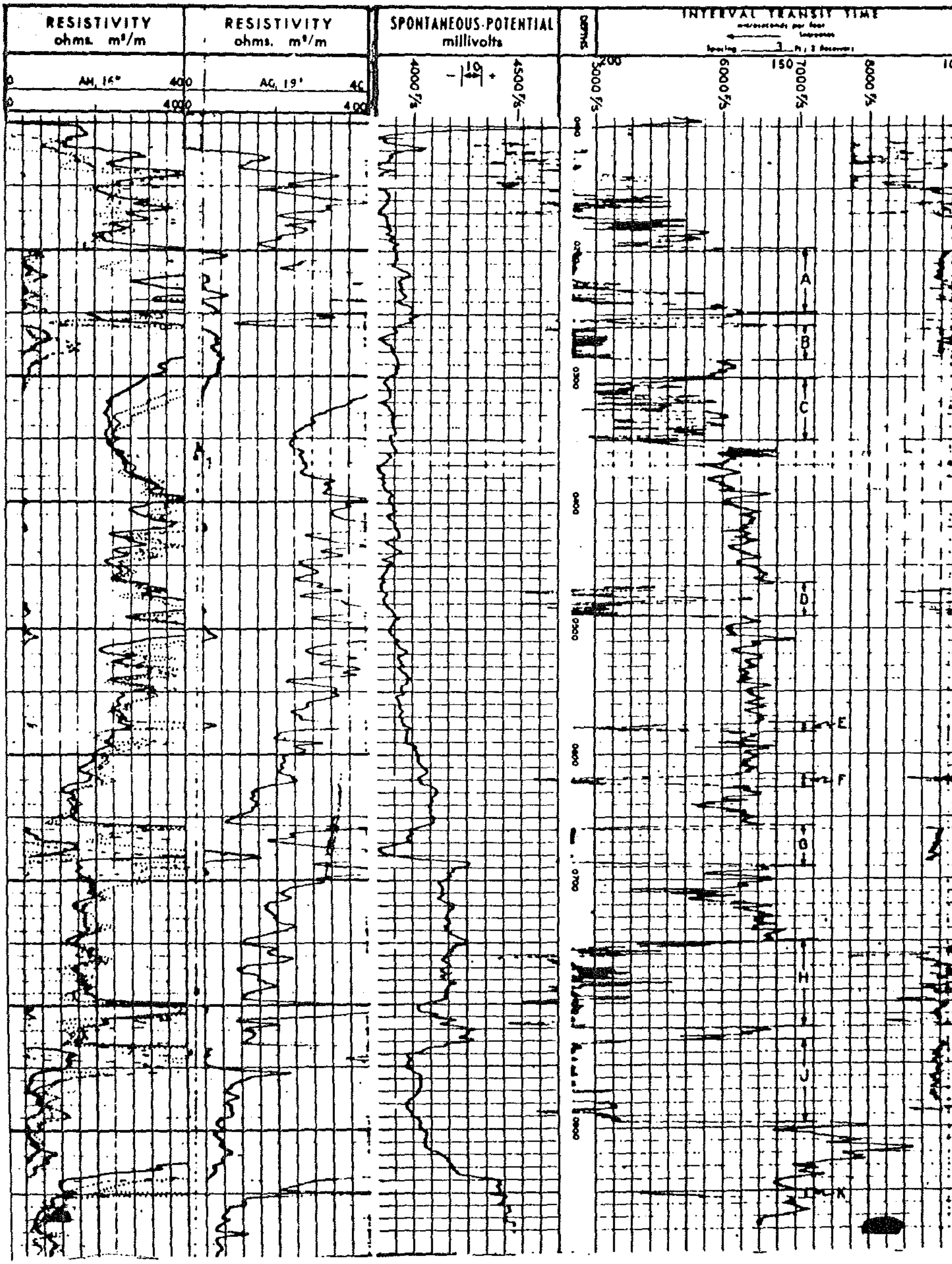

Figure 3-32

MINERALIZED ZONE

Mineralized zones, which are commonly associated with volcanic dikes, can sometimes be recognized on electric logs by unusually low resistivity and erratic (usually negative) S.P. departure. The unusually low resistivity is caused by metallic conductivity of mineral veins and the S.P. is affected by oxidation potentials.

On the example I-ES log, Figure 3-33, the mineralized zones are immediately above and below a volcanic dike or sill at 9315'-9470', and at 9940'-9970'. The lower zone may have been connected to the dike by a high angle fracture or fissure. The vein mineral primarily responsible for the metallic conductivity in this well is pyrite, which was recovered in large amounts in cuttings samples from the three zones.

The geologic significance is obvious because any oil accumulation predating the dike or sill would be dissipated from the volume of sediments affected by the intrusive.

MINERALIZED ZONES

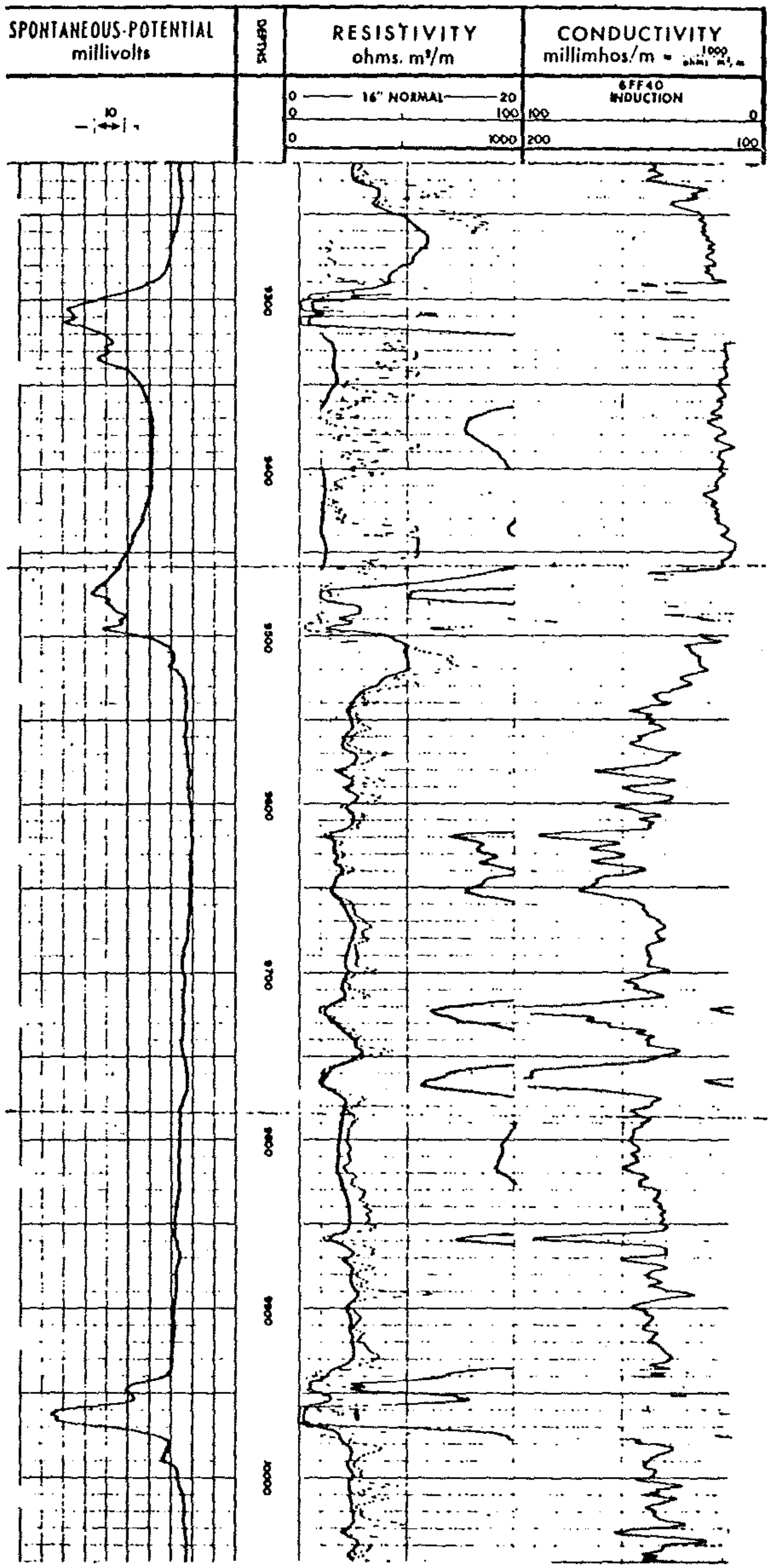

Figure 3-33

BASEMENT ROCKS

The term "basement" usually denotes any igneous or metamorphic complex which lies beneath the sedimentary section. Igneous basement rocks are usually referred to as "granitic basement" and the metamorphics are identified by rock type, geologic age, or formation name like "Franciscan basement" in California.

Solid granitic basement is easily recognized on electric logs, as shown on Figure 3-34, but if the rock is deeply weathered or covered with a basal conglomerate, or granite wash, containing large granitic boulders, a solid core 20 feet or more in length may be required to distinguish true basement from overlying sediments. (Figure 3-35).

Metamorphic basement is usually not as well defined on electric logs because these rocks are normally fractured and/or deeply weathered, resulting in a secondary porosity which may equal or exceed the porosity of overlying sediments. For example, fractured schist normally resembles fractured, cherty shale in electrical character and weathered serpentine may be indistinguishable from argillaceous shale. Consequently, good lithologic information may be necessary for electric log interpretation. If density and/or velocity logs are available, however, top of basement is usually well defined because of the higher grain densities and matrix velocities of most metamorphic minerals compared with overlying sediments. (See Figures 3-14 and 3-36).

GRANITIC BASEMENT

TEJON AREA
CALIFORNIA

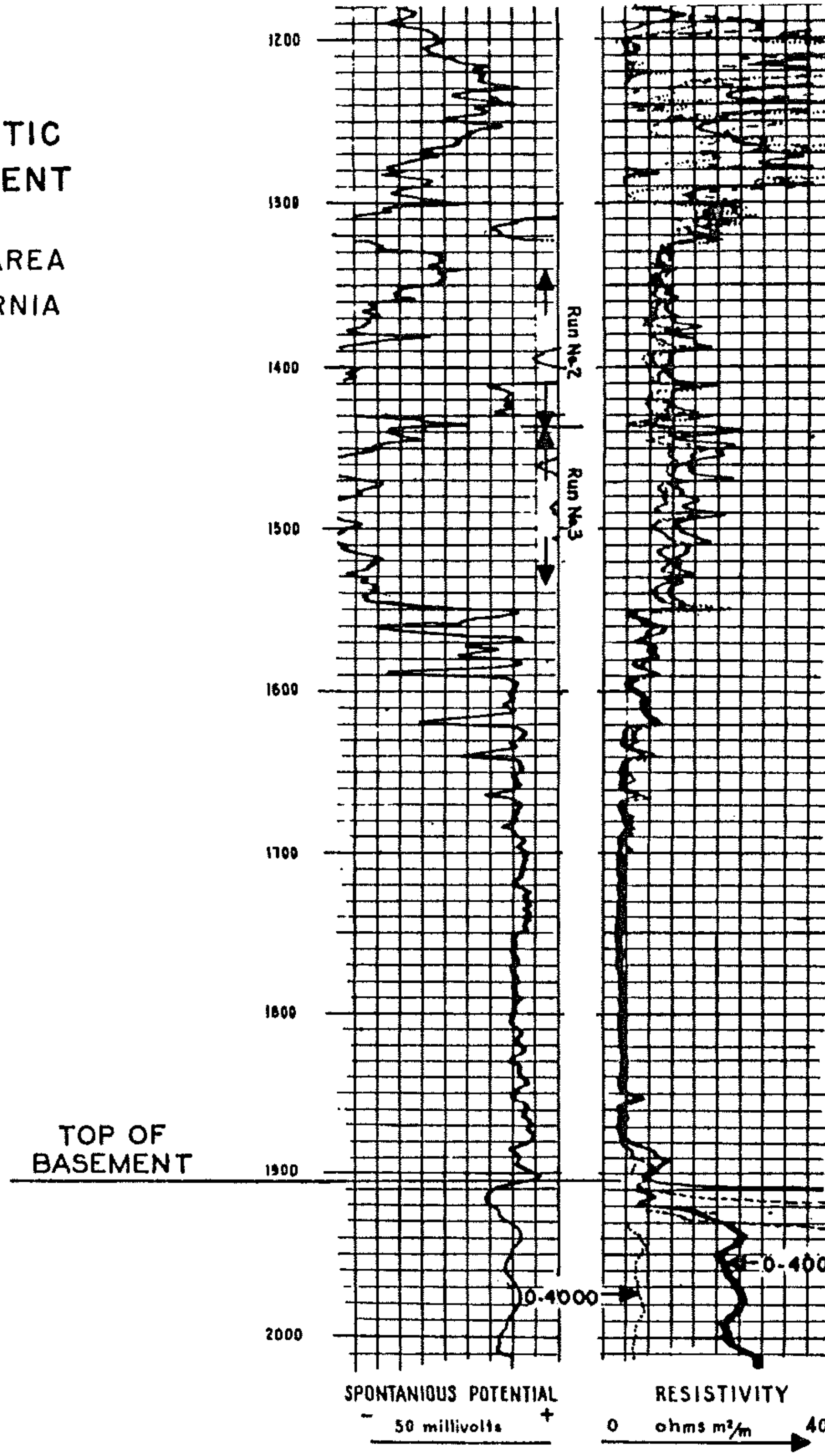

Figure 3-34

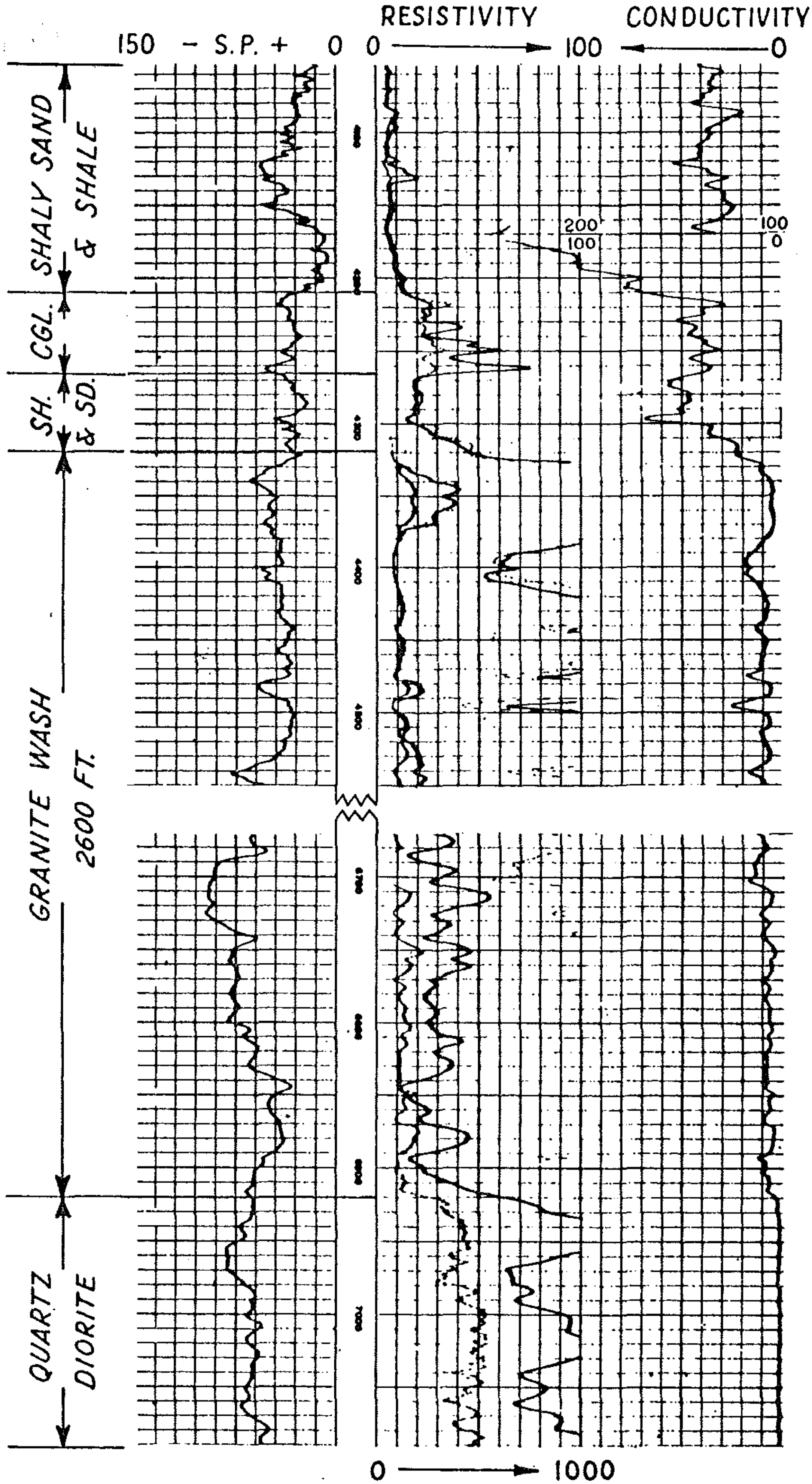
RESISTIVITY
CONDUCTIVITY
150 – S.P. + 0
0
100
0
200
100
100
0
SHALY SAND & SHALE
CGL.
SH. & SD.
GRANITE WASH 2600 FT.
QUARTZ DIORITE
0
1000

Figure 3-35

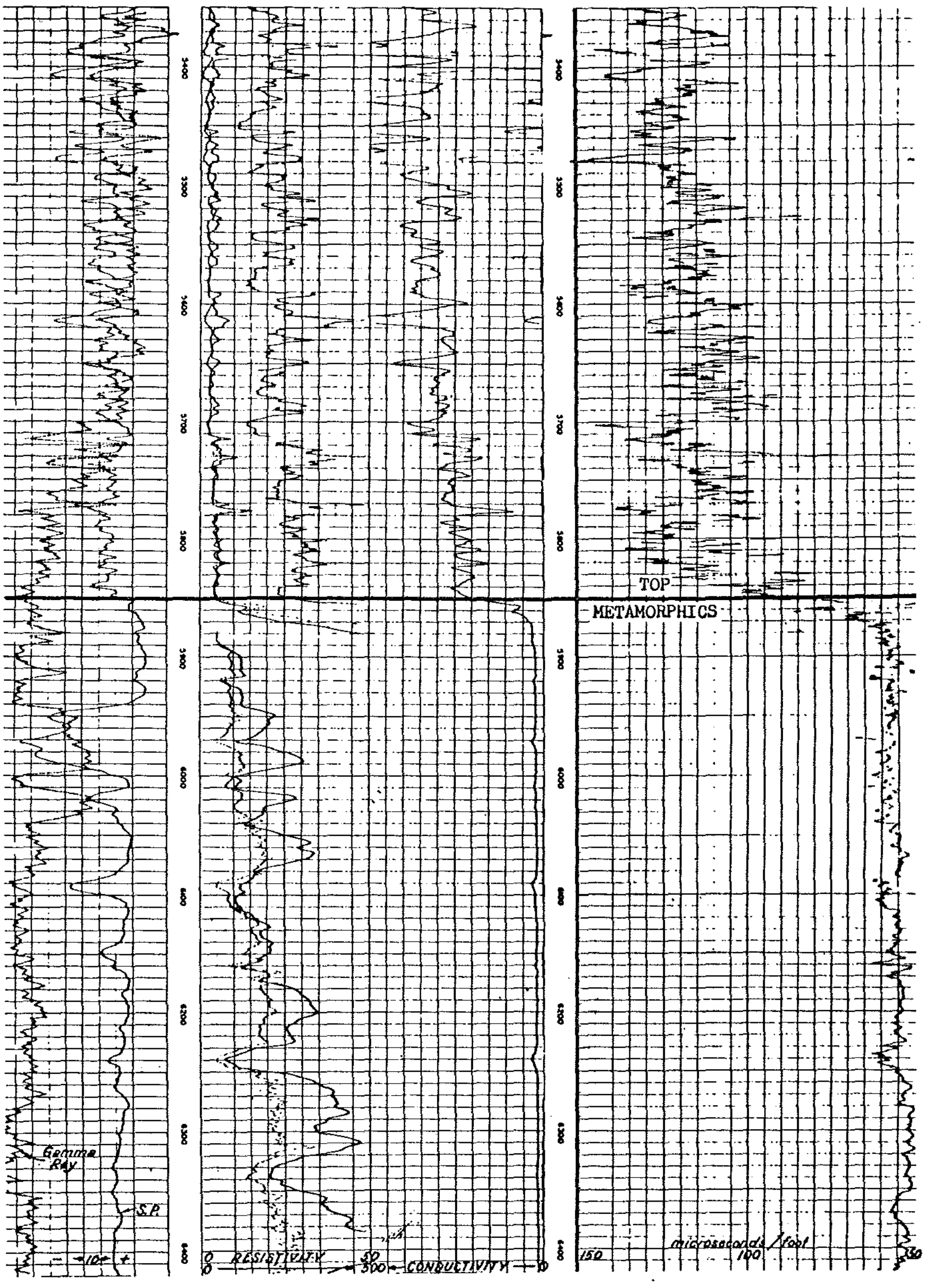
TOP
METAMORPHICS
Gamma Ray
S.P.
10
+
0 RESISTIVITY 50
0 500 CONDUCTIVITY 0
150 microseconds/foot 100

Figure 3-36

PART 4

STRUCTURAL INTERPRETATION FROM LOGS

STEEP DIPS

The effect of moderately steep dips on an electric log is an apparent thickening of equivalent intervals when compared with a log showing a normal section with low dips. If the dips are very steep, 50° or more, other effects become apparent as shown on Figures 4-1 to 4-4. In a thinly bedded section with contrasting resistivity (bedding anisotropy), the resistivity curves become rounded and flatten out because the depth of current penetration may include several beds, causing horizontal bed thickness effects in addition to the vertical effects which are dependent upon the ratio of bed thickness to electrode, or coil, spacing. In thick beds with relatively uniform resistivity and little or no permeability (no invasion effect), intervals of steep inhole dips may be detected by the effects of micro-anisotropy. A microanisotropic formation is one which is more conductive (less resistive) parallel to the bedding than normal to the bedding. Any formation with a preferred grain orientation parallel to the bedding will be electrically anisotropic, but shales and shaly siltstones will normally exhibit this property to the highest degree.

The effect of steep dips in an anisotropic shale section is most apparent on the induction-electrical (IES) log as shown on Figure 4-3. The radial, 3-dimensional current pattern for a short, 2-electrode spacing like that of the 16" normal results in a resistivity value greater than that parallel to the bedding but less than that normal to the bedding, and this resistivity value does not change appreciably with radical dip changes because of the predominance of the hole effect on a non-focused short spacing system. The current circulation which produces the induction log is in horizontal loops around the hole, and the hole effect is negligible because of the focusing coils in the system. Therefore, in a shale section, the 16" normal will usually show a higher resistivity than the induction curve where the inhole dip is less than 40°. Depending upon the anisotropy ratio (RN/RP), the curves will cross when the inhole dip is between 40° and 60°, and above 60° the induction curve will show a higher resistivity because the current loops must now travel obliquely across the bedding.

The response of the IES log opposite thin resistive beds may also provide a clue to the amount of dip. If the dips are low, the induction and short normal curves will indicate approximately the same apparent bed thickness, and if the bed is uniform, the peak values of the two curves will occur at essentially the same depth. However, with steep dips the bed thickness is exaggerated, particularly by the induction device because it has a much greater lateral investigation. Also, the peaks on the two curves usually occur at different depths with the normal curve characteristically deeper. The average dip of the intervals shown on Figure 4-4 is between 65° and 70°. In beds A, B, C, and D, the induction curve indicates greater apparent thickness than the short normal, and at B and E, the normal curve reaches a peak value about two feet deeper than the induction.

Anisotropic effects on the conventional electric log, which is a combination of 2 and 3-electrode systems with different spacings, are not as apparent in low dip sections as they are on the IES log. Although the longer spacings are affected more by the horizontal component, the difference is usually too small to be detected readily in long shale intervals. However, when the dip exceeds 50° in thick shale or shaly siltstone intervals, the longer spacing will show higher resistivities than the short normal with the separation increasing with the dip as shown on Figure 4-2. High dip effects on the conventional electric log are described in detail with an excellent example of a long interval in Geological Item of Interest #96 by Mr. H. E. Nagle, W.O.I., which was distributed in July, 1964.

Conditions other than steep dips which may cause similar relationships between the resistivity curves are mud saltier than the formation water, particularly in large holes, and hydrocarbon saturation in oil shales like the Green River in Utah and Wyoming.

INTERVAL THICKENING
FROM
HOLE DEVIATION AND DIPPING BEDS

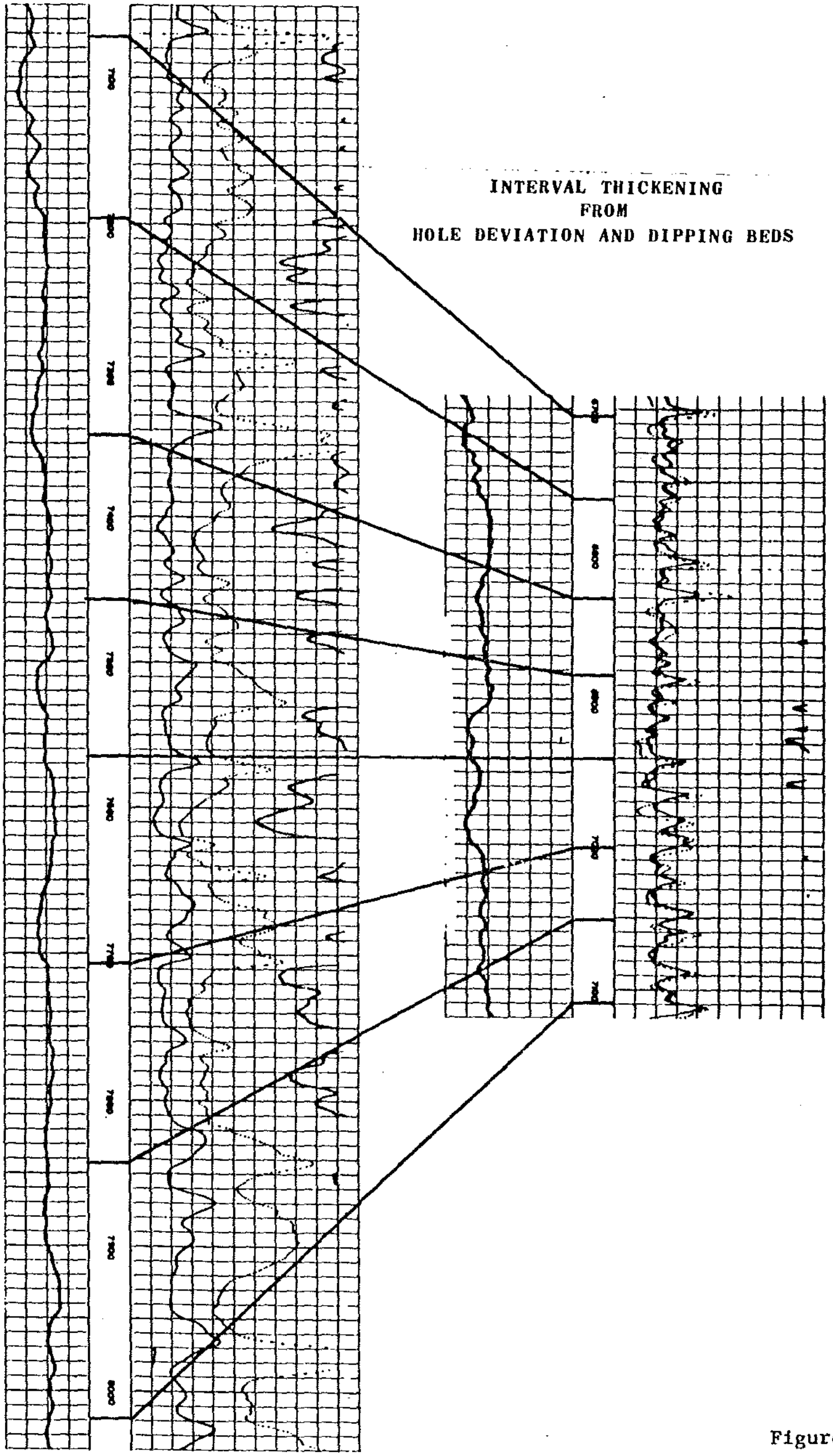

Figure 4-1

STEEP DIPS

ELK HILLS
CALIFORNIA

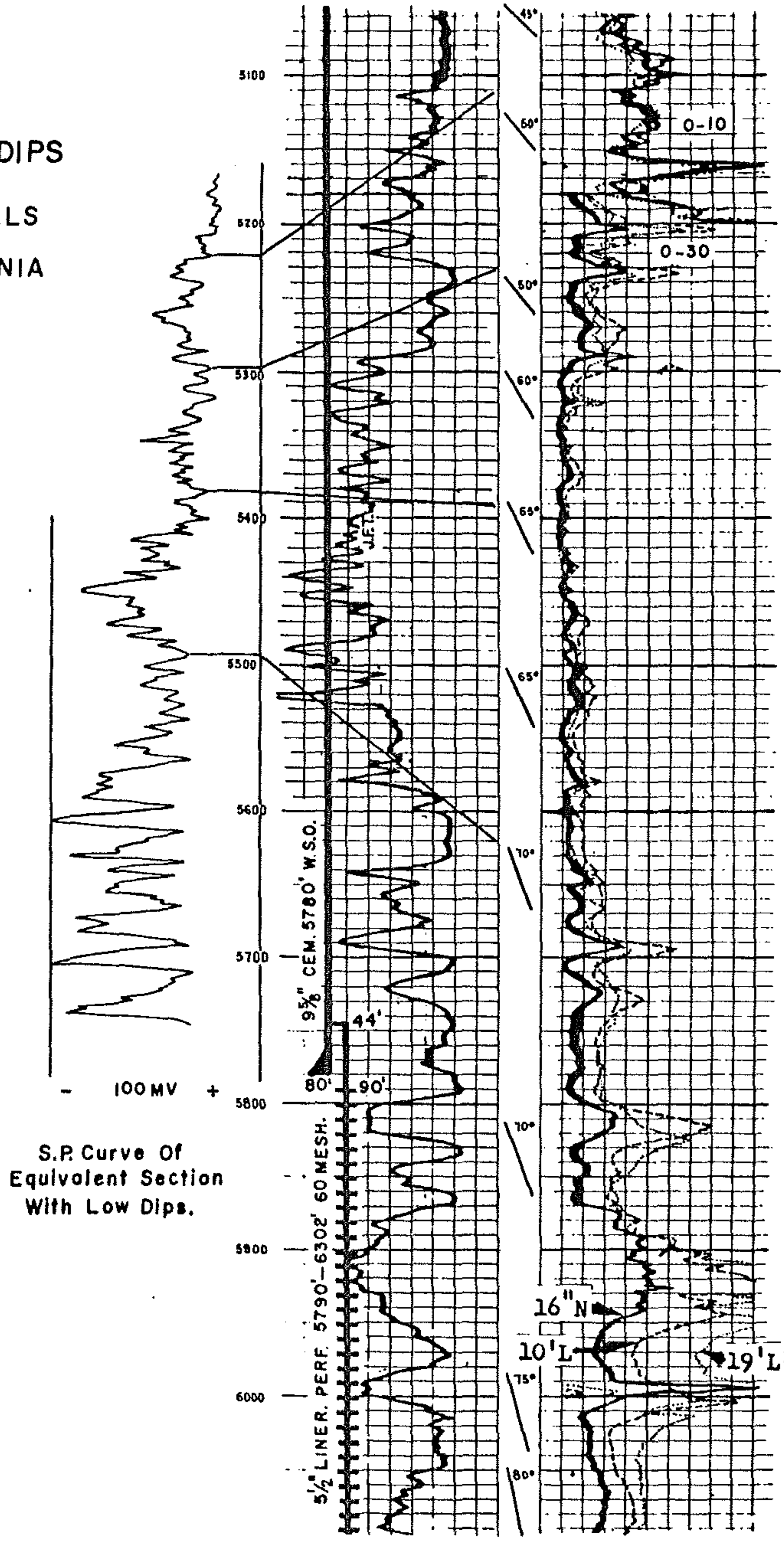

Figure 4-2

[redacted]

INDUCTION LOG SHIFT
CAUSED BY STEEP DIPS

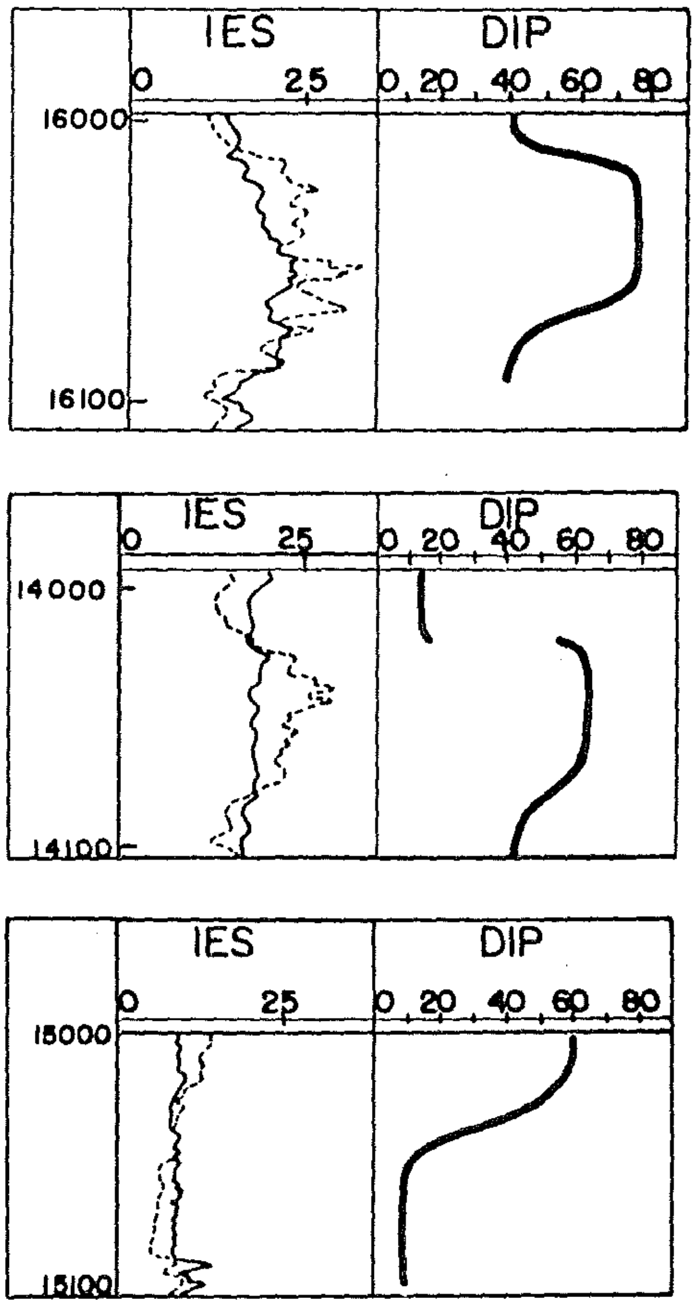

STEEP DIP BED THICKNESS AND BED DISPLACEMENT EFFECTS

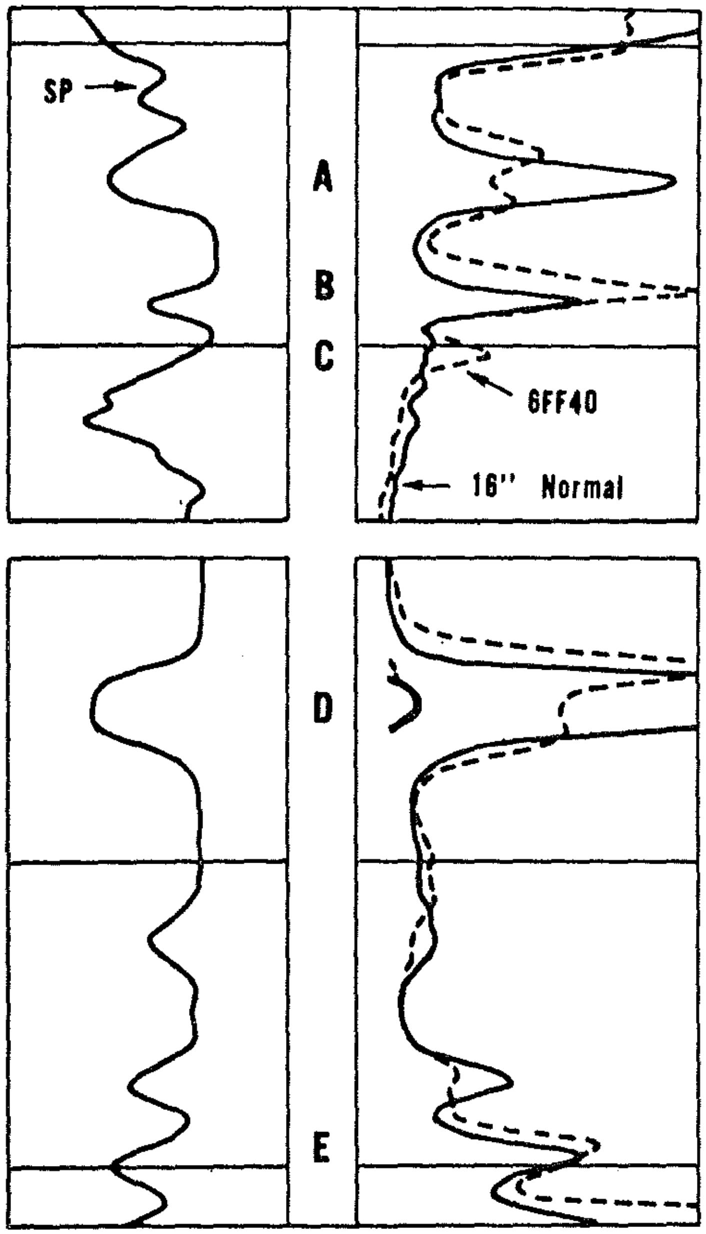

Figure 4-4

UNCONFORMITIES

Recognition of unconformities usually requires careful correlation of two or more logs, good age dating by paleontology or palynology to estabish a hiatus, and dips from cores or dipmeter computation to identify the feature as a disconformity or an angular unconformity.

Figure 4-5 shows an excellent example of truncation beneath an angular unconformity and an onlap sand above the unconformity. Many of the better stratigraphic traps were formed in this way. Consequently, recognition of unconformities, and angular unconformities in particular, is one of the first objectives in regional correlation.

ONLAP AND UNCONFORMITY

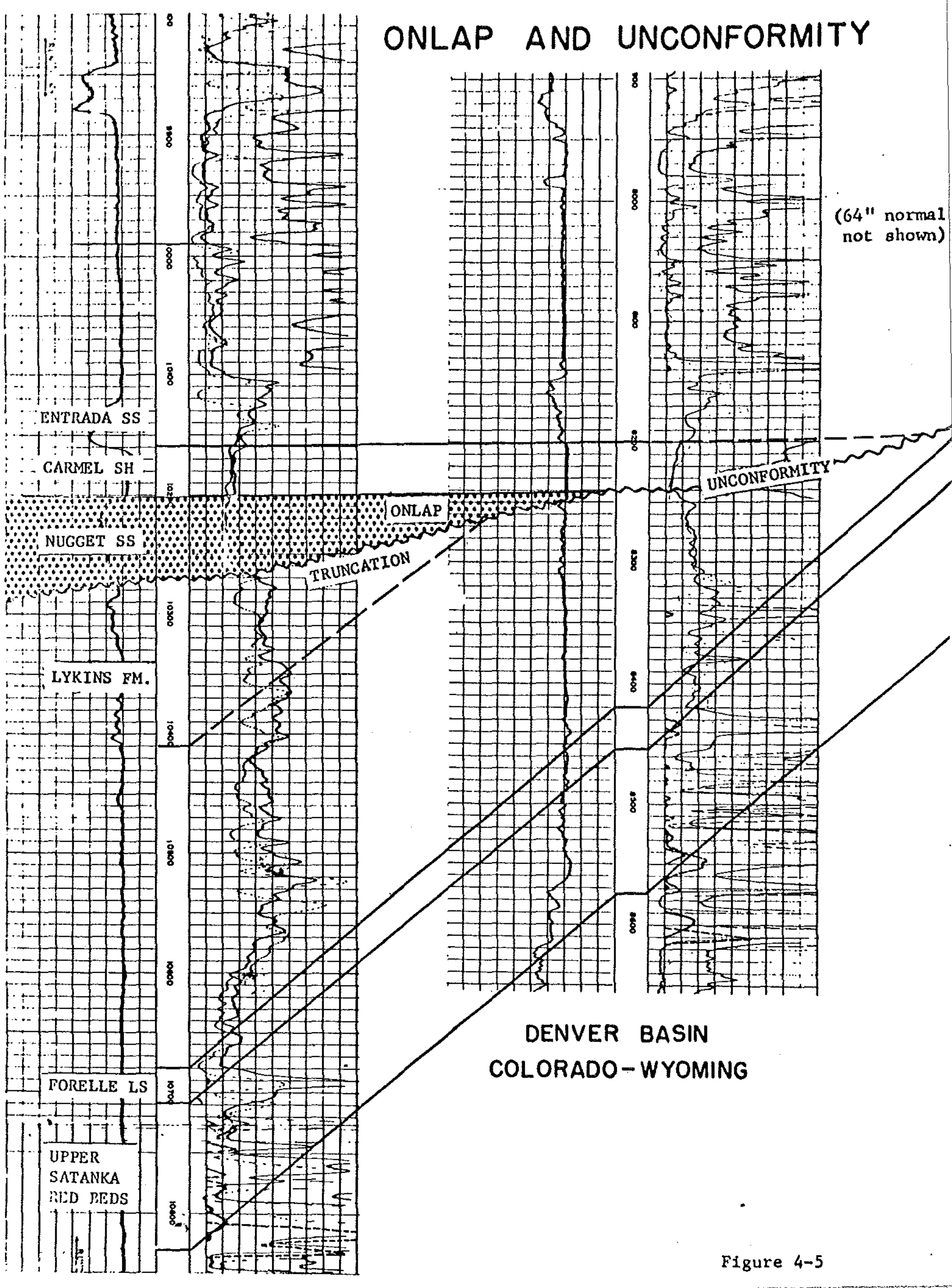

DENVER BASIN
COLORADO-WYOMING

Figure 4-5

NORMAL FAULTS

Missing section on an electric log when compared with logs from nearby wells may be indicative of normal faulting. Because of the continuous record provided by electric logs, many more such faults can now be recognized and defined than was possible when drillers' logs and core records and cuttings were the only material available for detailed correlation. However, as was pointed out in the section on correlation, electric logs by themselves may be misleading. Many workers have become "fault happy" by disregarding the possibilities of rapid facies changes and/or unconformities. Erroneous fault interpretations can usually be avoided if the regional and local lithologic relationships are studied in conjunction with the correlation of electric logs. To this end, all faunal evidence and core and cuttings records should be assembled and plotted on the logs.

Figure 4-6 shows a good example of correlations based on recognition of lithologic units and log character to define a missing interval. Note the absence of the Timpas limestone on the log to the left.

Disturbed and unusual fluid relationships associated with faulting may also be recognized on electric logs, particularly if the fault has a strike-slip component, as shown on Figure 4-7.

NORMAL FAULTING

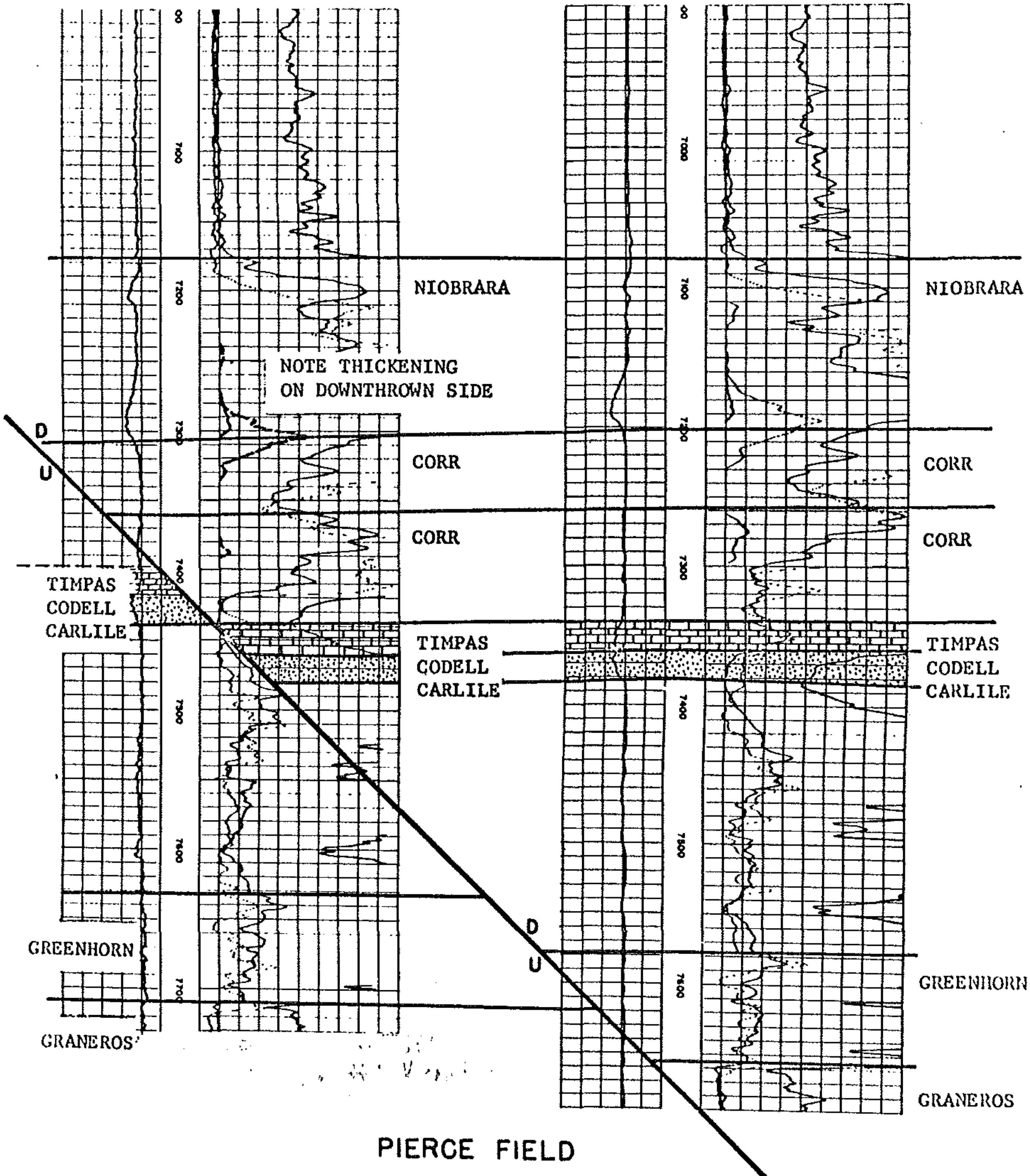

PIERCE FIELD
DENVER BASIN
COLORADO

Figure 4-6

UNUSUAL FLUID RELATIONSHIP

RESULTING FROM STRIKE–SLIP FAULT

SALT CREEK AREA
CYMRIC FIELD
CALIFORNIA

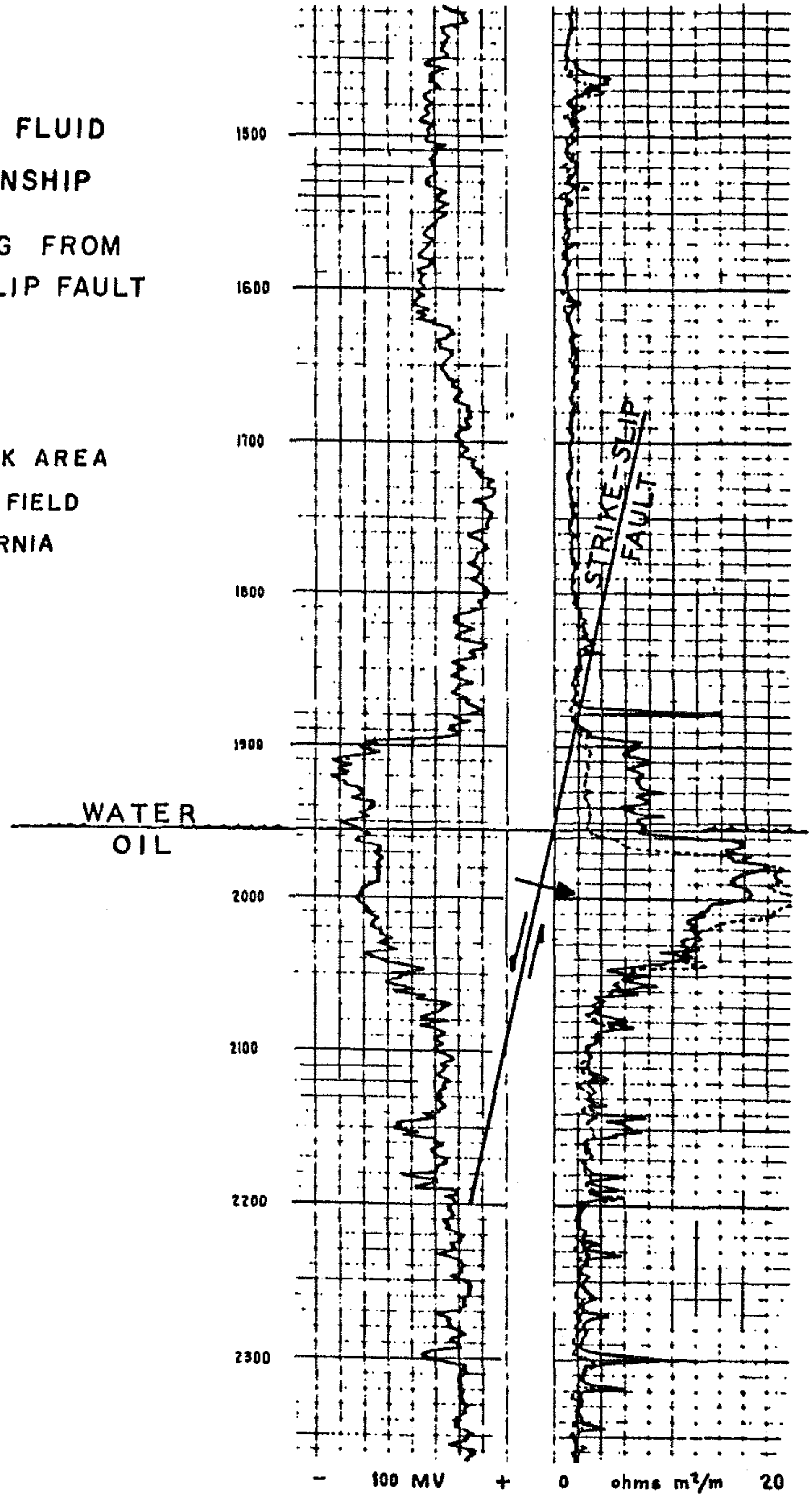

Figure 4-7

REVERSE FAULTING AND OVERTURNING

Repetition of section by reverse faulting and/or overturning may sometimes be recognizable on electric logs, particularly if good dip information and faunal records are available. Approximate similarity of character, though indicative of repetition, is not by itself sufficient criteria for reverse faulting or overturning. However, when abrupt changes in amount or direction of dip and/or unusual faunal relationships are noted, the electric log may be used to define the structural feature. Recommended practice for recognizing repeated section is to obtain two copies of the electric log and compare detail by superimposing one interval over the other on a light table, making allowance for differences in amount of dip. If overturning is suspected, one of the logs should be turned upside down. Character similarity which might otherwise be missed sometimes becomes readily apparent when duplicate logs are used in this manner.

Figure 4-8 shows the effects on an IES log in a deviated hole which crossed the axis of a tight anticlinal fold. The inhole dip changed from 26° right-side-up to 76° overturned in the interval 4160'-4260'. The normal anisotropic effect which causes separation between the 16" normal and the induction curves disappears at about 4200' as the dip approaches 90° where the well crossed the anticlinal axis. Below that depth the beds are all overturned with respect to the hole and the inhole thickness is increased about 5½ times by the steep dips as shown by the interval between the conductive beds A and B.

Figure 4-9 shows an interval repeated by a thrust fault with a 150' interval of drag folding in the fault zone. The steep dips in the fault zone are indicated by the cross-over of the resistivity curves as explained in the discussion on steep dips.

Figure 4-10 shows a sand twice repeated by a possible combination of overturning and high angle reverse faulting. The vertical line on the right represents a well 330' away in which only the lower occurence of this sand was found. Faunal evidence and dip information, though meager, agree with the picture as drawn. A similar break thrust structure is shown on Figure 4-11 except that, in this case, the overturned beds are below the fault.

Figures 4-12 and 4-13 illustrate the effect of a high angle reverse fault on an overlying thick salt section. The structural movement was absorbed by the salt in diapir type folds draping over the fault scarp. Repetition of thin shale markers by overturning is clearly shown on the Gamma-Sonic log of part of the salt interval by comparing a right-side-up copy with one turned upside down.

A unique application of a velocity log used for the location of a fault zone is illustrated on Figure 4-14. The well crossed a reverse fault where Cambrian carbonates were thrust over Cretaceous sandstone. The abrupt change in velocity plus the abnormally low velocity at 3625'-40', which probably reflects a gouge or crushed zone, definitely locate the fault. The velocity log of this example is a single receiver log which is now largely replaced by two receiver logs.

Application of a focused wall resistivity log and caliper in locating a fault is shown on Figure 4-15. The fault zone around 7700' was brecciated causing the hole to erode beyond the range of the caliper. That a fault was responsible for the brecciation was, of course, proven by other means.

STEEP DIPS AND OVERTURNED BEDS

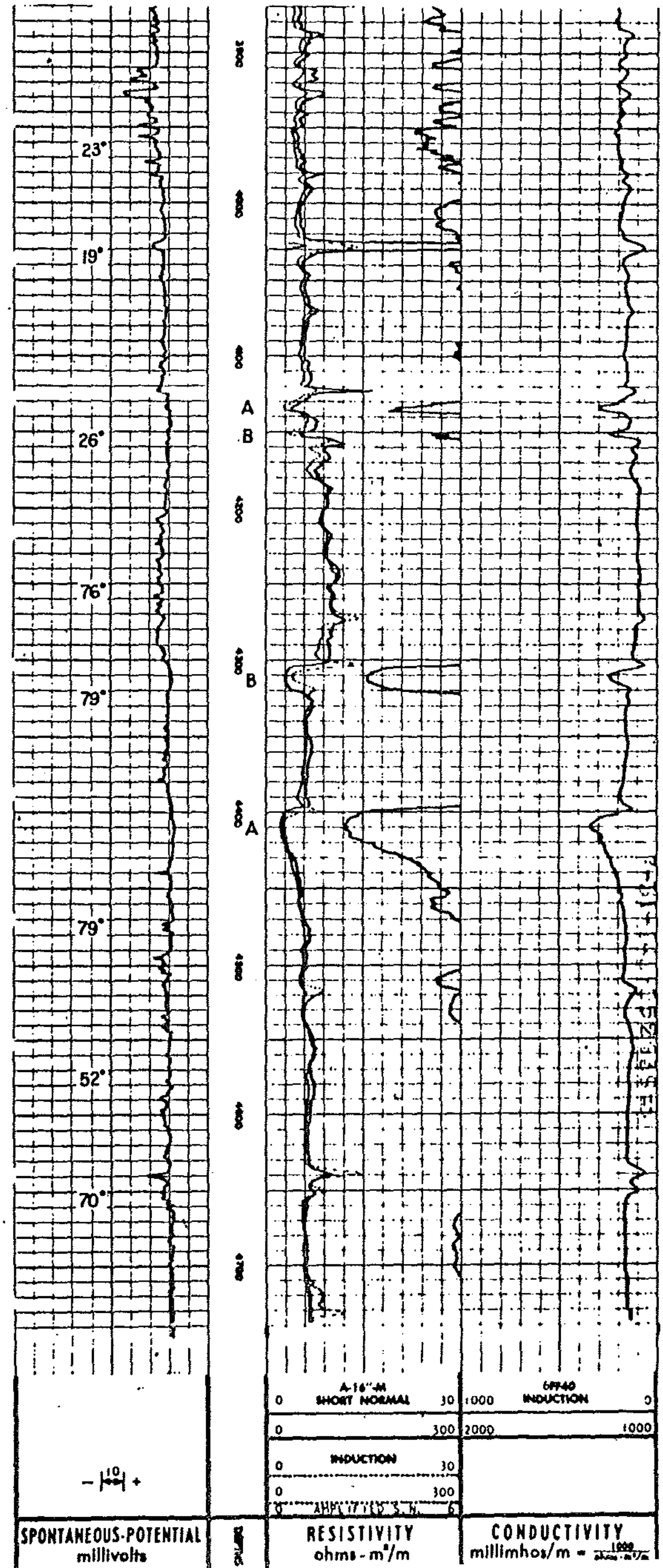

Figure 4-8

REVERSE FAULTING

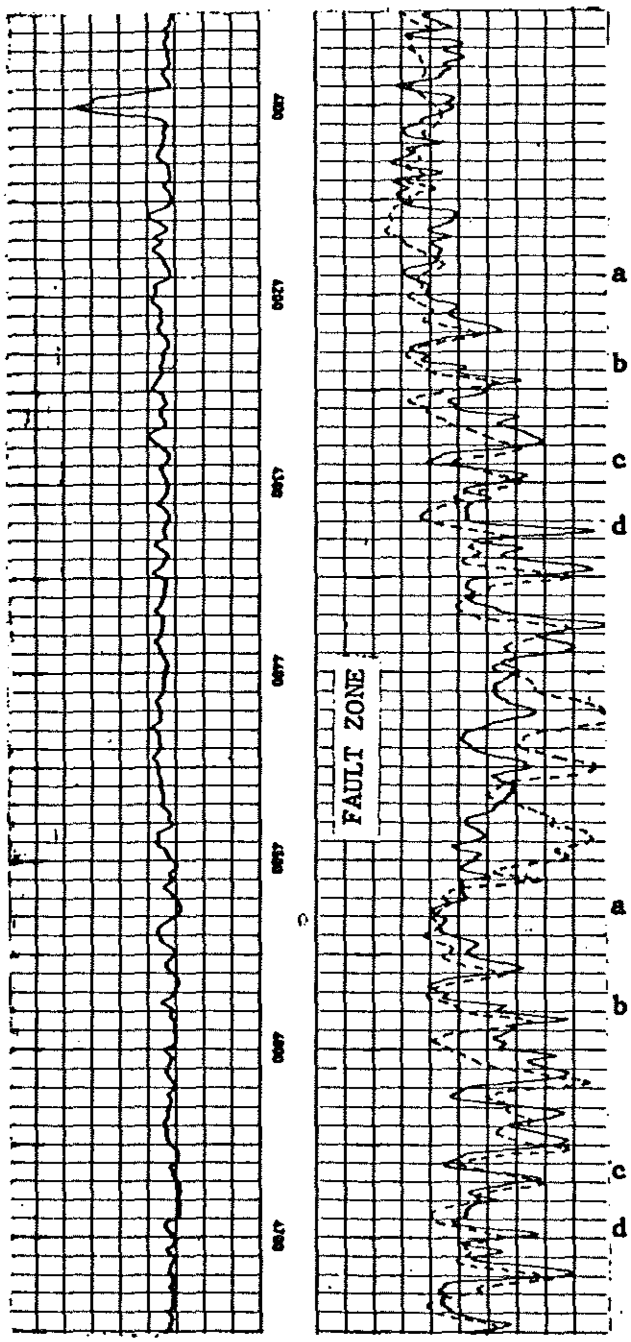

LARAMIE BASIN
WYOMING

Note use of short normal for correlation. Correlations a, b, c, and d show bed repetition from reverse faulting. Correlation is based entirely on electrical resistivity character.

Figure 4-9

REPETITION OF SECTION BY OVERTURNING AND REVERSE FAULTING

SALT CREEK AREA
CYMRIC FIELD
CALIFORNIA

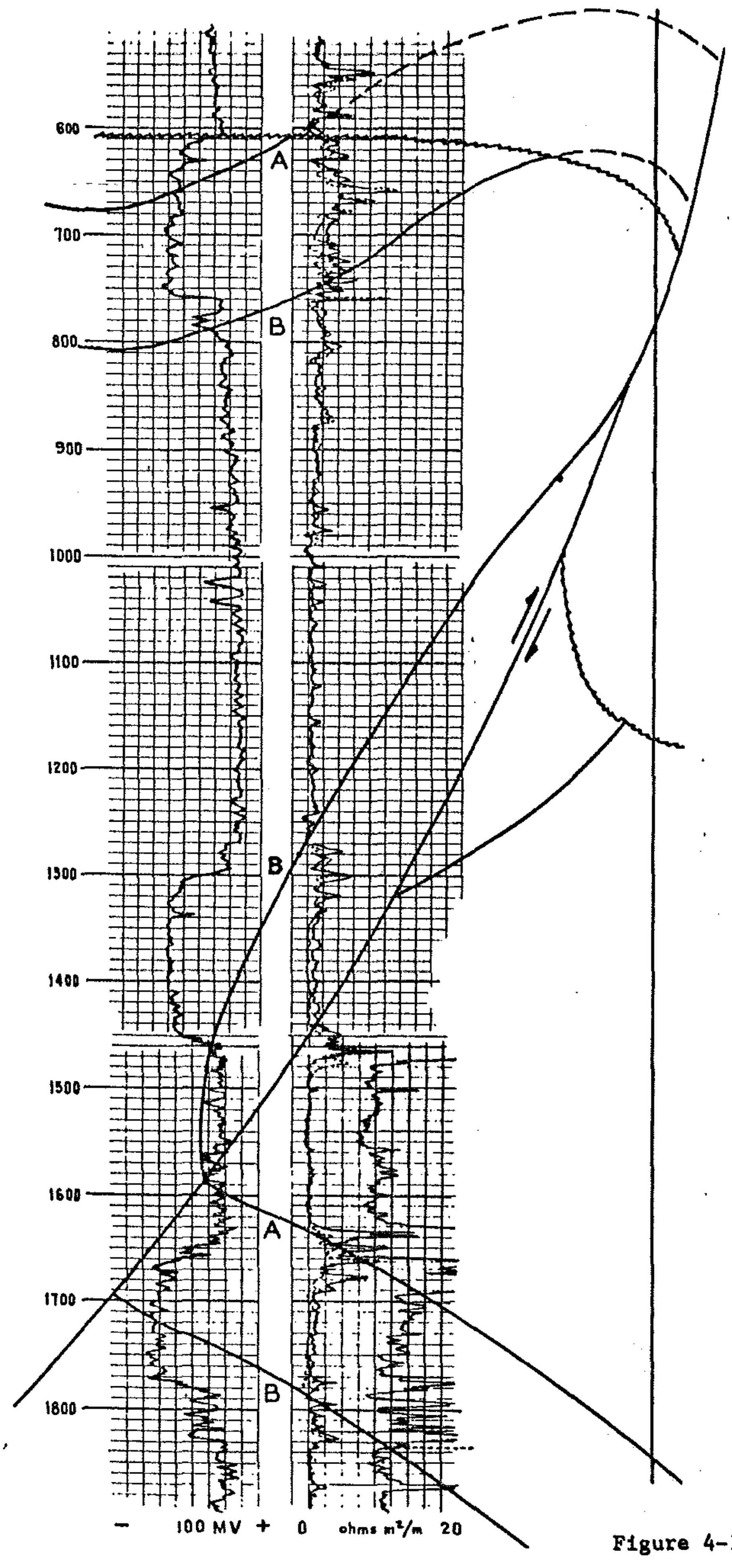

Figure 4-10

REPETITION OF SECTION BY REVERSE FAULTING AND OVERTURN
S.E. DURANT AREA BRYAN CO. OKLA.

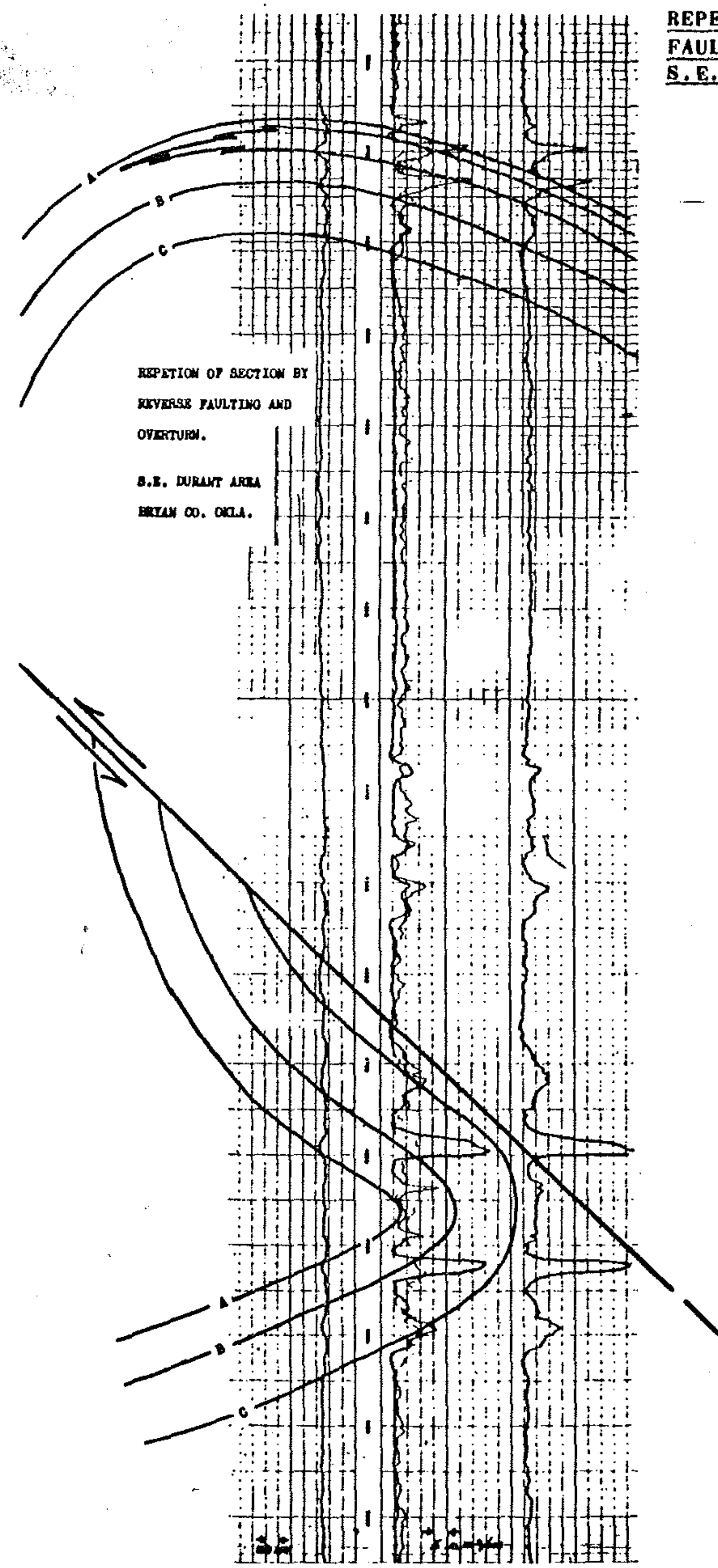

Figure 4-11

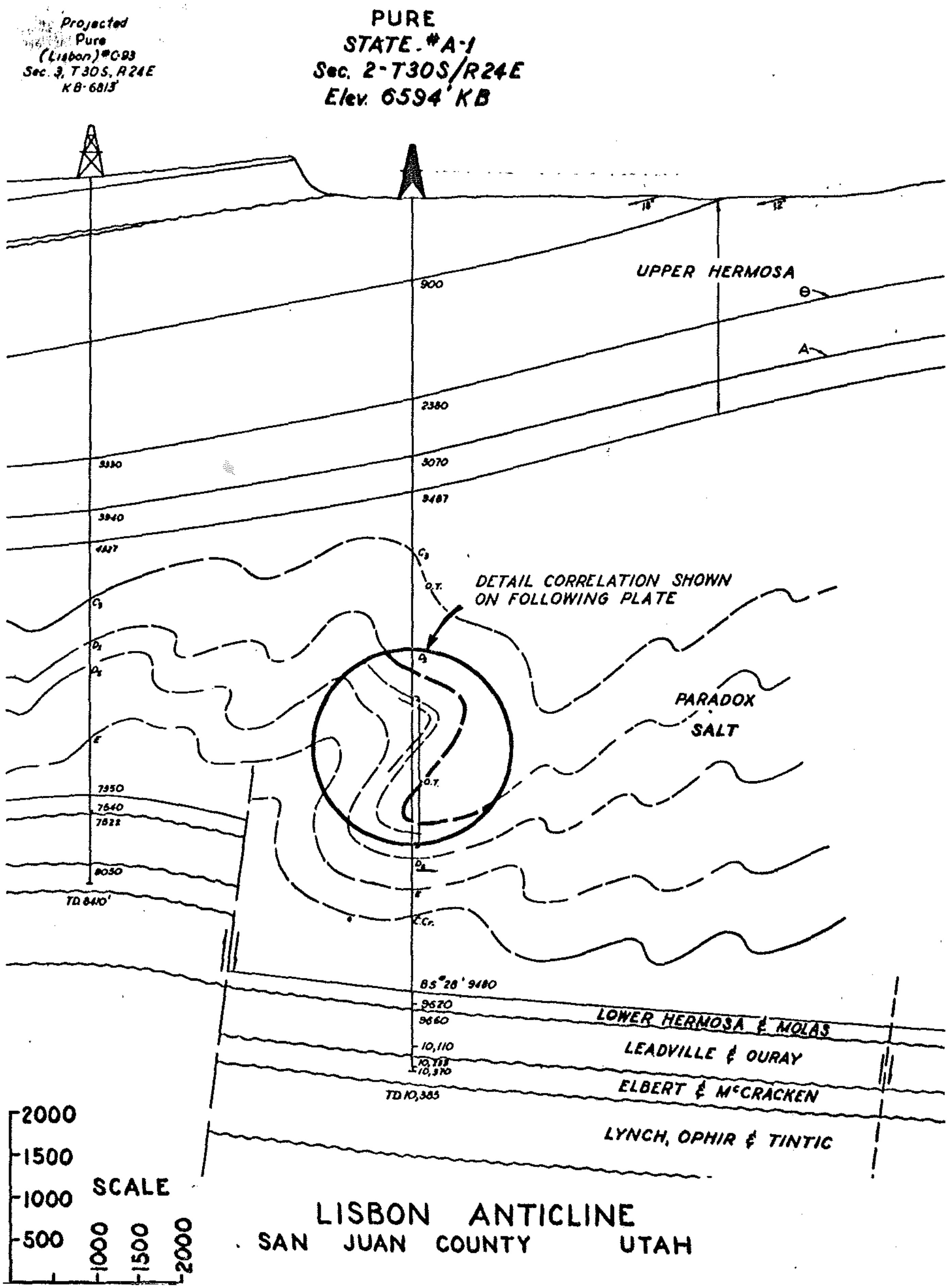
Projected
Pure
(Lisbon) #C-93
Sec. 3, T30S, R24E
KB-6813'
PURE
STATE #A-1
Sec. 2-T30S/R24E
Elev. 6594' KB
UPPER HERMOSA
900
2380
3070
3487
3940
7350
7640
8050
TD 8410'
DETAIL CORRELATION SHOWN
ON FOLLOWING PLATE
PARADOX
SALT
9620
9660
10,110
TD 10,385
LOWER HERMOSA & MOLAS
LEADVILLE & OURAY
ELBERT & McCRACKEN
LYNCH, OPHIR & TINTIC
2000
1500
1000
500
SCALE
1000
1500
2000
LISBON ANTICLINE
SAN JUAN COUNTY UTAH

Figure 4-12

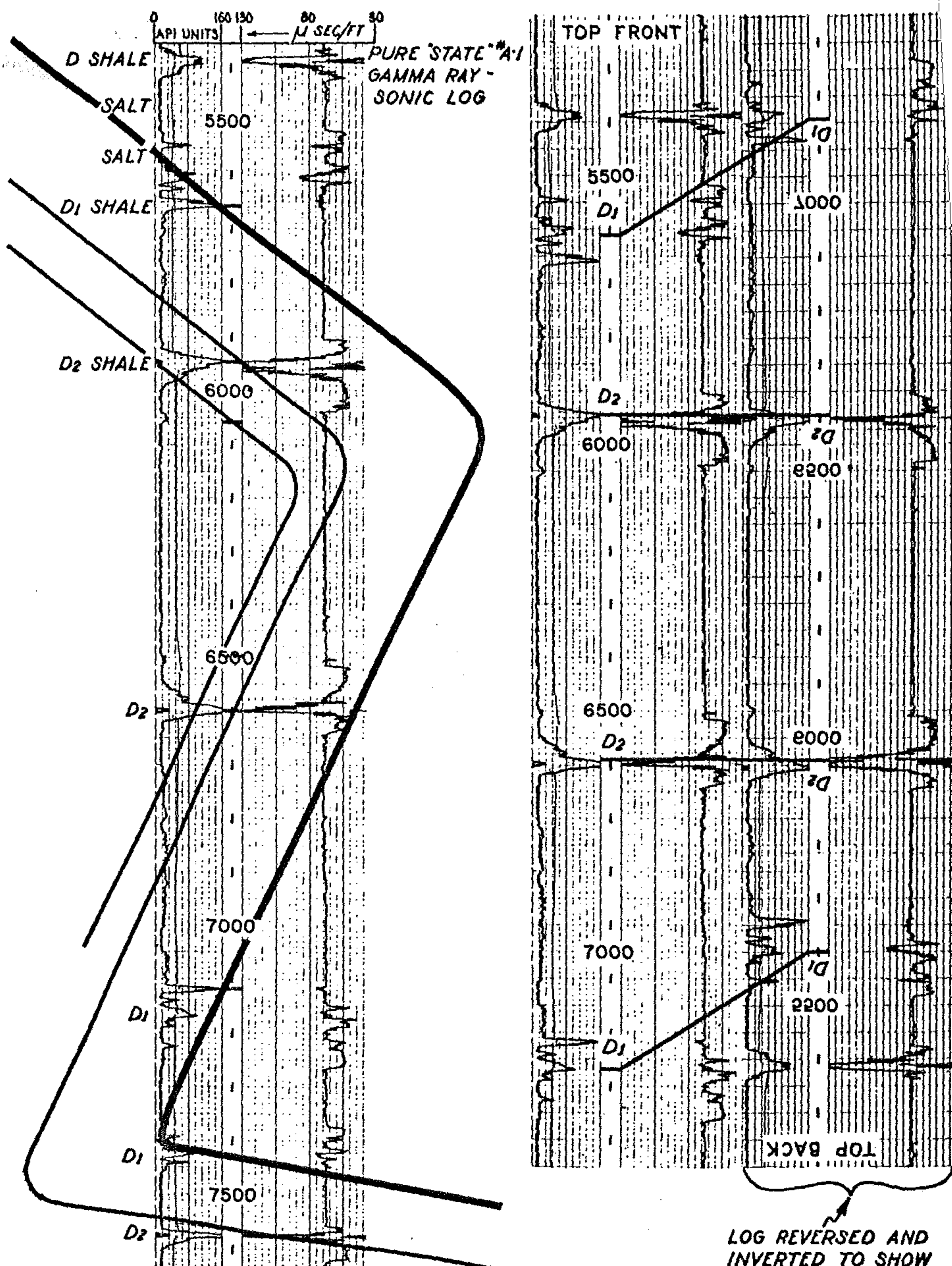

EXAMPLE OF REPEATED AND OVERTURNED BEDS
ON GAMMA-SONIC LOG

THRUST FAULT EXPRESSION
ON VELOCITY LOG
ROCKY MOUNTAINS

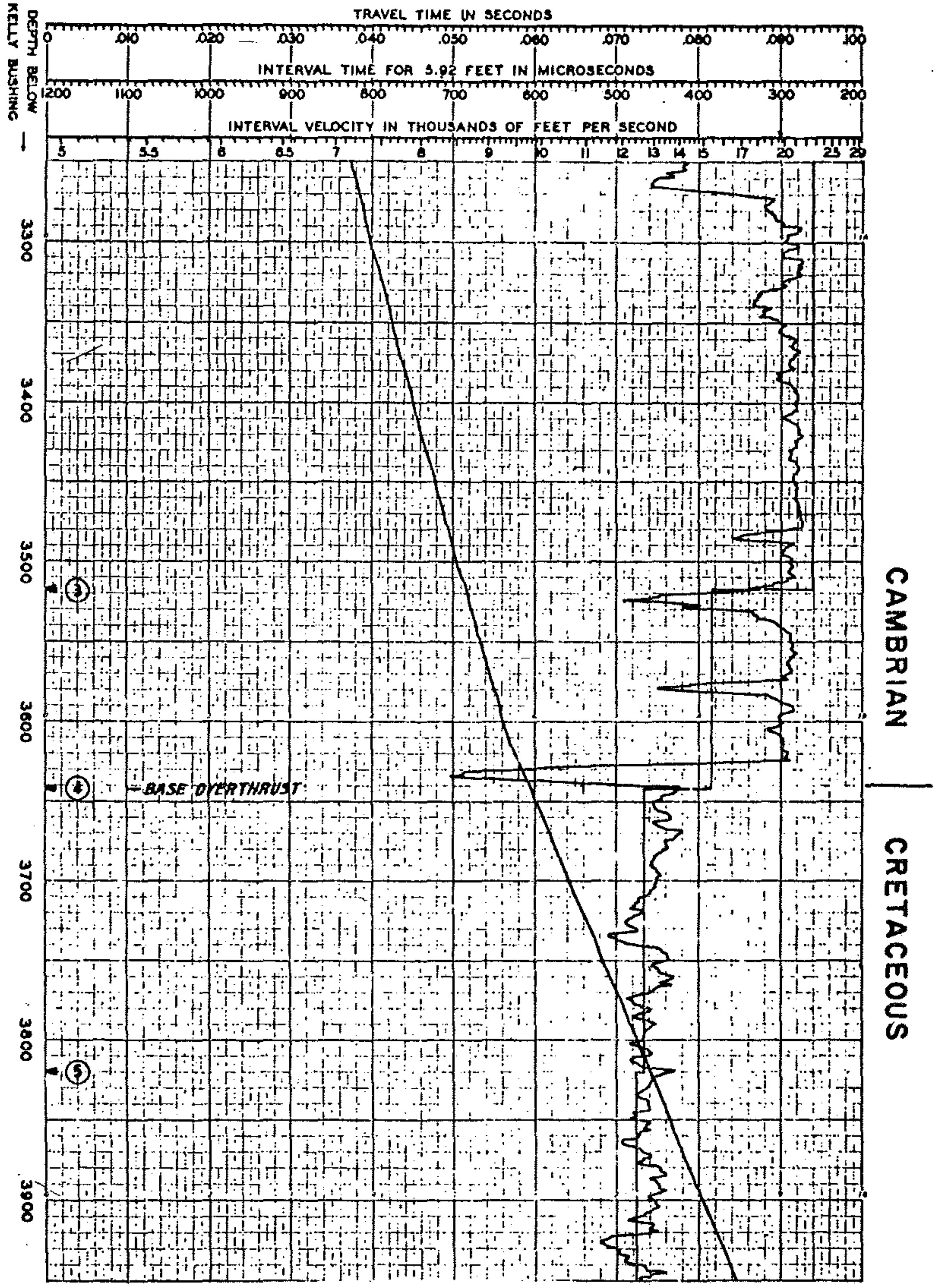

Figure 4-14

HOLE ENLARGEMENT IN FAULT ZONE

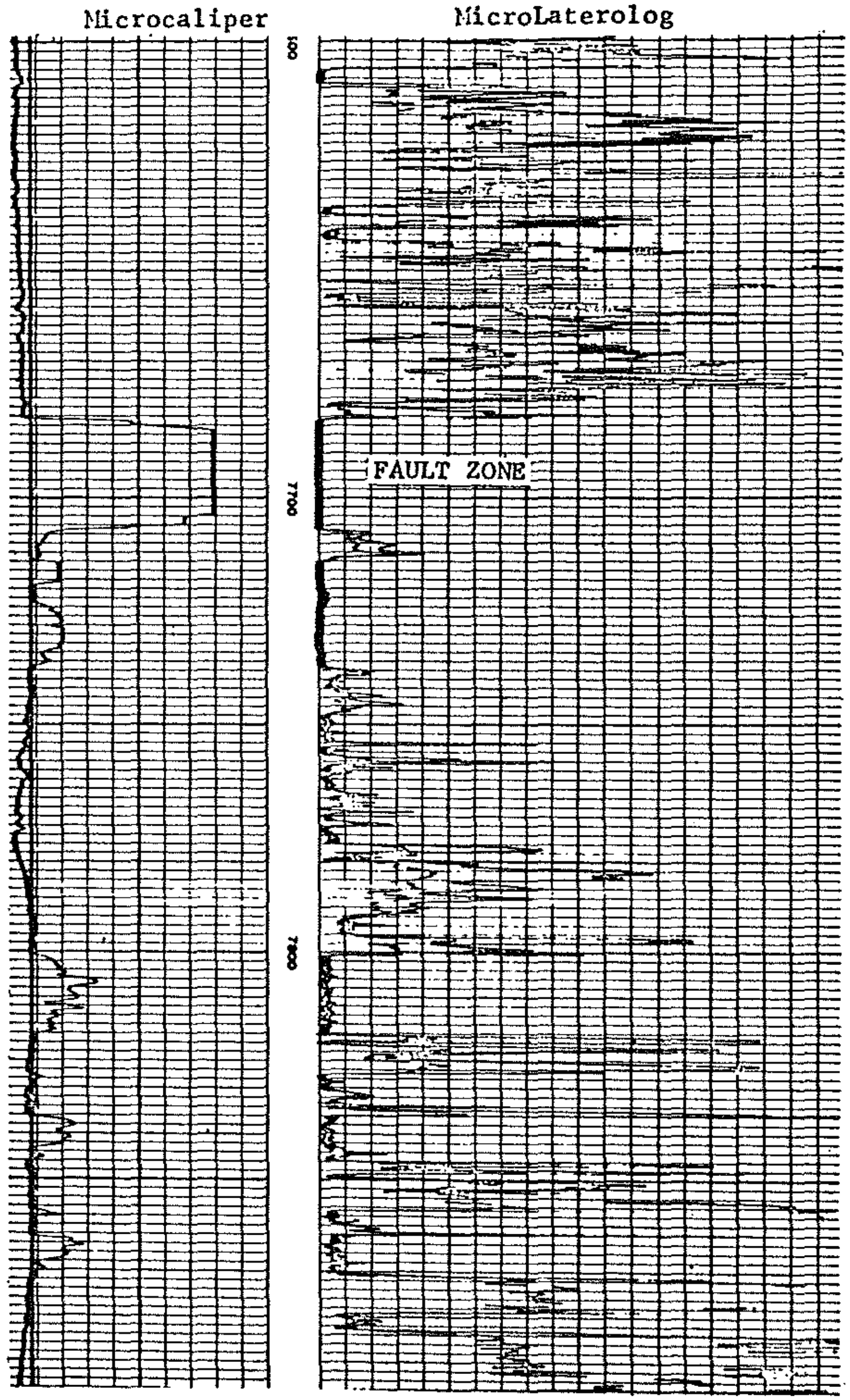

A reverse fault was found in this well. The fault zone around 7700 feet was brecciated and developed marked hole enlargement as indicated by the Microcaliper.

GYPSUM BASIN
COLORADO

Figure 4-15

STRUCTURAL INTERPRETATIONS FROM DIPMETER DATA

Since the early forties computed dips and strikes from dipmeter logs have been used with core dips to determine structural trends and establish the position of a particular well with regard to local structure. Until recently the computations were used individually or averaged over short intervals in the same way that core dips had been used in the past.

The detail now available from modern continuous dipmeter surveys is best handled by statistical analysis techniques. Several different approaches are used with the resultant display determined by the type of problem. Regional structure, unconformities, and stratigraphic detail, such as cross bedding, require statistical averaging techniques like those used in the MDSTR (Mean Dip and Strike) computer program. This program averages dip and dip azimuth data vectorially and the results are usually displayed in a similar fashion to that shown on Figures 2-18 to 2-22 in Part 2 of this manual. The vector averaging technique is described in detail in a report entitled "MDSTR Program for Computing Vectorial Averages of Dip and Dip Azimuth," by L. R. Litsey in the report on the March, 1965, Formation Evaluation Committee Meeting.

The statistical approach for detailed structural analysis of dipmeter data requires several types of plots which are obtained from the SCAT (Statistical Curvature Analysis Techniques) computer programs developed by C. A. Bengston of Chevron Research. The displays which can now be automatically plotted from the computer output are shown on Figure 4-16. The six kinds of geological surfaces which can be interpreted from SCAT plots are shown on Figure 4-17. The type of curvature is deduced from Dip vs. Azimuth plots like those shown on Figure 4-18.

The objectives of the SCAT programs are:

1. To determine the structural dip as accurately as possible at as many places as possible along the well bore.

2. To locate and identify geometric singularities, i.e., faults, unconformities, crestal planes, axial planes, and inflection planes.

3. To orient structural elements, i.e., find the bearing and plunge of crestal lines and dip and strike of axial planes.

4. To determine the geometric properties of the region near the well bore, i.e., to identify regions of anticlinal and synclinal curvature, distinguish between prolate and oblate curvature and conformal and disharmonic structural style.

5. To account for the effect of stratigraphic convergence on structural change with depth.

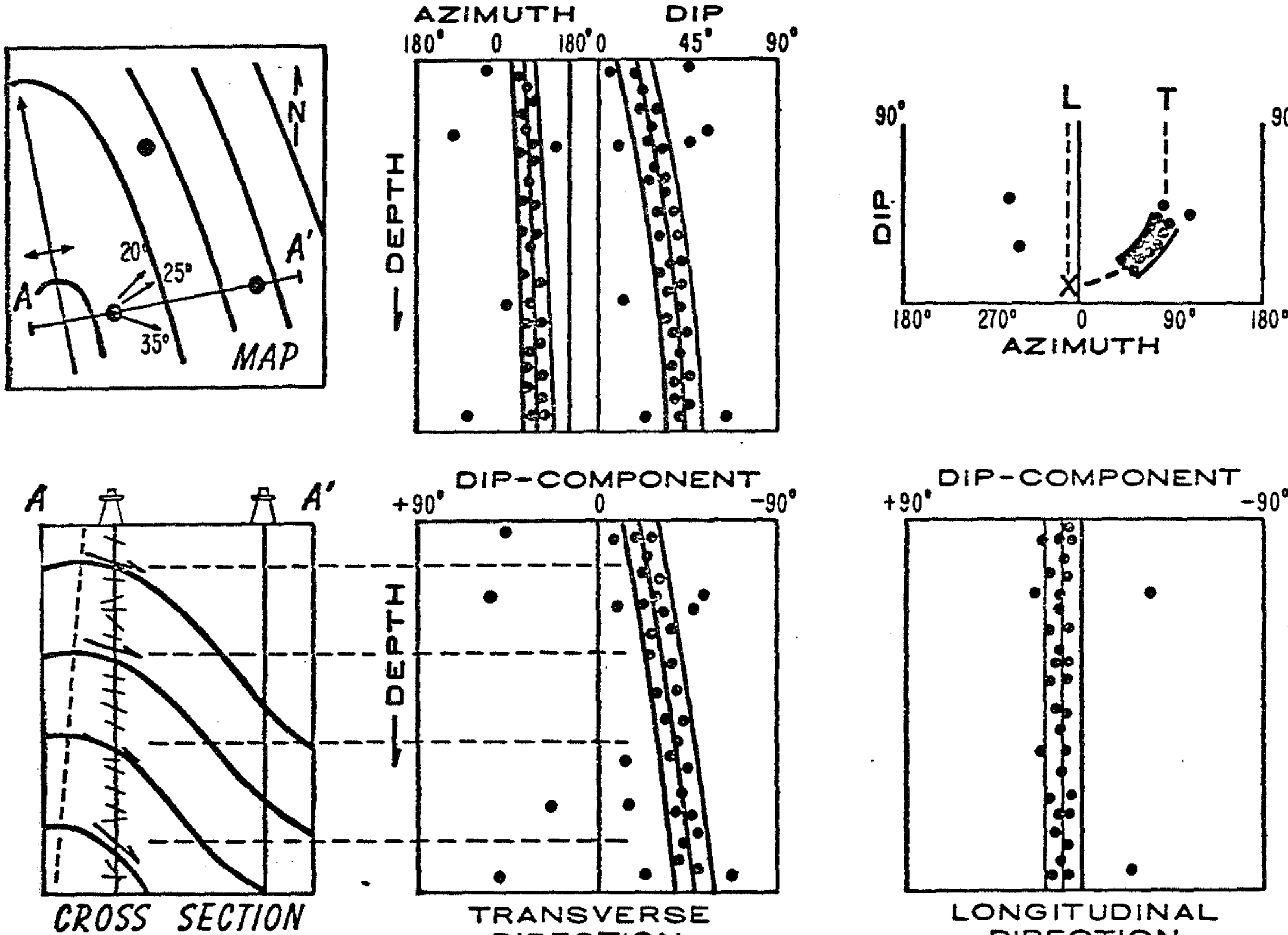

VECTOR AND GRAPH-TYPE DISPLAYS OF DIPMETER DATA

Figure 4-16

SIX KINDS OF GEOL. SURFACES

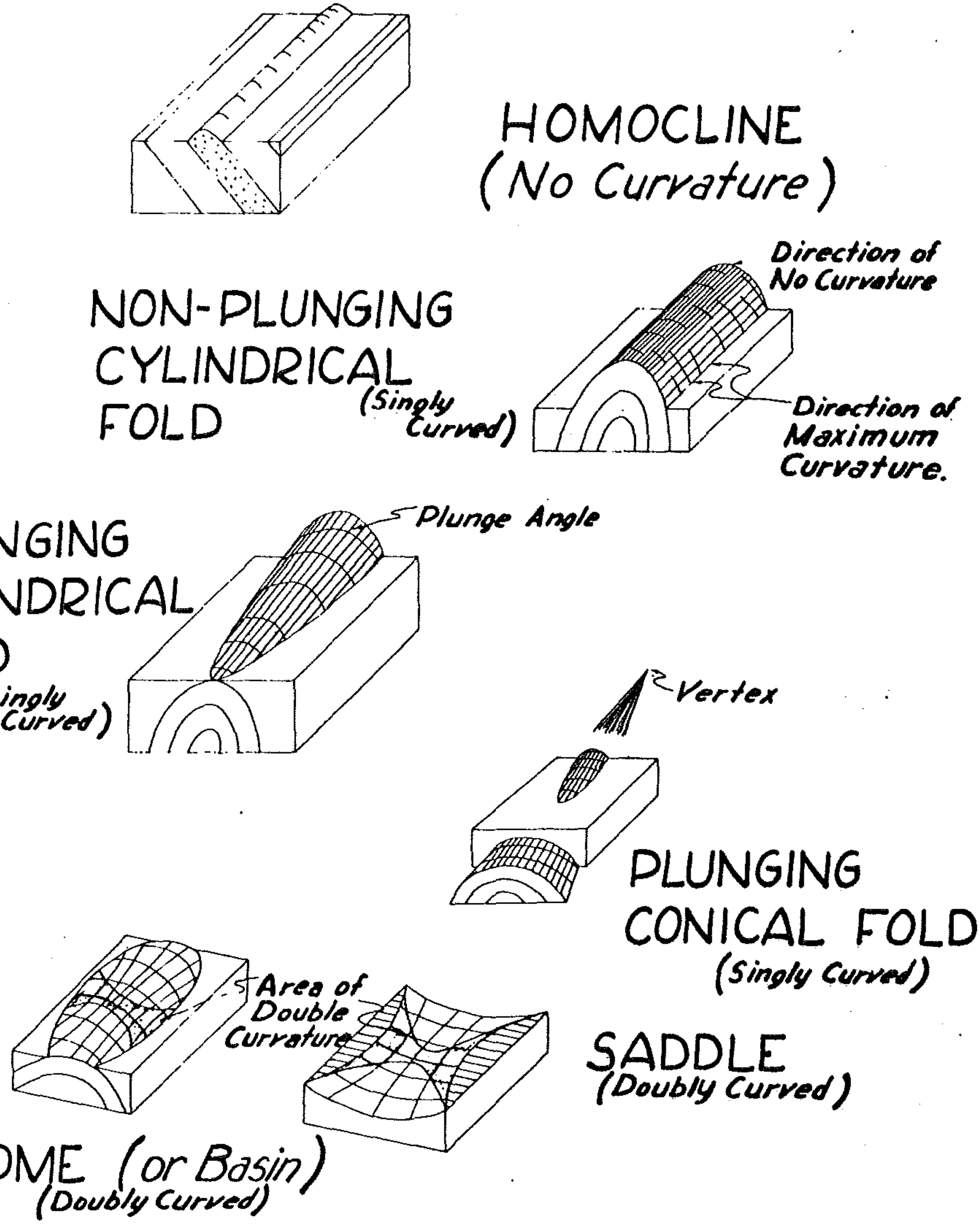

Figure 4-17

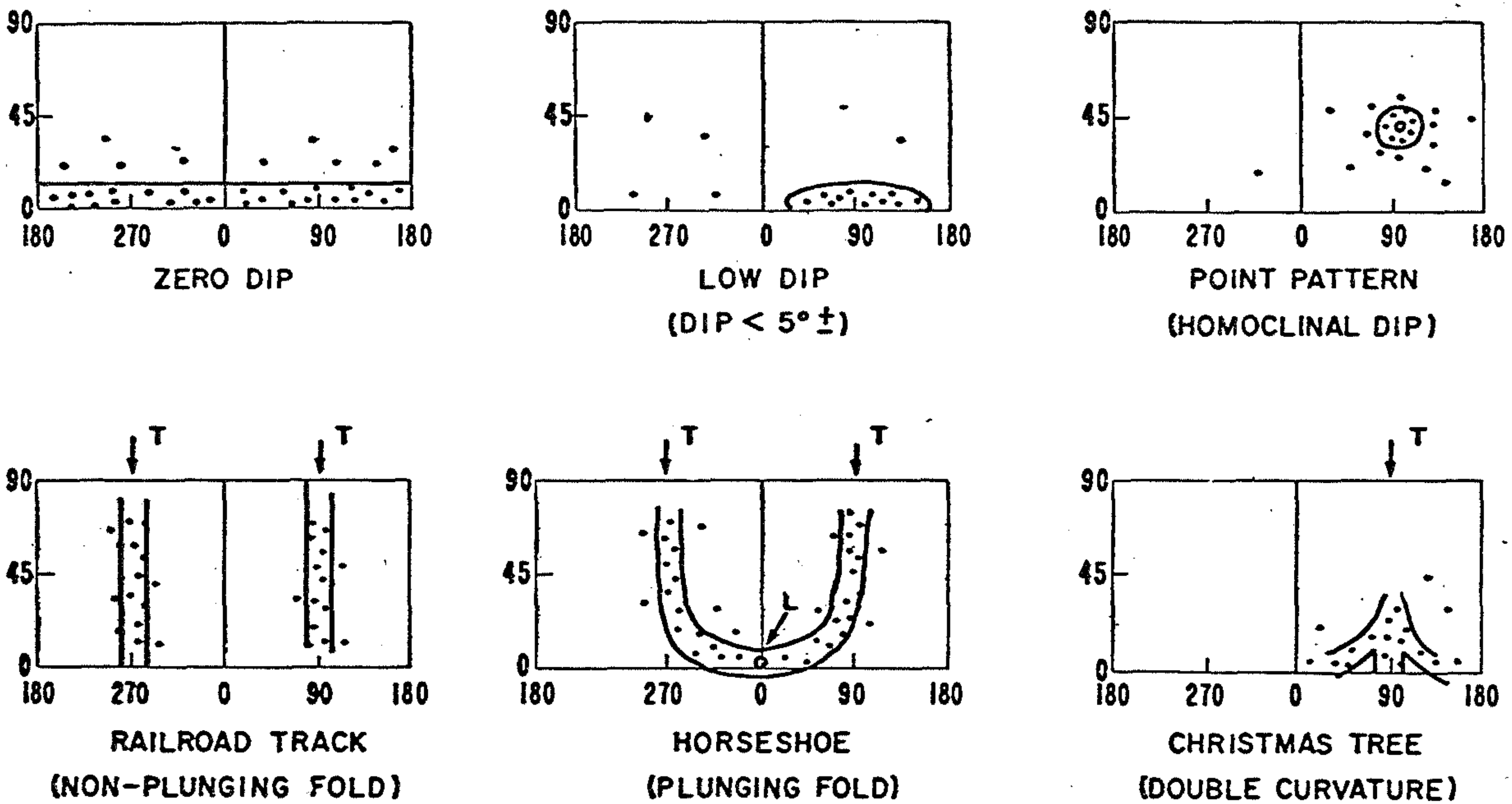

THE SIX VALID DIP vs AZIMUTH PATTERNS

Figure 4-18

PART 5

HYDRODYNAMICS AND ABNORMAL PRESSURE EFFECTS

TRANSITION FROM FRESH WATER TO SALT WATER

The normal character of an electric log run through the fresh water-salt water interface is shown on Figure 5-1. The transition zone on this example extends from approximately 1150' to 1550'.

In a sand-shale section the resistivity curves and the S.P. curve will show opposite effects if all of the sands are wet. The resistivity curve will show high contrast in the fresh water sands and the S.P. curve will show high contrast in the salt water sands. The transition zone will always be gradational on the resistivity curves because of the changing water salinity in both sands and shales, but the S.P. curve will normally show a step-like pattern as on the example. The S.P. opposite the fresh water sands will be positive if the formation water is fresher than the mud, as in this case, and will change from positive to negative in the transition zone. Shifts in the shale base line of the S.P. curve may be caused by either a change in the shale mineralogy or changing salinity in a sand between two shale intervals. In a continuous shale interval as at 1450'-1550' the S.P. will not change with the change in water salinity shown by the resistivity curves.

TRANSITION ZONE

FROM FRESH TO SALTY WATERS

R_M = 3.4 OHM–M AT 60°F

HUNTINGTON BEACH CALIFORNIA

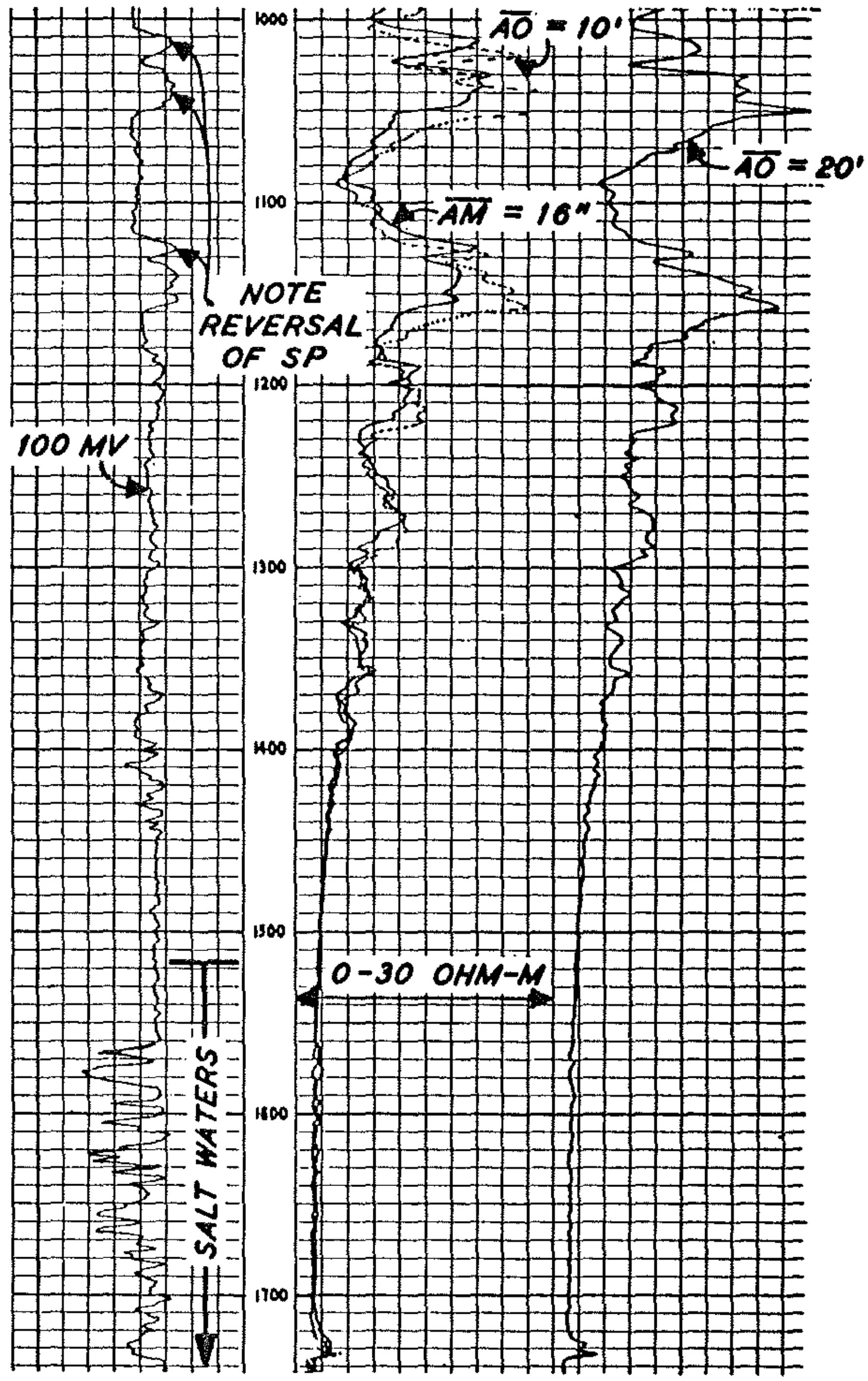

Figure 5-1

HYDRODYNAMIC EFFECTS

Partial flushing of a deep sand reservoir by meteoric waters is shown on Figure 5-2. The decreasing resistivity in the downward direction in this sand could be ascribed to increasing porosity with a resultant decrease in formation factor, decreasing hydrocarbon saturation, or increasing water salinity. The Sonic log eliminates the first cause, and the second was ruled out by the complete absence of hydrocarbon shows on the mud log and in sidewall cores. Positive evidence to support the third cause is provided by the shift in the S.P. shale base line between the top and base of the sand. Calculations of water resistivity from the S.P. curve check calculations from the resistivity and velocity curves. The salinities from those calculations are about 200 G/G in the top of the sand and 500 G/G near the base.

An unusually deep fresh water aquifer is shown on Figure 5-3. The sandstone in the interval 12,980'-13,085' is apparently continuous to the surface outcrop on the north slope of the Brooks Range, whereas the sands with negative S.P. and low resistivity in the interval 12,700'-12,800' are not continuous. Calculations indicate a salinity of about 200 G/G in the lower sand interval compared with about 1600 G/G in the upper sands.

FRESH WATER FLUSHING

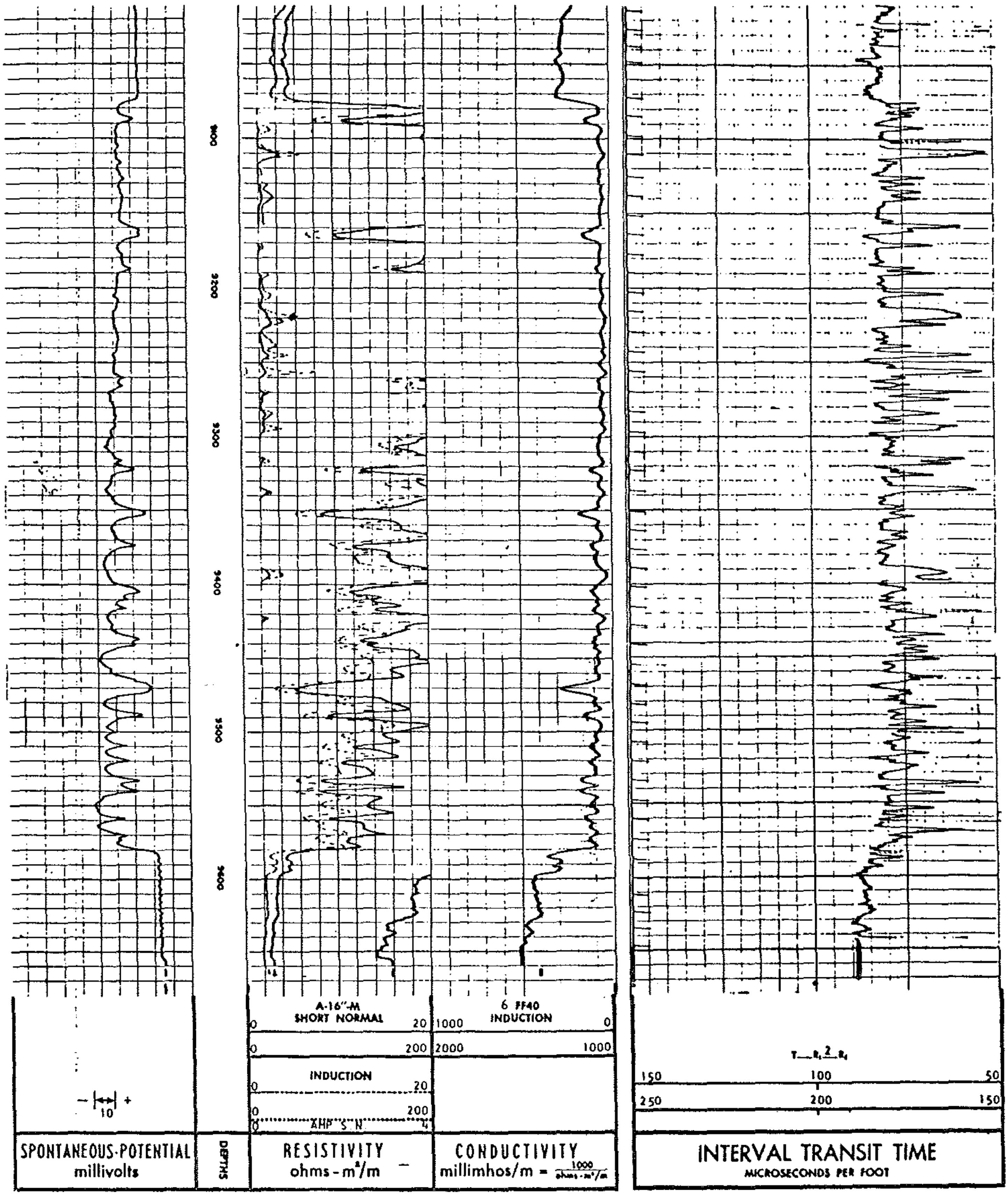

Figure 5-2

FRESH WATER AQUIFER

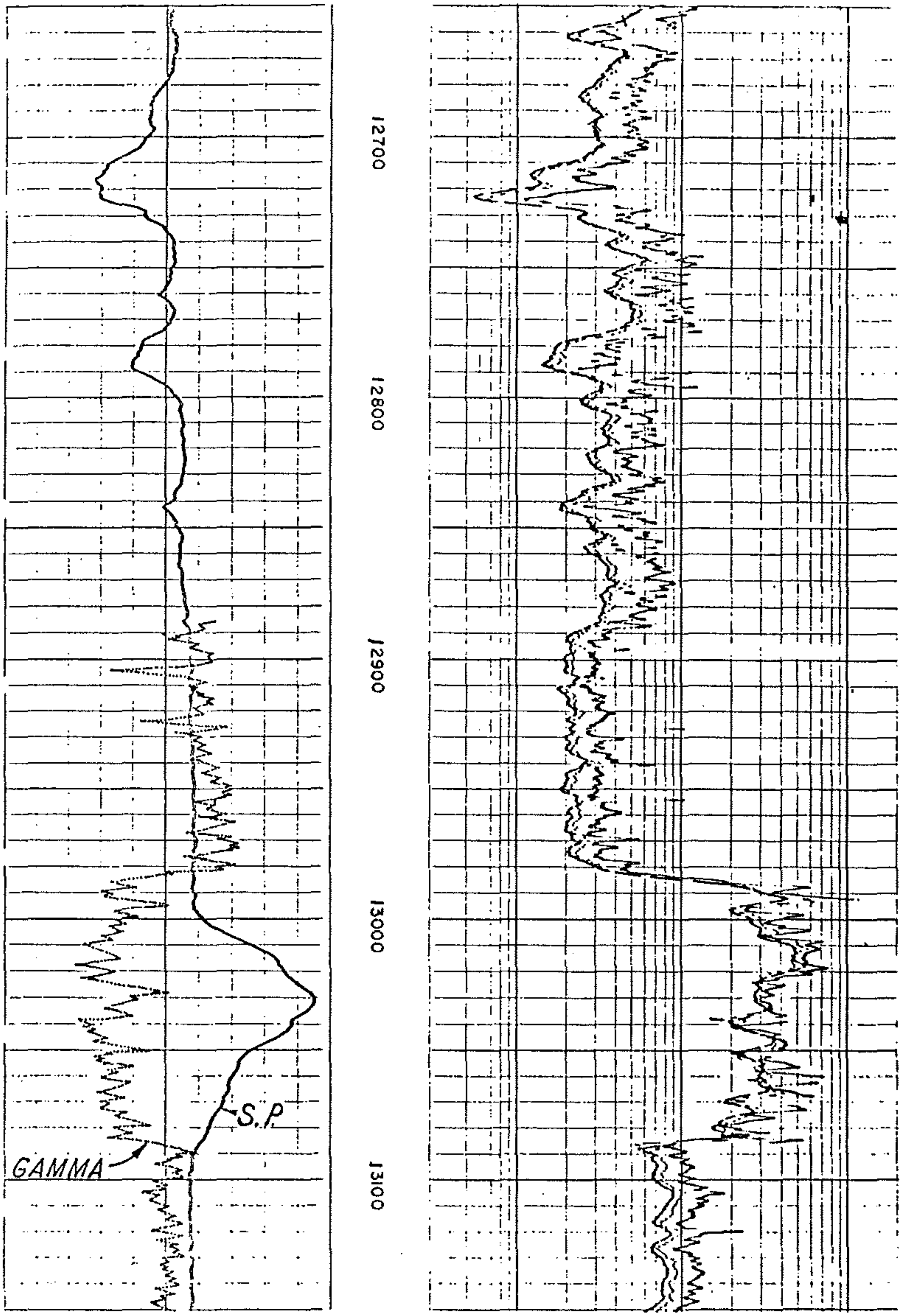

Figure 5-3

[redacted]

ABNORMAL PRESSURE EFFECTS ON WELL LOGS

During the last few years pressure effects on well logs have received considerable attention from log analysts. This interest has been stimulated by both geologists and drilling engineers. Geologists are primarily interested in the origin of abnormal pressures and the relationship to hydrocarbon accumulation and entrapment, whereas drilling engineers are looking at the problem of mud weight control when drilling into high pressure zones. A study group was recently selected by Mr. K. H. Crandall for a Corporation-wide survey of abnormal formation pressures, and their work to date indicates exploratory applications may be more widespread than was formerly realized.

The discussion and examples in this manual will be limited to the more obvious effects of abnormal pressures on resistivity, velocity, and density which can be readily recognized on well logs. For more complete coverage, a selected bibliography is appended.

The effect of increasing depth on shale resistivities with a normal hydrostatic pressure gradient is a gradual increase as porosity is decreased by compaction, if the shale mineralogy and formation water salinity do not change appreciably. A sudden increase in formation pressure at the top of an abnormal pressure zone will reverse the resistivity trend because the fluid pressure supports part of the load and maintains a higher than normal porosity. Figure 5-4 shows the abrupt change from the normal Gulf Coast shale resistivity gradient down to 4940' to one of decreasing resistivity below that depth. In this area and others on the Texas and Louisiana Gulf Coast, the shale resistivity gradients are sufficiently uniform to permit quantitative calculations of formation pressure and pressure gradient and thereby provide positive mud weight control for drilling into high pressure zones.

Similar pressure effects in shale intervals are common in the Cretaceous "E" and "F" zones in the Sacramento Valley in California, as shown on Figure 5-5. The effect on the velocity log is very similar to that on the resistivity because both logs are responding primarily to the changes in shale porosity. A plot of recorded pressures on tests in this well at 3890', 5397', and 6035' indicate the formation pressure gradient departs from normal hydrostatic at about 3500' and extrapolates to about 0.9 psi/ft at 7400'. The extrapolation indicates an increase of about 3 psi/ft in the interval 7300'-7400', where the most abrupt change is observed on the logs. Quantitative interpretation from logs, like that conducted on the Gulf Coast, is limited because of vertical and lateral changes in shale mineralogy and formation water salinity.

The density log can also be used to locate abnormal pressures in shale intervals if the mineralogy is fairly uniform. However, grain densities in shales may vary from about 2.2 gm./cc. in an opaline shale to about 2.75 gm./cc. in a chlorite-mica clay shale. The mineralogy must, therefore, be checked before considering pressure effects. Figure 5-6 shows an example of a plot of shale densities from cuttings samples compared with a density log in a high pressure zone. This shale density plot is now part of the mud logging service offered by Baroid and has been used successfully for mud weight control on the Gulf Coast where shale mineralogy is uniform.

References

Dickinson, George, 1953, Geological Aspects of Abnormal Reservoir Pressures in Gulf Coast Louisiana, AAPG Bulletin, Vol. 37, pp. 410-432.

Hottman, C. E., and Johnson, R. K., 1965, Estimation of Formation Pressures From Log-Derived Shale Properties, Jour. Pet. Tech., June.

MacGregor, J. R., 1965, Quantitative Determination of Reservoir Pressures from Conductivity Log, AAPG Bulletin, Vol. 49, pp. 1502-1511.

Wallace, W. E., 1965, Abnormal Subsurface Pressures Measured from Conductivity or Resistivity Logs, SPWLA Transactions, Vol. 2, May, and Log Analyst, Feb.-March, 1965, pp. 26-38.

ABNORMAL PRESSURE EFFECT ON RESISTIVITY TEXAS GULF COAST

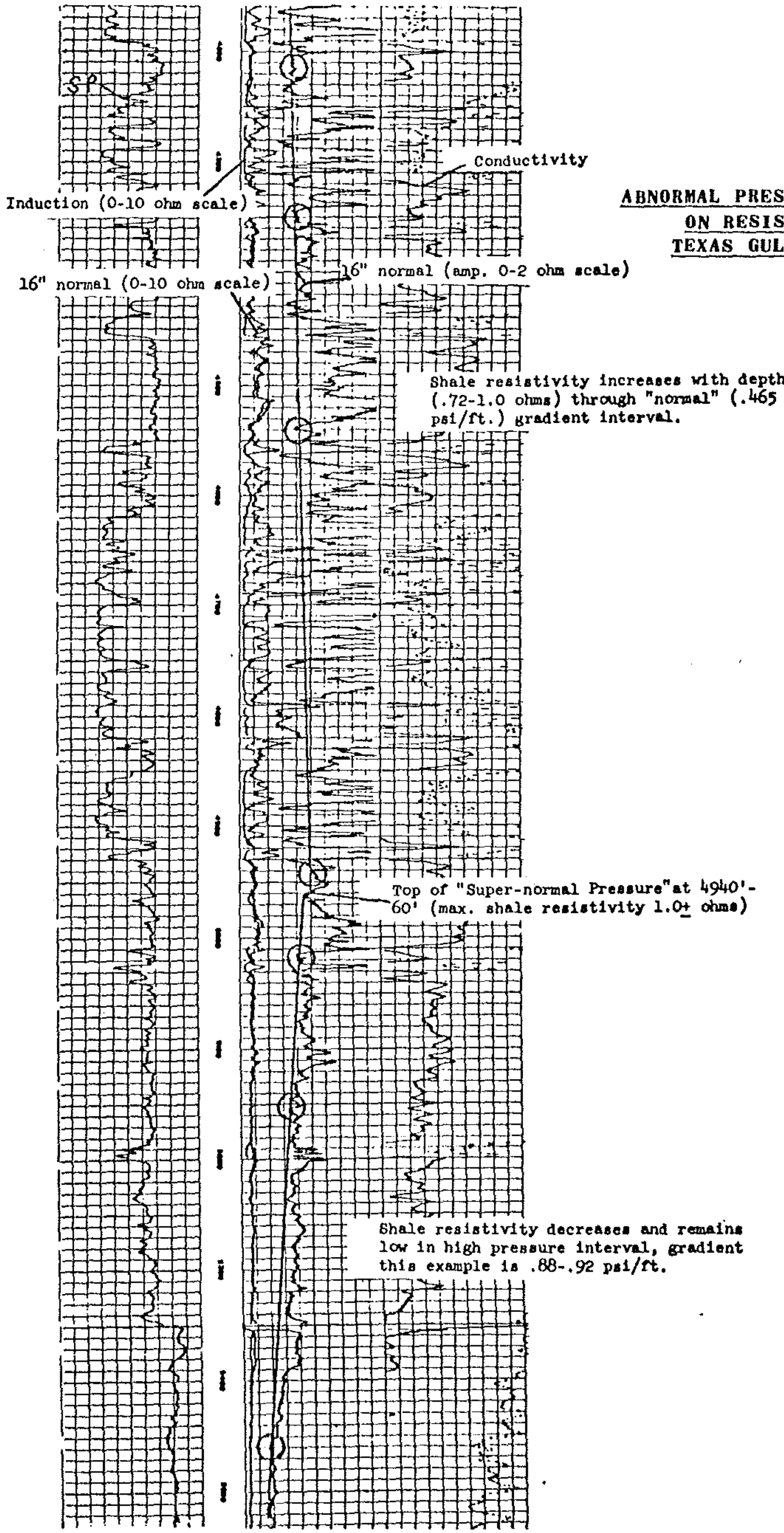

Figure 5-4

ABNORMAL PRESSURE EFFECT ON RESISTIVITY AND VELOCITY
SACRAMENTO VALLEY, CALIFORNIA

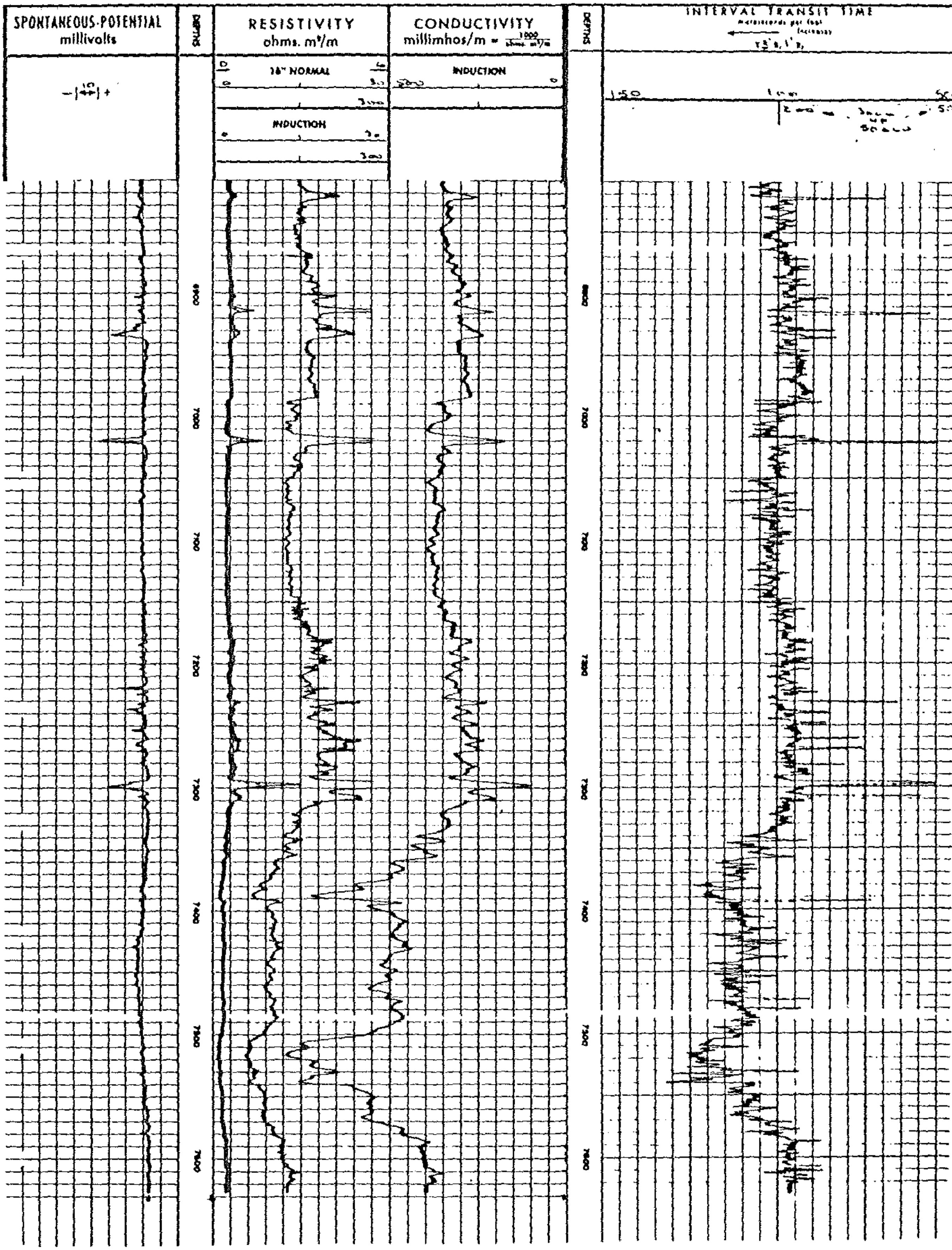

Figure 5-5

SHALE DENSITY PLOT COMPARED WITH DENSITY LOG
TEXAS GULF COAST

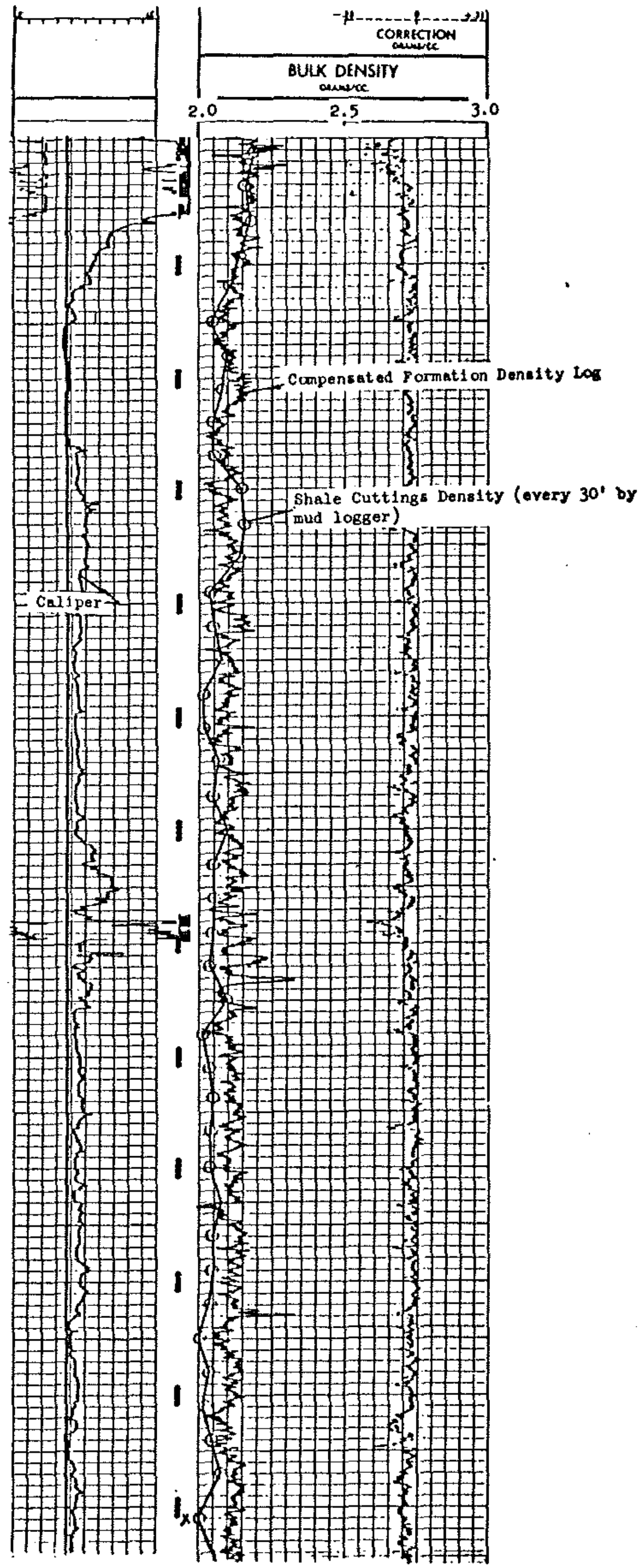

Figure 5-6

Geologic Interpretation From Well Logs
Rocky Mountain Log Supplement

Known Logs

Figure 1-3

top; sw/se/sw, 3-T9N-R79W, Conoco Oil, #5 Pollock, Jackson County, Colorado (McCallum Field).

middle; ne/se/ne, 20-T10N-R79W, Lion Oil Company, #1 Eva, Jackson County, Colorado (McCallum Field).

bottom; sw/nw/ne, 22-T10N-R79W, Monsanto Corp., #1 Perkins, Jackson County, Colorado (McCallum Field).

Figure 1-4

left; se/se, 15-T8N-R66W, California Oil Company, #1 Vernable, Weld County, Colorado (Pierce Field).

right; nw/se, 27-T8N-R66W, California Oil Company, #1 Jennings, Weld County, Colorado (Pierce Field).

Figure 1-7

left; nw/se, 27-T8N-R66W, California Oil Company, #1 Jennings, Weld County, Colorado (Pierce Field).

right; se/sw, 23-T8N-R66W, California Oil Company, #4 Priddy, Weld County, Colorado (pierce Field).

Figure 1-8; se/se/ne, 14-T3S-R85W, California Oil Company, #1 Benton Land and Livestock Company, Routt County, Colorado.

Figure 1-9; nw/ne, 13-T148N-R98W, California Oil Company, #1 Rough Creek Federal, McKenzie County, North Dakota.

Figure 2-2; sw/nw/se, 1-T26N-R90W, Sinclair Oil Company, #35-B Wertz, Sweetwater County, Wyoming (Wertz Field).

Figure 2-5; sw/ne/nw, 14-T27N-R113W, California Oil Company, #1 Birch Creek, Sublette County, Wyoming (Birch Creek Field).

Figure 2-7; c/ne/se, 13-T7S-R23E, California Oil Company, #35 Redwash, Unitah County, Utah (Red Wash Field).

Figure 2-8, ne/se/nw, 19-T29N-R114W, Belfer Natural Gas, #43-19G, Sublette County, Wyoming.

Figure 2-12

left; ne/nw, 7-T32N-R85W, Seaboard Oil Company, #1 Olds-Skiles, Natrona County, Wyoming (Grieves Field).

middle; ne/se, 17-T32N-R85W, Forest Oil Comapny, #45 Govt. 17-1, Natrona County, Wyoming (Grieves Field).

right; se/ne, 18-T32N-R85W, True Oil Company and Mule Creek Oil Company, #42-18 Dumbell, Natrona County, Wyoming (Grieves Field).

Figure 2-13

left; ne/nw, 31-T51N-R69W, True Oil Company, #1-A Heptner, Campbell County, Wyoming (Pleasant Valley Field).

right; ne/sw, 30-T51N-R69W, Shell Oil Company, #23-30 Heptner, Campbell County, Wyoming (Pleasant Valley Field).

Figure 2-14; se/se, 32-T7S-R44E, Standard Oil of California, #1 Dry Valley, Caribou County, Idaho.

Figure 2-15; sw/sw/se, 31-T160N-R81W, California Company, #1 Thompson, Bottineau County, North Dakota

Figure 3-15; nw/ne 13-T148N-R98W, California Company, #1 Rough Creek Federal, McKenzie County, North Dakota.

Figure 3-17; ne/se, 22-T9S-R43E, Hose Austin Company, #1 Kendrick, Big Horn County, Montana.

Figure 3-19; c/sw/nw, 9-T41S-R24E, Standard Oil of California, #12-9 Navajo, San Juan County, Utah (Aneth Field).

Figure 3-24

top; c/nw/nw, 22-T33N-R19W, California Oil Company, #1 Ute Tribal, Montezuma County, Colorado.

bottom; nw/sw 20-T148N-R97W, California Oil Company, #1 Danielson, Dunn County, North Dakota.

Figure 3-28

left; ne/se, 36-T26S-R20E, Texas Oil Company and Gulf Oil Company, #1-X Federal, Grand County, Utah.

right; ne/se, 36-T26S-R20E, M.G.M. Petroleum, #1 MGM, Grand County, Utah.

Figure 4-5

left; nw/ne/ne, 5-T11N-R66W, L.H. Amer-Chicago Corp., #1 Warren-Livestock, Weld County, Colorado.

right; c/se/ne, 36-T41N-R61W, Ginther-Warren and Ginther, #1 Fritz, Laramie County, Wyoming.

Figure 4-6

left; se/se, 15-T8N-R66W, California Oil Comapny, #1 Vernable, Weld County, Colorado (Pierce Field).

right; se/sw, 23-T8N-R66W, California Oil Company, #4 Priddy, Weld County, Colorado (Pierce Field).

Figure 4-9, nw/sw/sw, 18-T17N-R76W, California Oil Company, #8 Wilson, Albany County, Wyoming (Quealy Dome Field).

Figures 4-12 and 4-13, sw/se, 2-T30S-R24E, Pure Oil Company, State #1-A, San Juan County, Utah (Lisbon Field).

Figure 4-15, se/se/ne, 14-T3S-R85W, California Oil Company, #1 Benton Land and Livestock Company, Routt County, Colorado.

Rocky Mountain Wells With Unknown Locations

Figure 3-10, Pierce Field area?, Weld County?, Colorado.

Figure 3-16, Powder River Basin, Wyoming.

Figure 3-22, Paradox Basin, San Juan County, Utah

Figure 4-14, Rocky Mountains (United States or Canada?).